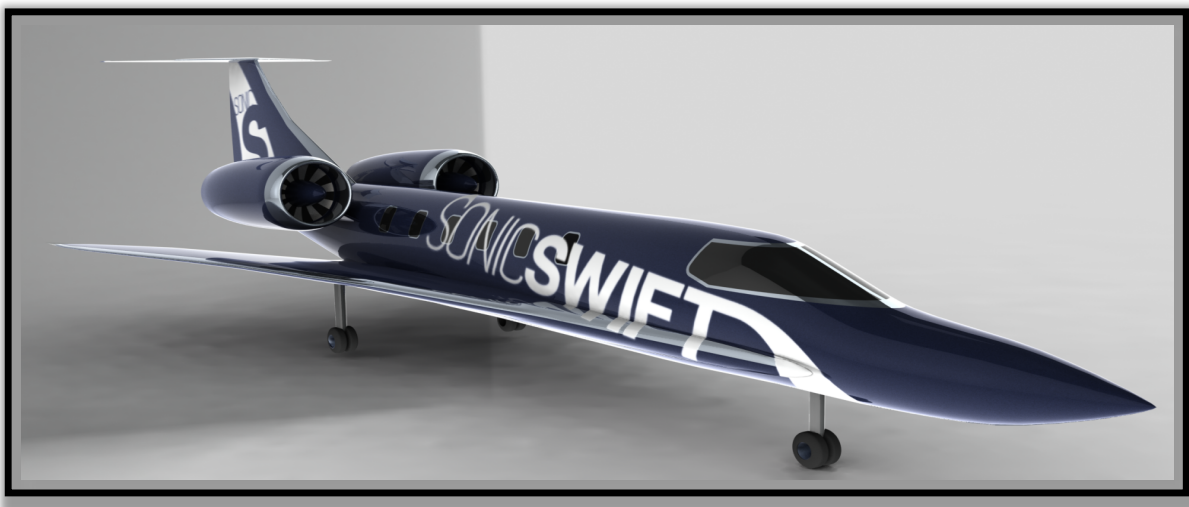


# SUPersonic BUSINESS JET

## CONCEPTUAL DESIGN TEAM



**FINAL REPORT**  
03 MAY 2012

**VIRGINIA POLYTECHNIC INSTITUTE & STATE UNIVERSITY**  
AEROSPACE AND OCEAN ENGINEERING DEPARTMENT

AOE 4154: SENIOR DESIGN  
PROFESSOR R. KAPANIA

**SONICSWIFT**

Final Report  
*Supersonic Business Jet Design Team*

## **EXECUTIVE SUMMARY**

This report provides detailed explanations and results relating to the preliminary vehicle sizing and subsequent initial design iteration of a supersonic business jet concept vehicle. Due to the current lack of supersonic transportation options for corporate, political and military leaders, there is a demand for a vehicle that can provide extremely fast transportation, even enabling single day, round-trip trans-Atlantic travel. With a design cruise speed of Mach 2.2, and a range of nearly 5,000nm, this vehicle is designed to carry a maximum of 12 passengers. This report outlines the evolution of aerodynamic design to a highly swept delta wing, optimized in a NASA supersonic aerodynamics study. Drag was calculated using the component build-up method, FRICTION code, and Cart3D CFD analysis. The wings and empennage were analyzed using beam bending and flat plate stress based analysis, and was optimized using an in-house optimizer. The final propulsion unit is a civil derivative engine of the GE F118. Detailed performance calculations and analysis were performed to determine realistic vehicle performance, complying with FAA and ICAO regulations. Landing gear was sized, and placed in the vehicle to retract into the fuselage without landing gear pods. Interior, cabin and cockpit systems were sized semi-empirically, as well as hydraulic, electrical and auxiliary power systems. Emergency systems were integrated according to FAA regulations. For sonic boom mitigation, an extendable nose boom, shaped nose and careful adherence to the supersonic area rule allows for significantly decreased sonic boom noise when compared to the Concorde. Finally, this report describes the final design iteration, and outlines the vehicles performance, characteristic parameters and estimated sonic boom strength. This concept vehicle shows that it is technologically and economically feasible to break the sound barrier for business jets.

Final Report  
*Supersonic Business Jet Design Team*

**TABLE OF CONTENTS**

TEAM MEMBERS AND ROLES.....	6
1. INTRODUCTION.....	7
2. COMPETITOR RESEARCH	
<i>2.1. Retired Supersonic Commercial Aircraft</i> .....	8
<i>2.2. Commercially Developed Concept Vehicles</i> .....	9
<i>2.3 NASA Developed Concept Vehicles</i> .....	12
3. MISSION REQUIREMENTS	
<i>3.1. Initial Mission Requirements</i> .....	12
<i>3.2 Evolution of Mission Requirements</i> .....	13
4. MULTI-DISCIPLINARY OPTIMIZATION CODE	
<i>4.1. Design Goals</i> .....	15
<i>4.2. Code Structure: Modular Design</i> .....	15
<i>4.3. Code Structure: GlobalData Class</i> .....	16
<i>4.4. Applications Overview</i> .....	17
5. AERODYNAMIC DESIGN	
<i>5.1. Aerodynamic Configuration</i> .....	17
<i>5.2. Initial Geometries and Aerodynamic Performance Parameters</i> .....	20
<i>5.3. Optimization</i> .....	24
6. DRAG ESTIMATION	
<i>6.1. Component Buildup Method</i> .....	29
<i>6.2. FRICTION Code</i> .....	32
<i>6.3. CFD Drag Calculations</i> .....	33
<i>6.4. Induced Drag</i> .....	34
7. PROPULSION	
<i>7.1. Initial Research</i> .....	36
<i>7.2. Diffuser Cone</i> .....	40
<i>7.3. Engine Development</i> .....	42
8. Structural Analysis	
<i>8.1. Structural Configuration Design</i> .....	48
<i>8.2. Analysis: Intro</i> .....	49
<i>8.3. Analysis: Loading Conditions</i> .....	50
<i>8.4. Analysis: Stress Based Design</i> .....	53
<i>8.5. Analysis: Material Limits</i> .....	54

Final Report  
*Supersonic Business Jet Design Team*

8.6. Wing .....	57
8.7. Beam Bending Analysis.....	59
8.8. Thin Plate Analysis .....	62
8.9. Optimization .....	66
8.10. Configuration Case Study .....	67
8.11. Materials Case Study.....	68
8.12. Final Wing Results .....	69
8.13. Horizontal Tail .....	71
8.14. Horizontal Tail Configuration Case Study.....	72
8.15. Horizontal Tail Final Results .....	73
8.16. Vertical Tail.....	74
8.17. Vertical Tail Final Results .....	76
8.18. Future Work.....	77
 9. WEIGHTS ESTIMATION .....	80
 10. STABILITY AND CONTROL SURFACE SIZING	
10.1. Definition of Variables.....	81
10.2. Calculations .....	81
 11. PERFORMANCE	
11.1. Preliminary Performance Challenges and Investigations .....	84
11.2. Available Thrust Estimation .....	88
11.3. Normal Operation Envelope.....	90
11.4. Transonic Flight Considerations .....	91
11.5. Range and Fuel Consumption Estimation.....	92
11.6. Endurance Estimation.....	95
11.7. Reserve Fuel.....	95
11.8. Takeoff Calculation Method .....	95
11.9. Takeoff Results .....	97
 12. SYSTEMS	
12.1. Landing Gear.....	98
12.2. Fuel Systems .....	101
12.3. Internal Configuration .....	102
12.4. Hydraulic and Electrical Systems.....	103
12.5. Cockpit.....	104
12.6. Cabin .....	105
12.7. Emergency .....	106
 13. SONIC BOOM MITIGATION AND ESTIMATION .....	107
 14. COSTS ESTIMATION.....	113
 15. FAA REQUIREMENTS .....	114

Final Report  
*Supersonic Business Jet Design Team*

16. SIZING EVOLUTIONS.....	114
17. FINAL DESIGN	
<i>17.1. Final Vehicle Design .....</i>	117
<i>17.2. Vehicle Mockup and Branding .....</i>	121
<i>17.3. Comparison to Cessna Citation X.....</i>	122
18. CONCLUSION.....	124
REFERENCES .....	125
APPENDICES	
<i>Appendix I: Weights Breakdown .....</i>	127
<i>Appendix II: Costs Breakdown.....</i>	128
<i>Appendix III: FAA Requirements .....</i>	129

Final Report  
*Supersonic Business Jet Design Team*

## **TEAM MEMBERS AND ROLES**

### Project Management

Brian Groves: Lead

Maggie Nate: Associate

### Multi-Disciplinary Analysis/Optimization Code

David Gayman: Lead

Brian Groves: Associate

### Propulsion

Nathan Bingham: Lead

Alex Harrell: Associate, Eco-design

### Aero Configuration

Kevin Antcliff: Lead, Aero Configuration

Shyla Thomas: Drag Estimation

### Structures

David Gayman: Lead

Brian Groves: Associate, Weights

### Flight Performance

George Buhl: Lead, Mission Analysis & Performance

Chris Cramer: Stability and Controls

Maggie Nate: Stability and Controls

Shyla Thomas: FAR Regulations

Brian Groves: Project Costs

### Sonic Boom Mitigation

Brian Groves: Lead, Sonic Boom Mitigation

Karishma Pillai: Sonic Boom Measurement

### Systems

Karishma Pillai: Lead, Landing Gear

Kevin Antcliff: Fuel Systems

Maggie Nate: Cabin Systems, Internal Configuration

Shyla Thomas: Emergency Systems

Chris Cramer: Cabin Systems

Brian Groves: Systems Advisor

Final Report  
*Supersonic Business Jet Design Team*

## 1. INTRODUCTION

Currently there is no vehicle that enables corporate executives, heads of state, military leaders and other VVIP's to make realistic, transcontinental day trips. A supersonic business jet cruising at Mach 2.2 would revolutionize business and politics, making it possible to fly from NYC to Paris (3160 nm) and back in one day, eliminating jet-lag and decreasing total flight times from 15 hours to 8. Business trips from Seattle to Washington, D.C. (2025 nm) would take 3 hours, and Los Angeles to London (4750 nm) less than 6. Although current FAA and ICAO regulations prohibit supersonic flight over land, careful design and sonic boom mitigation techniques demonstrate low sonic boom effects, leading to a strong argument to have these regulations relaxed to allow for low-boom supersonic flight over land.

With this vision, the design objectives were chosen to be competitive with similar current supersonic vehicle prototypes, and to be a leader in the performance of supersonic transport. The initial sizing goal is to allow for single day trans-Atlantic round-trip flights, while being comfortable and fuel-efficient. The vehicle must have sufficient range to cross the Pacific as well. The design will incorporate technologies that will mitigate the noise impact during each flight regime, with the goal to demonstrate acceptable over-land supersonic noise impact in anticipation of future changes in supersonic noise regulations. With increasing environmental awareness and regulations, the design will try to achieve as low of an environmental impact as possible, with a primary focus on emissions during flight. Lastly, in order to make this design viable, it must be shown that the design is profitable for both operators and manufacturers.

Design began with careful research into past, present and future aircraft with similar missions and flight conditions. This research allowed for an educated preliminary sizing, resulting in parameters that were used for further design iterations and analysis through a multi-disciplinary optimizer (MDO) code developed in house.

Final Report  
*Supersonic Business Jet Design Team*

## 2. COMPETITOR RESEARCH

### 2.1. Retired Supersonic Commercial Aircraft

Supersonic flight is dominated by two main categories: the large supersonic transport and military vehicles. Defense aircraft such as fighter jets and reconnaissance vehicles routinely fly at supersonic speeds, but do so with few crewmembers and intense operating flight conditions. The design goals for these vehicles are in a completely different flight regime than a business jet, so they were not analyzed on a vehicle level. Rather, component and configuration designs were analyzed to provide insight for our conceptual design.

The BAC Concorde and Russian Tupolev Tu-144 are the only successful commercial supersonic transports, but both have since retired. These aircraft are an order of magnitude larger than the business jet concept, carrying in excess of 120 passengers; the supersonic business jet concept will carry 12. Due to the similar mission profiles, these aircraft were analyzed and viewed as the 'big brothers' to the initial design. As such, many common features were utilized but on a smaller scale.

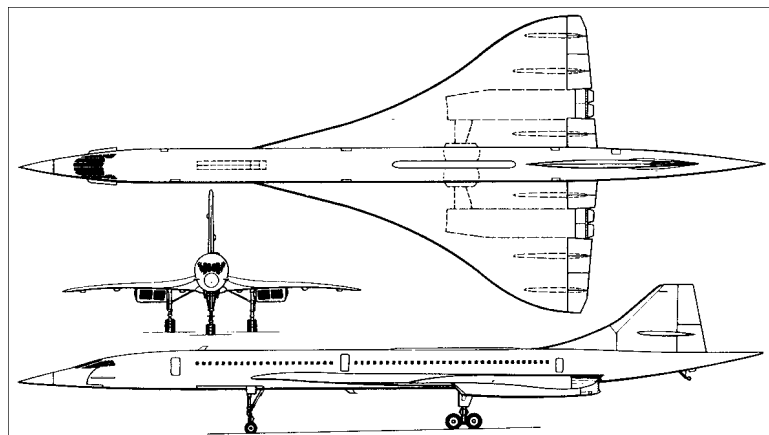


**Figure 2.1.1: BAC Concorde**  
([http://www.aviastar.org/air/inter/inter\\_concorde.php](http://www.aviastar.org/air/inter/inter_concorde.php))

Final Report  
*Supersonic Business Jet Design Team*

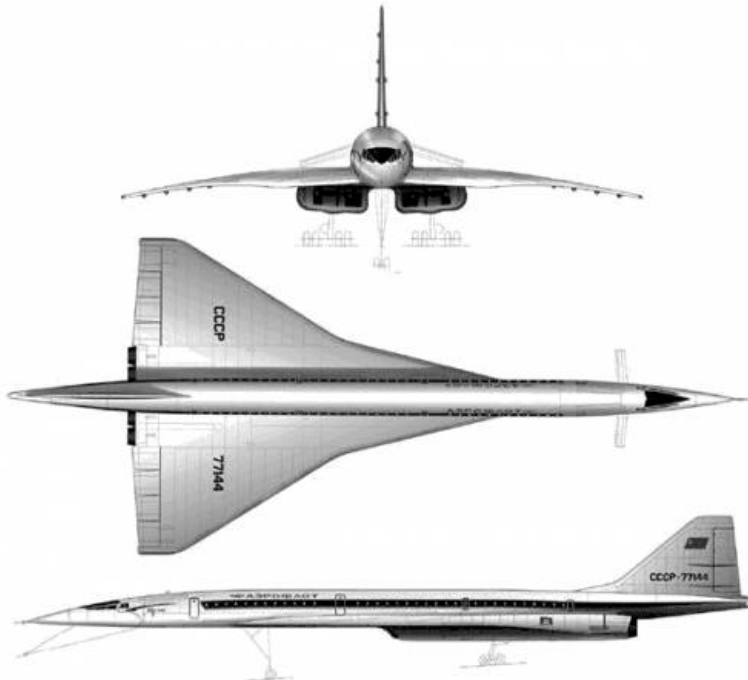


**Figure 2.1.2: Tupolev Tu-144**  
([http://www.the-blueprints.com/blueprints/modernplanes/tupolev/20253/view/tupolev\\_tu-144\\_supersonic\\_airliner/](http://www.the-blueprints.com/blueprints/modernplanes/tupolev/20253/view/tupolev_tu-144_supersonic_airliner/))

## 2.2. Commercially Developed Concept Vehicles

Finally, several supersonic business jet conceptual vehicles are currently in development. Most notably, the Aerion SBJ (Supersonic Business Jet, Figure 2.2.1) appears to be the closest to development (entry goal of 2014). Our vehicle was designed to be a direct competitor to this aircraft.

Final Report  
*Supersonic Business Jet Design Team*

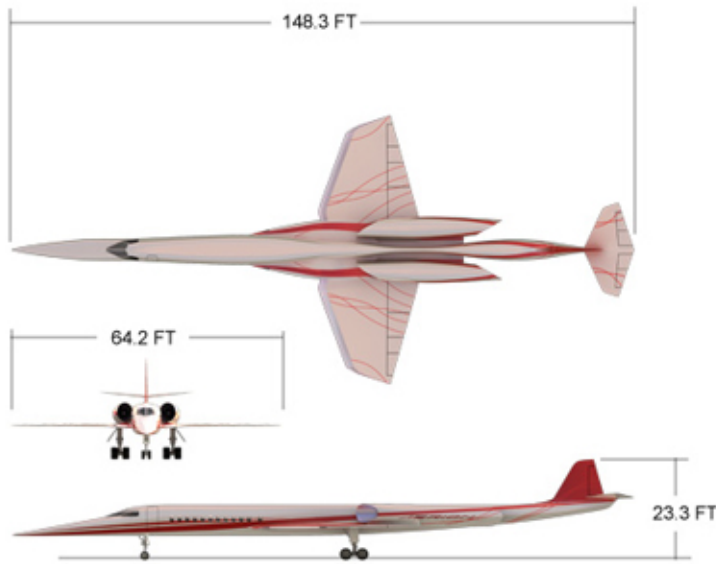


**Figure 2.2.1:** Aerion Supersonic Business Jet (SBJ)  
(<http://avia.superforum.fr/t675-le-projet-aerion-supersonique>)

Additionally, the HyperMach SonicStar is a slightly larger and much faster concept, with an expected entry date of 2025 (Figure 2.2.2). Further prototype designs have been developed by Tupolev (Tu-444), Lockheed Martin (Quiet Supersonic Transport) and NASA, but these are all either abandoned or have no firm plans to enter the market (Figures 2.2.3 and 2.2.4).



**Figure 2.2.2:** HyperMach SonicStar  
(<http://hypermach.com/>)

Final Report  
*Supersonic Business Jet Design Team*

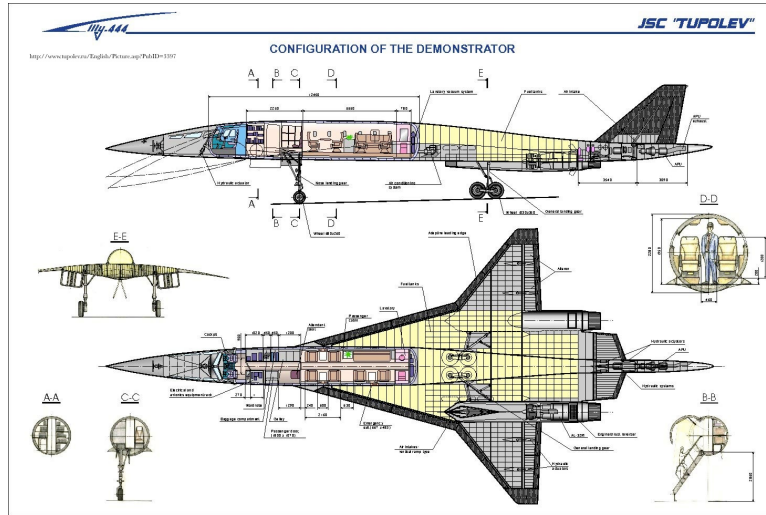


**Figure 2.2.3:** Tupolev Tu-444  
([www.tupolev.ru](http://www.tupolev.ru))



**Figure 2.2.4:** Lockheed Martin Supersonic Green Machine  
(<http://www.popsci.com/technology/article/2012-04/jets-future>)

These concept vehicles provide few details beyond the overall aerodynamics and sonic boom mitigation techniques, with the exception of the Tupolev Tu-444, which has a publically available systems and interior layout diagram. These vehicle designs were primarily used for the development of our vehicle's aerodynamic design.

### **2.3. NASA Developed Concept Vehicles**

In contrast to the commercial supersonic vehicle design concepts, the NASA N+2 and N+3 vehicle designs were immensely useful in this design project. Both of these designs are for larger scale, commercial supersonic vehicles, but provide key insight into how to design a supersonic vehicle. The N+2 document was used as a primary source in the design evolution process, providing key insights.

Additionally, a NASA Technical Memorandum on designing a supersonic executive jet (Memorandum 74055, 1977) was useful in designing the vehicles interior and systems configuration. A final NASA study on supersonic business jet design provided key insights into the wing configuration and sonic boom mitigation techniques (NASA/TM-2003-212435).

Each of these NASA documents and studies was used for insight on how to design a supersonic business jet and provided the backbone for the success of this design project.

## **3. MISSION REQUIREMENTS**

### **3.1. Initial Mission Requirements**

The vehicle was being designed to meet several strict mission requirements and objectives, detailed as follows.

The design will achieve a supersonic cruise speed of at least Mach 2.2 and a cruise range of at least 9000 kilometers [4860 nm], enabling a direct flight across the Pacific from Los Angeles to Tokyo. The aircraft will accommodate 2 crewmembers, 12 passengers and their luggage. Noise emissions should comply with the Type 4 certification as specified in 14 CFR Part 36, and engine emissions must meet proposed EPA Tier 8 standards ("EPA NOx Standards") Additionally, there should be no increase in perceived noise levels on the ground while the aircraft cruises overhead at supersonic speeds.

The mission profile selected for the vehicle is similar to that of typical commercial transport aircraft (see Figure 3.1.1). The goal for initial takeoff length is to be 1800 m, the

Final Report  
*Supersonic Business Jet Design Team*

usual takeoff field length for most airports around the world, and the takeoff length shall not be greater than 2400 meters. This aircraft will then climb subsonically to a cruise altitude of 12,000 meters. Once at this altitude, the aircraft will accelerate to supersonic speeds. Once the aircraft reaches approximately Mach 1.1, it will continue to accelerate to the design supersonic cruise speed Mach number of 2.2 and climb to the super cruise altitude of 20,000 meters. For safety reasons, it will carry fuel reserves, in case the intended airport or landing field is closed according to NBAA IFR recommendations.

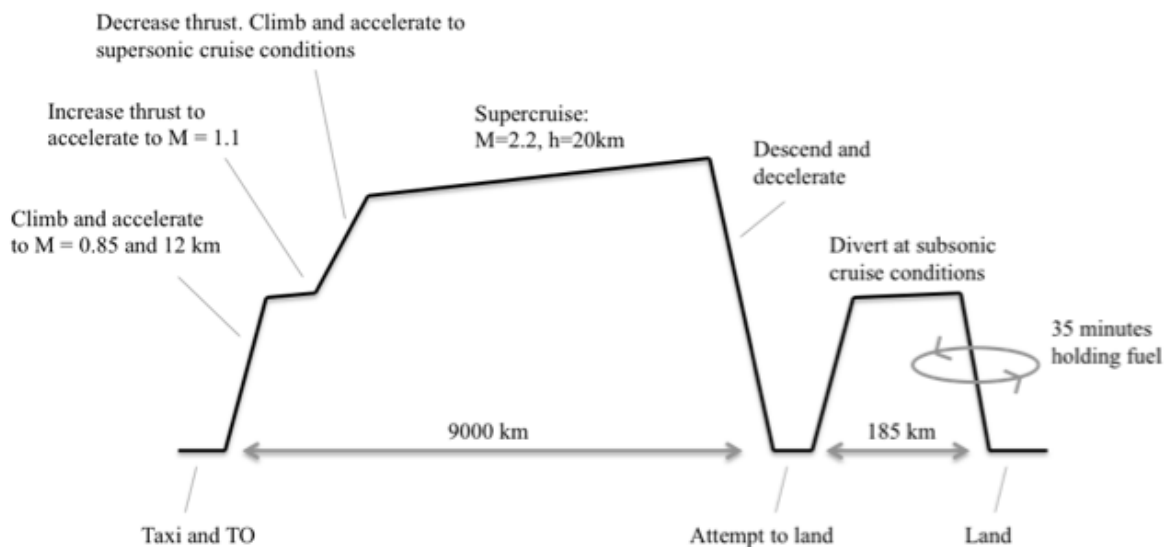


**Figure 3.1.1:** The anticipated mission profile for the supersonic business jet.

### 3.2. Evolution of Mission Requirements

Since most initial design requirements were met, few changes were made to the original specifications created at the start of the project. However, due to time constraints, noise and engine emission requirements were deemed unnecessary for the completion of the design project and were changed from requirements to goals. If the project were to continue and more detailed design work were to be done, it is expected that these emissions standards would become requirements again. The design originally also called

Final Report  
*Supersonic Business Jet Design Team*

for a life cycle analysis to be done on the aircraft, but this was also considered too time consuming for the conceptual design phase.

The requirement of a takeoff length less than 1800 m [6000 ft] was specified at the beginning of the project. This requirement was chosen based on research of similar aircraft designs such as the NASA N+2 aircraft and the Aerion SBJ. However, while performance calculations showed that the design can takeoff in less than 1800 m, it would not meet safety requirements in the case of an engine failure. Therefore, the takeoff requirement was increased to 2400 meters. This change was considered an acceptable sacrifice in takeoff and subsonic performance since the teams' focus and time would be better spent on supersonic optimization. However, an 1800 meter balanced field length remains as a goal if the design team had more time to consider including high lift devices such as a canards.

Changes were made to the mission profile in light of engine performance discoveries and safety suggestions. The original mission profile, shown below, it was expected that the aircraft would climb to approximately 20,000 feet before accelerating to supersonic speeds. However, this proved to be impossible with the design. At higher altitudes, the induced drag became too high at subsonic speeds to overcome. The modified mission profile, shown in Figure 3.1.1, has the aircraft enter two major climbing phases after takeoff. After the first climbing phase, we found the aircraft could accelerate to supersonic speeds and then continue to climb to the desired supersonic cruise altitude as induced drag decreased.

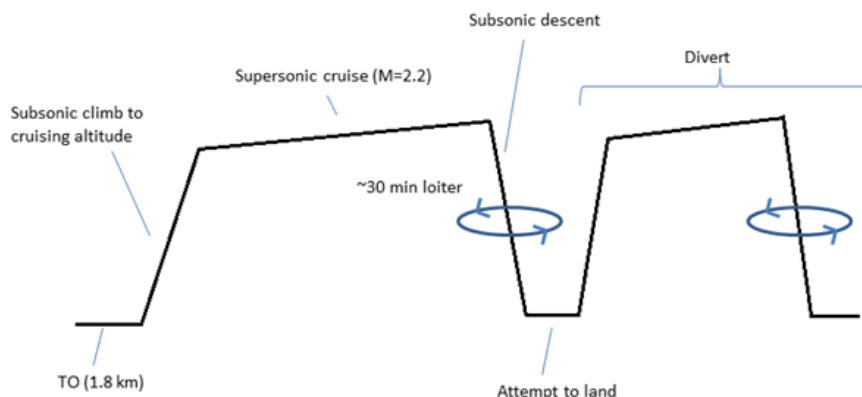


**Figure 3.2.1:** The initial mission profile for the supersonic business jet.  
This profile was used to estimate the initial aircraft weight sizing.

Final Report  
*Supersonic Business Jet Design Team*

Another change was made to the amount of reserve fuel held on board. The initial mission profile accounted for 30 minutes of loiter fuel as suggested by Chapter 3 of Raymer and an additional 6% reserve fuel for cruise to an alternate airport and trapped fuel. As more work was done to understand fuel consumption, the reserve fuel was changed to equal 185 km [100 nm] of subsonic cruise fuel and 35 minutes of holding fuel in compliance with NBAA IFR recommendations.

## 4. MULTI-DISCIPLINARY OPTIMIZATION CODE

### 4.1. Design Goals

The Multi-Disciplinary Optimization (MDO) code is understood to involve three primary goals. The most important aspect is centralized information storage. Secondly, the code should provide a robust programming framework in which numerical analysis appropriate to the aircraft design can operate. The final goal is to enable future optimization over a set of parameters, to be determined by trial-and-error. In addition, the code base should be highly adaptable to allow the rearrangement of processing stages.

### 4.2. Code Structure: Modular Design

With these capabilities in mind, a modular structure was designed. Algorithms specific to engineering aspects of the aircraft were functionalized and grouped into modules. A central module containing parameters that effectively define the airplane, such as geometric, performance, cost, stability, and weight variables, was also written. All modules have access to this GlobalData class. A more detailed description of this class can be found in the next section.

Modules are instantiated as objects in a single high-level script. This script then calls the “process” function in each object, which requests that any internal calculations be

Final Report  
*Supersonic Business Jet Design Team*

performed. For example, if the process function for the Performance object is called, aircraft performance resulting from the current set of global parameters is computed. Important results are then stored in the GlobalData class.

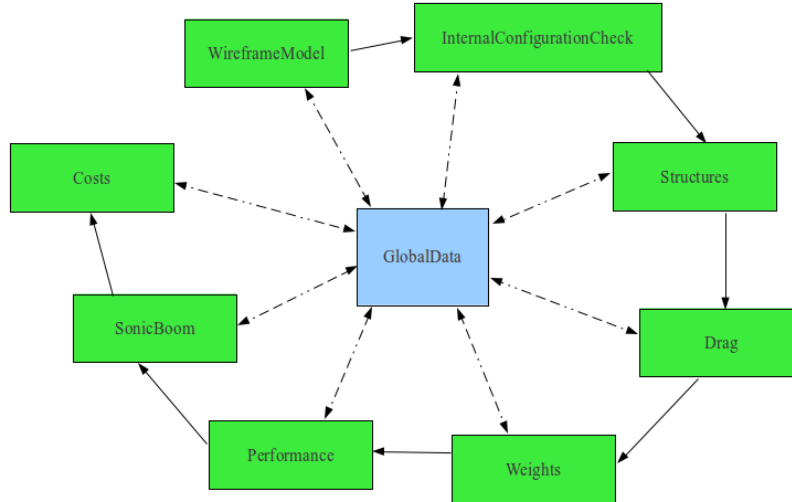


**Figure 4.1:** Block diagram showing execution path (solid lines) and allowed data access (dashed lines)

### 4.3. Code Structure: GlobalData Class

The GlobalData class is central to the project. This class encapsulates all parameters that define the aircraft, and is responsible for all access and storage of these values. The types of data that can be stored are double-precision values, arrays and structures (known as “structs”). All can be arranged into arbitrarily large tree structures, giving each module the ability to organize their parameters.

Functions in the GlobalData class automatically store and recall these global parameters. Files containing the information are saved using a chronological naming sequence to enable a history of the airplane to be examined at any time. Additionally, diaries of input and output text from all interactions with the MDA code are automatically logged for future reference.

Final Report  
*Supersonic Business Jet Design Team*

#### **4.4. Applications Overview**

Initial applications for the optimizer included sizing the wing and empennage to optimize range. Constraints included wing loading (indirect constraint) and marginal static stability, while areas of the wing, horizontal and vertical tail were allowed to vary independently. Dependent variables included takeoff gross weight, drag and propulsion sizing.

Additionally, a sub-optimizer in the MDO code was utilized in the structural analysis to better determine the optimal number of ribs and spars. Combinations of different materials were also included in this optimizer, yielding a structure that is a desirable balance between weight, cost and allowable deflections and stresses.

Detailed results of optimization studies can be found in their respective sections. Applying this optimizer was crucial in converging to a design, and since the MDO code incorporated all aspects of the vehicle design (withstanding: aerodynamics), the optimizer could be used to investigate the widespread impact of each varied parameter.

### **5. AERODYNAMIC DESIGN**

#### **5.1. Aerodynamic Configuration**

Initially, this group began by researching current designs of supersonic business jets, creating designs similar to those and presenting them to the team. Most of the team agreed to a design similar to the QSST with the inverted tail. However, the people who did not agree to the QSST design brought up a point. No one had really researched why previous supersonic jets were shaped like they were. Therefore, the design and aerodynamic configurations group decided to research the different configurations possible and create an original configuration specific to the requirements of this design project.

Final Report  
*Supersonic Business Jet Design Team*

The design arrangement of an aircraft is important for its aerodynamic efficiency. Poor wing-fuselage arrangement can cause lift issues and unstable handling qualities. We created a table layout of many wing, tail, and engine configurations that are possible and listed the pros and cons for each. The wing configurations we brainstormed consisted of rectangle, trapezoidal, swept, delta and blended wing body. The rectangular wing configuration is used for low-speed performance, so it was not considered as an option for our design. The blended wing body configuration has a high lift to drag ratio, but the dimensions were considered unrealistic for small civil aircraft. This left the trapezoidal, swept, and delta wing as possibilities for our design. They are high-speed performance wings and generally have a good lift-to-drag ratio.

A wider variety of options existed for the tail configuration. The options were as follows: box tail, double vertical, conventional (low, middle, and high horizontal), and the inverted tail. The box tail is reliable structurally, but created more drag than the other options. The double vertical tail only seemed useful when configured with a delta wing, which would limit our wing options. This analysis left the conventional and inverted tail as options for our initial design.

The engine configuration had yet to be decided at this point in the design process because we were awaiting the decision of what engine we would use. The specifications of the engine chosen will play an important role in the configuration result. However, the configuration options we were considering, pending a final engine selection, included inboard (above or below the wing), outboard (above or below the wing), and blended into the wing. After the propulsion system was selected later in the design process, we decided on mounting the engines inboard and above the wing.

The group came up with 12 total configurations (3 wing and 4 tail configurations), shown in Figure 5.1.1. We presented all of them to the team and decided on three final configurations: trapezoidal wing with conventional tail, swept wing with conventional tail, and swept wing with inverted tail (Figure 5.1.2). The primary design was chosen to be the swept wing with a conventional tail. The team as a whole felt that one primary design would be necessary for initial parameters and calculations.

Final Report  
*Supersonic Business Jet Design Team*

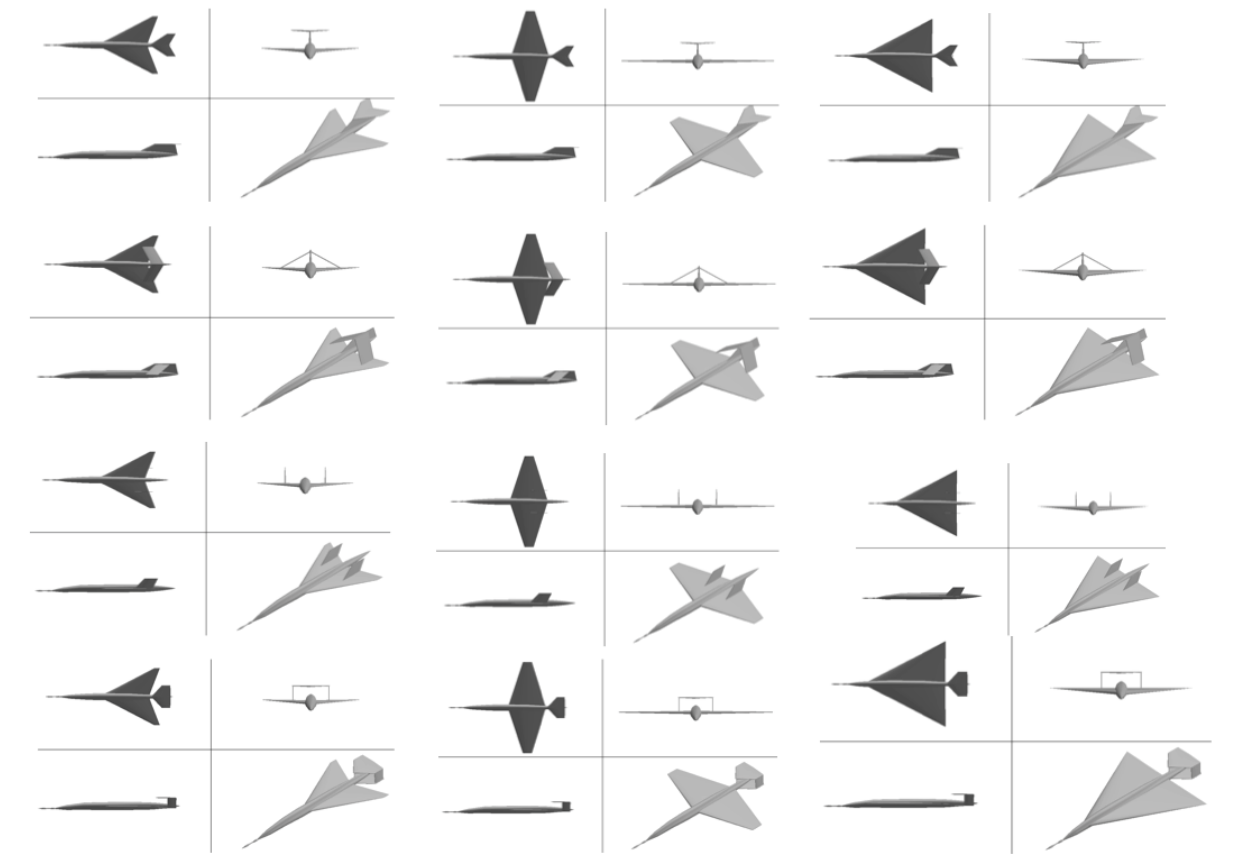


**Figure 5.1.1:** 12 Initial Configurations

Final Report  
*Supersonic Business Jet Design Team*

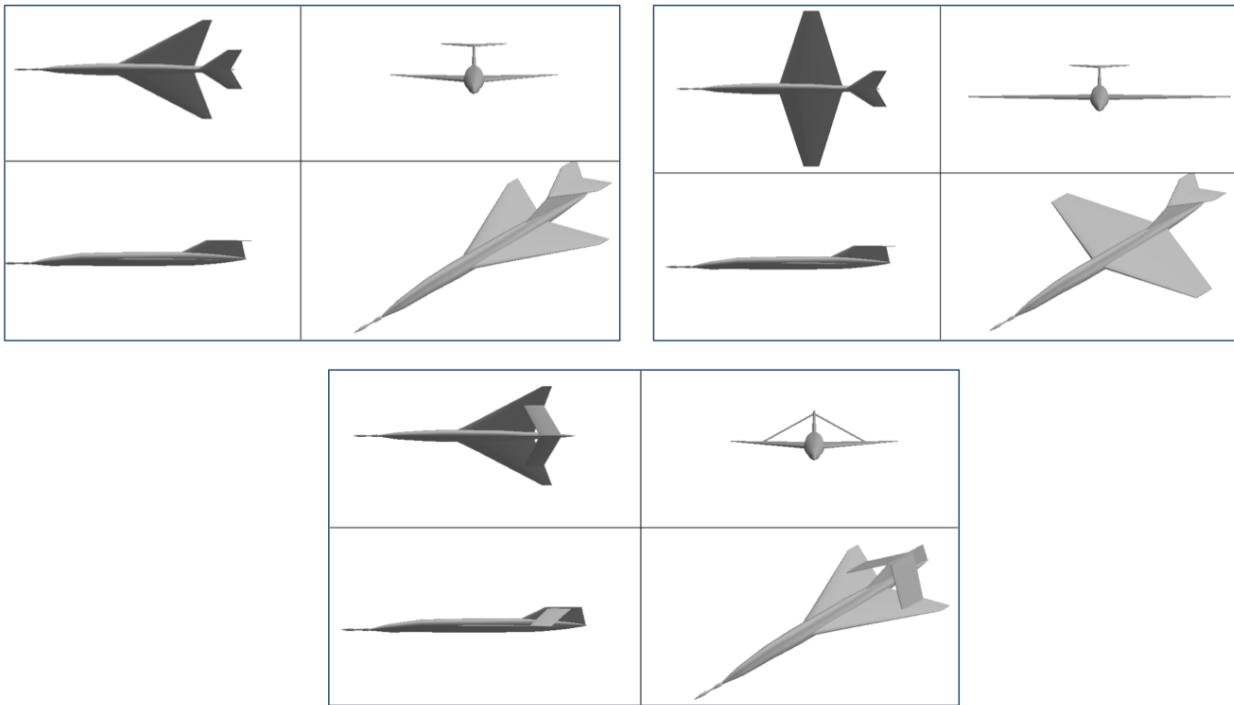


**Figure 5.1.2: 3 Configuration Finalists**

## 5.2. Initial Geometries and Aerodynamic Performance Parameters

The analysis of aircraft geometric and performance parameters begins with the initial specifications. While no official Request for Proposal, or RFP, is available for commercial supersonic business jets, a set of specific requirements and parameters over which optimization must be performed can be specified.

The primary goal of the supersonic business jet is to provide a marketable service to a paying set of customers. For ventures which employ novel technology or concepts, it is often necessary that the initial customers be members of the financial and political sectors, due to the financial backing that they can provide. As such, the primary customers for the supersonic business jet are members of the business class.

Amenities must be tailored to fit this important customer base. A cabin, which provides sufficient personal space while offering as much seating as possible, is desired. A midsized business jet traditionally has a maximum capacity of twelve, which allows a

**Final Report**  
*Supersonic Business Jet Design Team*

significantly large number of seats in which business transactions may be carried out. Two pilots are standard aboard passenger aircraft for safety, bringing the total number of people aboard to fourteen.

Defining minimum passenger spacing requirements allows interior fuselage dimensions to be determined. With the goal of minimizing aircraft weight, and taking into account the passenger cabin, cockpit, kitchen space, and restroom, the fuselage length was fixed at 126 ft. The exterior fuselage dimensions were taken to include the interior space, in addition to a fixed fuselage thickness based on the approximate thickness of similar aircraft. This and other values were chosen using statistical data and research, and are intended merely to serve as a reasonable starting point for aircraft sizing.

Values for the overall aircraft performance are tabulated below for clarity.

**Table 5.2.1:** Initial Requirements

Wing aspect ratio	2.3	
Wing planform area	511.79 m <sup>2</sup>	1679.2 ft <sup>2</sup>
Thrust per engine	90.99 kN	20458 lbf
Fuselage length	38.40 m	126 ft
Fuselage width	2.35 m	7.7 ft
Fuselage height	2.35 m	7.7 ft
Center of gravity location	19.20 m	63.0 ft
Number of passengers	12 People	
Crew	2 People	
Total number of people	14 People	
Range	9000 km	5592 miles
Cruise altitude	19.8 km	65,000 ft
Cruise Mach number	2.2	
Cruise lift-to-drag ratio	8.19	
TOGW	51,655.3 kg	113,925 lbf
Fuel weight	30,367.9 kg	66,976 lbf
Fuel volume	39.2 m <sup>3</sup>	1384 cu. ft
Wing loading	3.9 kPa	82.4 lbf/sq. ft
Cruise lift coefficient	0.158	
Thrust required per engine	91.88 kN	20,500 lbf

Beginning with these specifications, an aspect ratio is chosen for the wing. Based on an analysis of supersonic aircraft of varying sizes, as well as subsonic business and passenger aircraft, an aspect ratio of 2.3 was chosen. This number comes from a weighted

Final Report  
*Supersonic Business Jet Design Team*

average of wing aspect ratios, which have been successfully employed for aircraft similar to the supersonic business jet.

To fully specify wing geometry, taper ratio and angles of sweep and dihedral must be specified. These values, like the aspect ratio, are taken from weighted averages of aircraft, which have similar performance to the SBJ and are tabulated below for clarity. The leading edge of the wing is initially placed at 40% of the fuselage length. This number was chosen based on similar values for business jets, and without regard for stability considerations. This location serves as an initial starting point, and will be iterated after further aerodynamic and structural analyses have been performed, at which point the aerodynamic center and center of mass will be known.

**Table 5.2.2:** Initial Wing Sizing Parameters

Sweep angle	0.6108 rad	35 degrees
Location of wing leading edge	15.361 m	50.4 ft
Taper ratio		0.4
Dihedral angle	0.04363 rad	2.5 degrees
Horizontal tail volume	0.4503 m <sup>3</sup>	15.9 cu. ft
Vertical tail volume	0.0538 m <sup>3</sup>	1.90 cu. ft

**Table 5.2.3:** Resulting Initial Wing Geometry

Wingspan	18.93 m	62.1 ft
Mean aerodynamic chord	8.23 m	27.0 ft
Root chord	11.76 m	38.6 ft
Tip chord	4.69 m	15.4 ft
Distance of m.a.c. line from centerline	8.23 m	27.0 ft
Aerodynamic center (supersonic)	15.51 m	50.9 ft
Section lift coefficient		0.127
Horizontal tail area	31.8 m <sup>2</sup>	342.1 sq. ft
Vertical tail area	8.76 m <sup>2</sup>	94.4 sq. ft

Given the wing area, aspect ratio, taper ratio, quarter-chord sweep angle, and leading edge location, all basic wing geometries are specified and can be visualized (see Figure 5.2.1). Following a similar process for geometric parameter specification, the horizontal and vertical tails may be sized. The primary consideration for tail sizing comes from the first-order “tail volume” estimate from the study of aircraft control dynamics. The

**Final Report**  
*Supersonic Business Jet Design Team*

tail volume ratio relates measures of the effective “stabilizing power” to the power that the airframe requires. As a result of this assumed relation, the horizontal and vertical tail areas are determined as first-order approximations by the selection of appropriate tail volume ratios.

The horizontal and vertical tail volume ratios are chosen based on the values employed by similar aircraft. Using these values, in conjunction with the main wing geometric parameters, tail planform areas were calculated. To fully specify swept tail surface geometry, reasonable aspect ratios and sweep angles were chosen. Taper ratios and a tail dihedral angle were also specified. The parameters that determine tail surface shape do not have as significant an effect on aircraft performance as planform area, but do have a direct impact on structural design considerations, manufacturability, and sonic boom mitigation. As such, these values serve as a reasonable starting point for aerodynamic analysis, and will be changed as the design is iterated. The tail was placed at the rear of the fuselage, and can be displaced in future design iterations if necessary.

**Table 5.2.4:** Horizontal Tail Independent Parameters

Horizontal tail volume	0.45 m <sup>3</sup>	15.9 cu. ft
Horizontal tail moment arm	18.29 m	60.0 ft
Horizontal tail aspect ratio		1.2
Horizontal tail sweep	0 rad	0 degrees
Horizontal tail LE location	37.49 m	123.0 ft
Horizontal tail taper ratio		0.8
Horizontal tail dihedral angle	0 rad	0 degrees

**Table 5.2.5:** Horizontal Tail Dependent Parameters

Horizontal tail area	31.78 m <sup>2</sup>	342 sq. ft
Horizontal tail span	6.19 m	20.3 ft
Horizontal tail root chord	5.73 m	18.8 ft
Horizontal tail tip chord	4.57 m	15.0 ft
Horizontal tail m.a.c.	5.15 m	16.9 ft
Horizontal tail location of m.a.c. line	21.88 m	71.8 ft
Horizontal tail aerodynamic center (subsonic)	38.70 m	127 ft
Horizontal aerodynamic center (supersonic)	15.54 m	51.0 ft

**Final Report**  
*Supersonic Business Jet Design Team*

A similar procedure allows for the dimensioning of the vertical tail. The values chosen for taper ratio and other parameters of minor influence are chosen somewhat arbitrarily according to the engineers' best judgment concerning structural design, ease of manufacture, and wave drag reduction. These values, in addition to those for the horizontal tail, will be improved iteratively in future calculations.

**Table 5.2.6:** Vertical Tail Independent Parameters

Vertical tail volume	0.054 m <sup>3</sup>	1.91 cu. ft
Vertical tail moment arm	18.19 m	59.7 ft
Vertical tail aspect ratio		1
Vertical tail sweep	0 rad	0 degrees
Vertical tail LE location	11.4 m	122.7 ft
Vertical tail taper ratio		0.9
Vertical tail dihedral angle	0 rad	0 degrees

**Table 5.2.7:** Vertical Tail Dependent Parameters

Vertical tail area	28.77 m	94.4 sq. ft
Vertical tail height	2.96 m	9.72 ft
Vertical tail root chord	3.1 m	10.2 ft
Vertical tail tip chord	2.8 m	9.21 ft
Vertical tail m.a.c.	2.96 m	9.72 ft
Vertical tail location of m.a.c. line	10.6 m	34.8 ft
Vertical tail aerodynamic center (subsonic)	38.15 m	125.2 ft
Vertical aerodynamic center (supersonic)	15.26 m	50.1 ft

### 5.3. Optimization

After the original aerodynamic arrangement and values were set, the cross sectional area was optimized. The group wanted to insure that the most efficient aircraft was being created. Therefore, the area rule was applied, the entire aircraft was resized, the engines were repositioned, the shape of the wing was drastically changed and CFD analysis was undertaken

Final Report  
*Supersonic Business Jet Design Team*

The Whitcomb Area Rule revolutionized the design of supersonic aircraft in the early 1950's. Richard Whitcomb was testing different fuselage and wing combinations in order to determine the design that would produce the least amount of drag. However, regardless of the combination, the drag was determined to be much higher than expected. This was determined to be the result of the sharp change in area due to the wings. Therefore, Whitcomb decided that it was necessary to decrease the area of the fuselage in order to decrease the added drag due to the wings.

In the initial design iteration, the area rule was taken into consideration but never quantified. The data was then fit to a second-degree polynomial. From this graph, the fuselage was enlarged or shrunk to more accurately depict a smooth curve. To create a more efficient aircraft, future endeavors will be focused on incorporating the Sears-Haack Area Distribution.

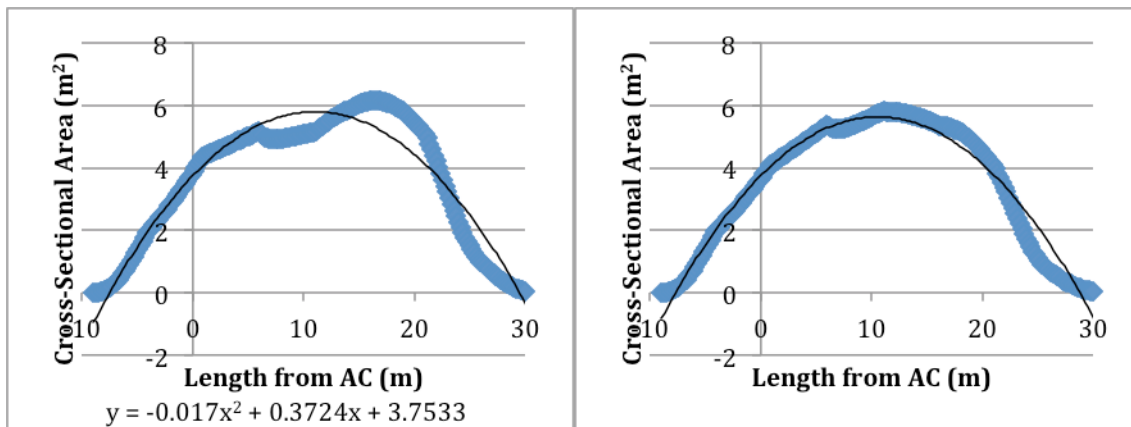


**Figure 5.3.1A/B:** Area Rule Optimization (Before and After)

Another major change was the shrinking of the aircraft (mostly the fuselage length and wing span). After running our master code through a couple iterations, it was found that our fuselage needed to shrink significantly. The incredibly large space that was thought necessary was deemed excessive. From this realization, the fuselage length was changed from 40 meters to 25 meters. This change puts the aircraft in line with typical subsonic business jets. It was also decided that the wings needed to be shortened in order to increase the aircraft's wing loading.

Final Report  
*Supersonic Business Jet Design Team*

Lastly, the engines were moved from the wing to the fuselage. This change was mostly decided because of the increase in weight due to the added structure on the wing. This added structure would also take up space in the wing, which would fill up some of the much-needed space for fuel. As confirmation that this was in fact a good decision, many small business jets designed today have also chosen to place their engines on the fuselage.

Another major change that was made was a drastic change in the shape of the wing. The original wing consisted of a typical swept wing with added strakes. However, the new design has a very smooth leading edge that transfers seamlessly from strakes to wing. This shape of the wing (shown below) was taken from a NASA study of supersonic business jets. The dimensions do not hold for our aircraft, as we scaled this shape to our span and area.

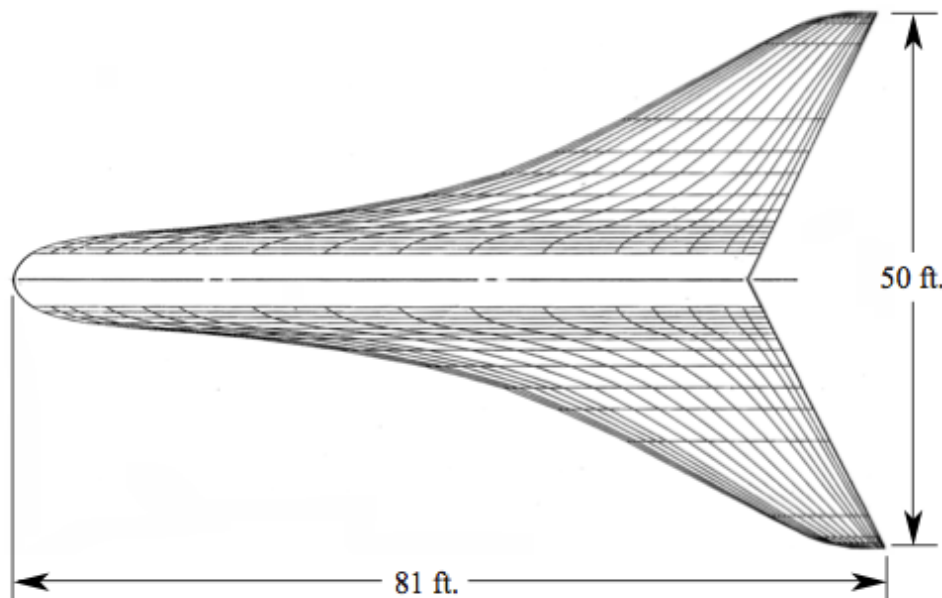


**Figure 5.3.2:** NASA Supersonic Business Jet Wing

All of the geometric modeling has been done in Vehicle Sketch Pad. In the past few weeks, in cooperation with NASA Langley, our model has been moved into Cart3D to perform CFD analysis in order to make sure that these design changes described above are effective.

In Figure 5.3.3, the local coefficient of pressure at a Mach number of 0.85 is shown. The coefficient of pressure ranges from around -0.7 to 0.35. The coefficient of pressure is

Final Report  
*Supersonic Business Jet Design Team*

largest at the nose and the cockpit window. It is lowest aft of the cockpit window and at the root of the wing at around 90% of the chord.

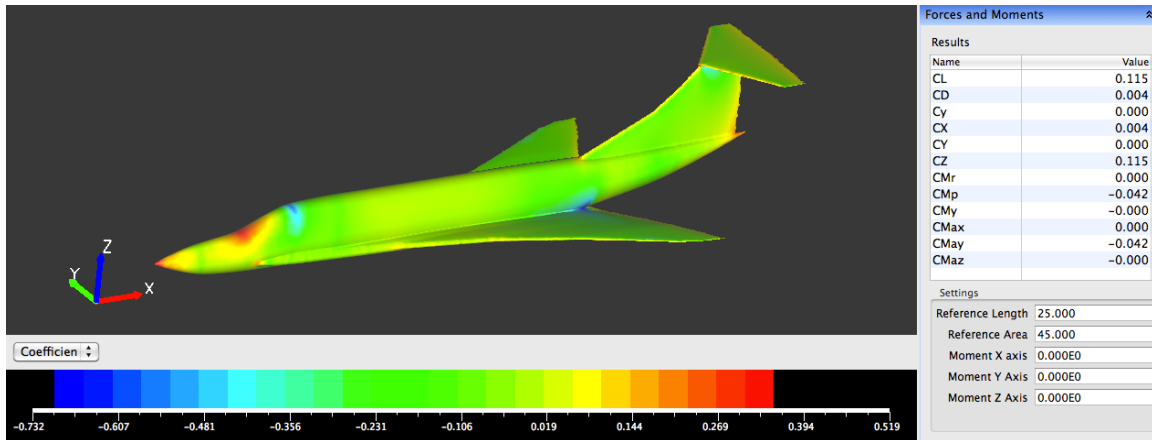


**Figure 5.3.3:** Local Coefficient of Pressure at M=0.85

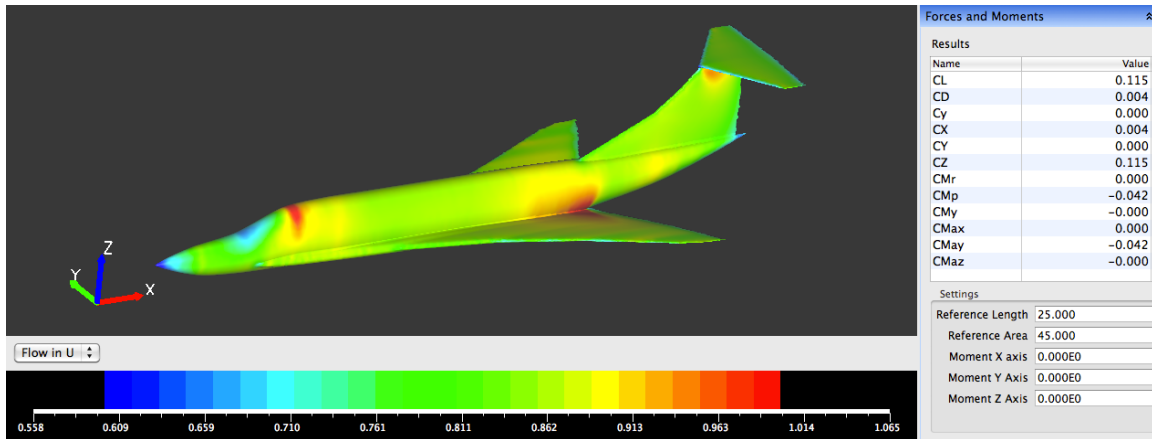


**Figure 5.3.4:** Local Flow Velocity at M=0.85

Final Report  
*Supersonic Business Jet Design Team*

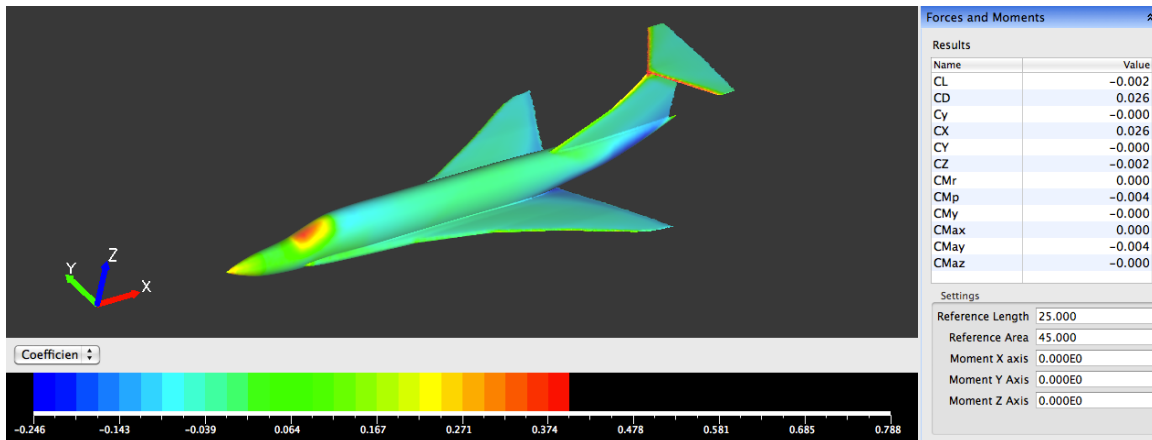


**Figure 5.3.5:** Local Coefficient of Pressure at M=2.2

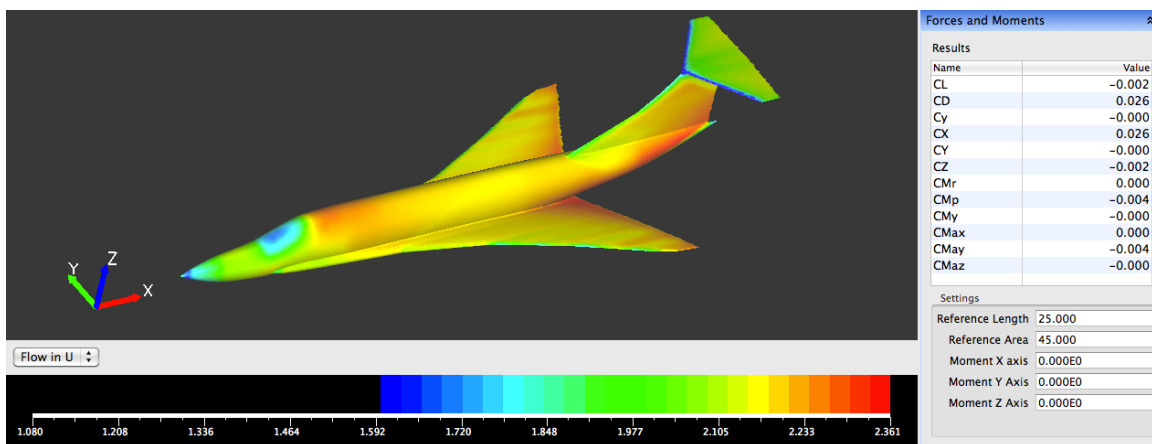


**Figure 5.3.6:** Local Flow Velocity at M=2.2

## 6. DRAG ESTIMATION

### 6.1. Component Build-up Method

The initial goal of the aerodynamics team was to estimate the parasite drag of our aircraft. The component build up method was used to compute the subsonic portion of the zero lift drag. This method analyzes each component by calculating the flat-plate skin-friction drag coefficient ( $C_f$ ) and form factor (FF), which estimates the pressure drag due to viscous separation. The Q factor takes into account the interference effects and the product of the wetted area,  $C_f$ , FF, and Q (approximately equal to 1 for all components) produce the total component drag. Therefore, the subsonic component drag estimation is defined as:

$$(C_{D0})_{subsonic} = \frac{\sum(C_f c^{FF_c} Q_c S_{wet,c})}{S_{ref}} + C_{D_{misc}} + C_{D_{L\&P}} \quad (6.1.1)$$

where the subscript “c” stands for component,  $C_{D_{misc}}$  is the miscellaneous drags (assumed to be negligible) from special features and the  $C_{D_{L\&P}}$  is the drag from leakages and protuberances (assumed to be 10% of the parasite drag).

The flat-plate skin-friction coefficient used in the subsonic parasite drag equation depends on the Reynolds number, Mach number, and the skin roughness of each component. The laminar equation used is defined as:

$$C_f = \frac{1.328}{\sqrt{R}} \quad (6.1.2)$$

and the turbulent equation is defined as:

$$C_f = \frac{0.455}{(\log_{10} R)^{2.58}(1+0.144M^2)^{0.65}} \quad (6.1.3)$$

The initial laminar and turbulent skin friction coefficients plots can be seen in Figure 6.1.1.

Final Report  
Supersonic Business Jet Design Team

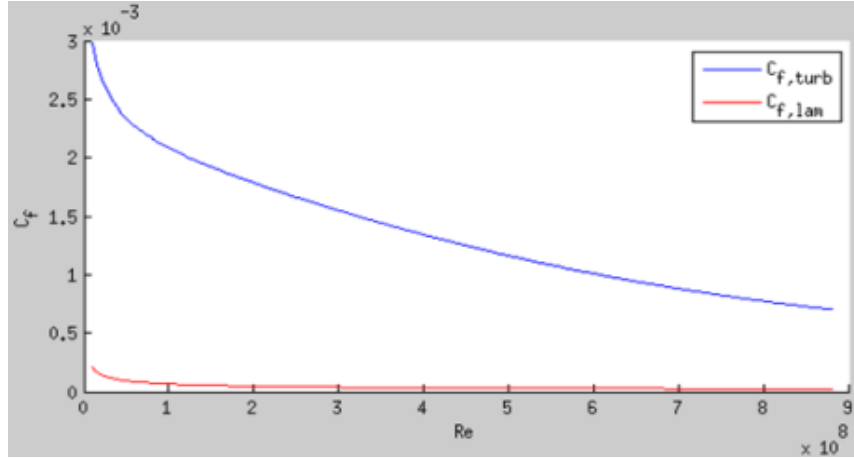


**Figure 6.1.1:** Laminar and Turbulent Skin Friction Plots

As one can see, the calculated laminar skin-friction coefficient is relatively small compared to known values (Raymer). The calculated turbulent skin-friction coefficient was closer to expected values and was thus used in the following calculations.

For the initial calculation of the component form factors, the following equations were used:

$$FF_{wing,tail,strut} = \left[ 1 + \frac{0.6}{(x/c)_m} \frac{t}{c} + 100 \left( \frac{t}{c} \right)^4 \right] [1.34M^{0.18}(\cos\Lambda_m)^{0.28}] \quad (6.1.4)$$

$$FF_{fuselage} = \left( 1 + \frac{60}{f^3} + \frac{f}{400} \right) \quad (6.1.5)$$

$$f = \frac{l}{\sqrt{\frac{4}{\pi} A_{max}}} \quad (6.1.6)$$

The supersonic parasite drag was calculated in a similar fashion to the subsonic component build up method. It is defined in the following equation.

$$C_{D0\,supersonic} = \frac{\sum(C_{fc}S_{wet,c})}{S_{ref}} + C_{D_{misc}} + C_{D_{L\&P}} + C_{D_{wave}} \quad (6.1.7)$$

Notice FF and Q are assumed to be 1. Also notice the new wave drag term. This accounts for the pressure drag due to the shock formation in supersonic speeds. The supersonic parasite drag was estimated using a supersonic area rule code (Ref 43, Raymer) similar to

Final Report  
*Supersonic Business Jet Design Team*

the classic Harris wave drag code. The initial transonic drag was estimated for the Mach regime between 0.8 and 1.2. The drag rise that occurs in that regime was solved empirically (Ref 37, Raymer).

The first parasite drag buildup estimation can be seen in Figure 6.1.2 as a function of Mach number. It consists of the parasite drag for subsonic, transonic, and supersonic flight.

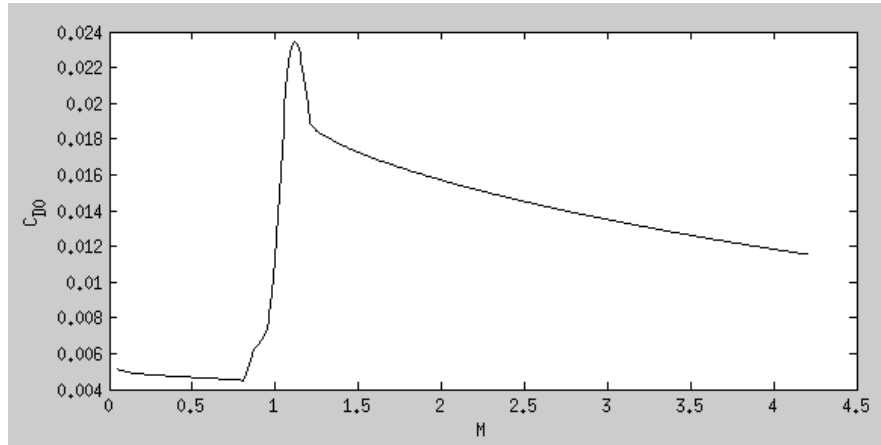


**Figure 6.1.2:** Parasite Drag Estimation

Again, the subsonic estimation includes the skin-friction drag with form factor and interference, as well as, miscellaneous and leak/protuberance drag. The supersonic estimation includes the supersonic flat-plate skin-friction drag, miscellaneous and leak/protuberance drag, and wave drag. Notice there is a difference between subsonic and supersonic skin-friction coefficient. The difference was calculated and plotted as a function of Mach number (Figure 6.1.3).

Final Report  
*Supersonic Business Jet Design Team*

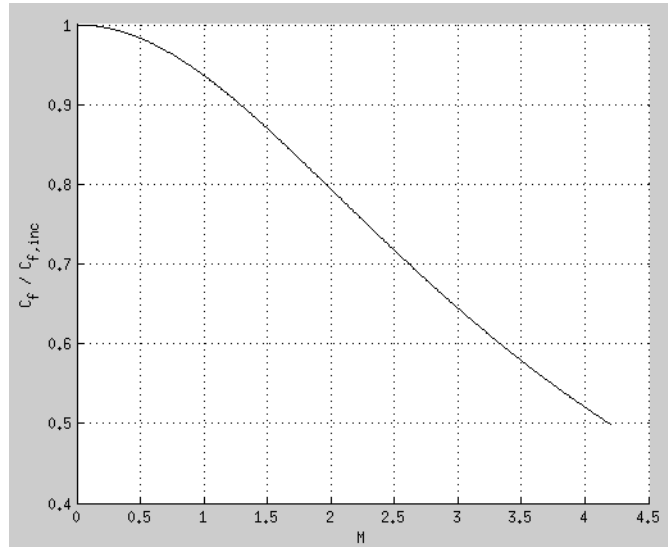


**Figure 6.1.3:** Skin Friction versus Mach Number

The difference in compressible and incompressible skin coefficient was approximately 3% around a Mach number of 0.5. As the Mach number increases, the difference between the compressible and incompressible values increases.

## 6.2. FRICTION Code

The first drag estimation was an order of magnitude too large at supersonic speeds. The team's drag code was verified with Dr. Mason's FRICTION drag calculation code and the initial sizing dimensions were reviewed. The value used for the fuselage area was quite large so the component drag estimation was reexamined. The team decided it was necessary to decrease the area of the fuselage. The new input was put into FRICTION and the new drag estimation is now comparable to the F-15's drag output. A wave drag code was added to the FRICTION coding which was then integrated into the MDA code. The resulting drag estimation is seen in Figure 6.2.1.

Final Report  
*Supersonic Business Jet Design Team*

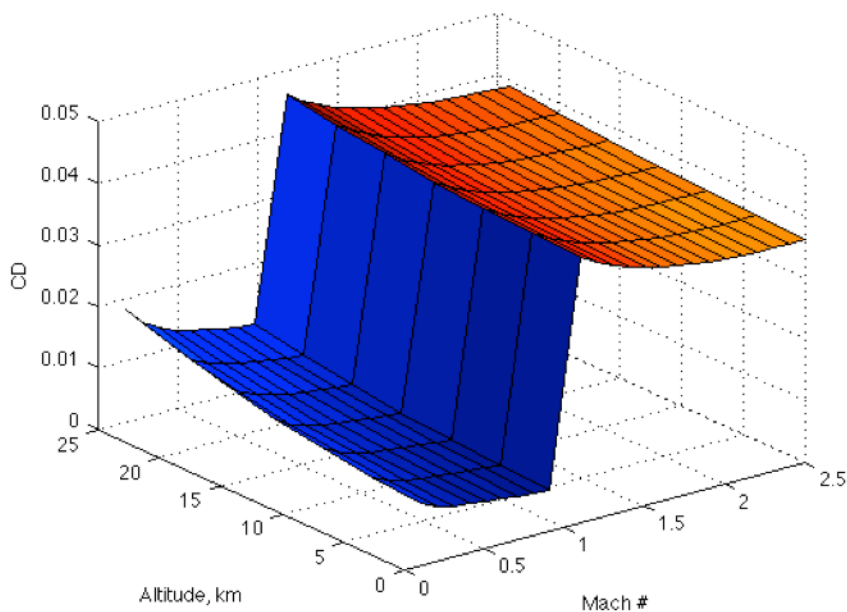


**Figure 6.2.1:**  $CD_0$  as a function of Altitude and Mach

The output from the FRICTION code yields  $CD,0$  values in the expected ranges for both subsonic and supersonic flight. This was further compared through a simple model of an F-15. The FRICTION code yields a “best case” drag coefficient for different flight speeds and altitudes, but provides little in the way of interference and protuberance drags.

### 6.3. CFD Drag Calculations

To account for the limitations in the simple FRICTION models, a three-dimensional model of the (near-final) vehicle design was meshed and then run through Cart3D – a computational fluid dynamics (CFD) simulation software package. These calculations were performed at NASA Langley, as described in the Aerodynamics section of this report.

The 3D model subsonic drag predictions were slightly lower than the FRICTION code would suggest (at sea level, and  $M=0.85$ ), by 2 drag counts. The drag code was updated to reflect these changes by artificially decreasing the FRICTION subsonic drag coefficient by one drag count (median value). For the supersonic  $CD,0$ , the drag coefficient was significantly lower (at sea level,  $M=2.2$ ) than predicted by FRICTION. Since the

Final Report  
*Supersonic Business Jet Design Team*

FRICTION drag predictions are in line with the F-15, and fall under expected ranges, the FRICTION predictions were taken to be more accurate than the Cart3D predictions. This was decided since our aerodynamicist could not independently verify the flow conditions fed into Cart3D, and since designing for the worse of two supersonic drag predictions errs on the side of being worse than actual.

#### **6.4. Induced Drag**

The induced drag coefficient at moderate angles of attack is the square of the lift coefficient multiplied by the induced drag factor, or K. Since the lift coefficient is already known throughout the flight, the value of K needs to be determined. The method used to determine the value of K is the Oswald span efficiency method as described in Raymer.

In order to find K, we consider the following equation:

$$K = \frac{1}{\pi A e} \quad (6.4.1)$$

Since the geometry of the vehicle and the aspect ratio,  $A$ , is known, we only need to determine the Oswald span efficiency factor,  $e$ . This value accounts for the extra drag due to a non-elliptical lift distribution and flow separation. The follow equation provides an estimate for  $e$  based on data from actual swept-wing (leading edge sweep > 30 deg) aircraft:

$$e = 4.61(1 - 0.045A^{0.68})(\cos\Lambda_{LE})^{0.15} - 3.1 \quad (6.4.2)$$

This equation, however, is only valid for aircraft traveling subsonically. At supersonic speeds, the induced drag factor increases significantly. The following equation provides a quick estimate of K at supersonic speeds:

$$K = \frac{A(M^2-1)\cos\Lambda_{LE}}{(4A\sqrt{M^2-1})-2} \quad (6.4.3)$$

Final Report  
*Supersonic Business Jet Design Team*

However, the leading edge suction described in Raymer provides is preferred to the above equation. The leading edge suction method includes changes in the value of K due to variations in lift coefficient during supersonic flight and provides a better estimate. However, due to time constraints on the aerodynamics analysis, this method was not incorporated into the design project.

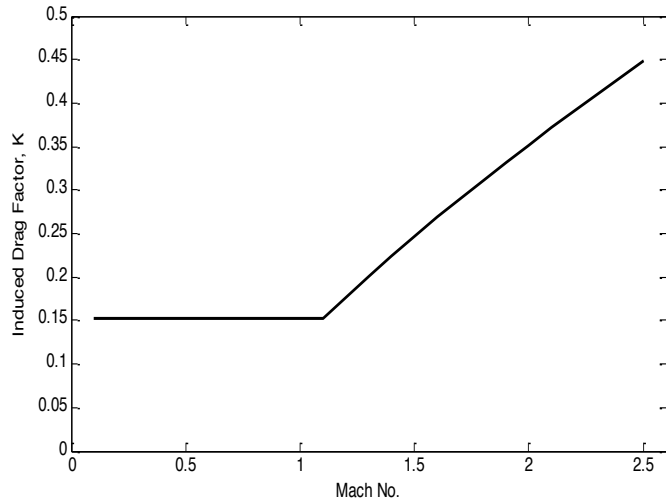


**Figure 6.4.1:** Estimated induced drag factor versus Mach number with a leading edge sweep of 45 degrees.

The above figure shows the estimated induced drag factor of the current supersonic business jet design using the equations described above.

## 7. PROPULSION

### 7.1. Initial Research

At the onset of the design process, since the target production date was at least two decades in the future, any and all advanced concept designs were considered for use in the supersonic business jet (SBJ). Due to this fact, at first many conventional designs such as the turbojet and turbofan were not given serious consideration. More time was spent researching types of propulsion systems such as pulse detonation engines (PDE), supersonic propeller configurations, propfans, and electrically-powered jet engines. Eventually and for various reasons each of these was thrown out in favor of a conventional turbofan. At various points later in the design process, after a general turbofan design had been selected, some modifications were proposed to enhance fuel savings or thrust but for reasons of simplicity development of these were terminated.

PDEs initially looked the promising because of the enhanced fuel savings they could offer, in theory. The PDE is similar to pulse jet engine, which mixes fuel and air in a chamber which is then ignited. The resulting combustion increases pressure and produces usable thrust via a nozzle at the rear. The combustion chamber must be refilled with the fuel-air mixture after each combustion, hence the ‘pulse’ aspect of operation. One benefit of this is that there are fewer moving parts than the jet engines in use today. Compressors, turbines, and spools are not needed, thereby reducing weight and cost of the overall system. Care must be taken in the implementation of the valves that control the flow of air and fuel to ensure that thrust is actually directed is a useful direction, and that combustion is not allowed to advance to the fuel supply (Kailasanath).

The difference between the pulse jet and PDE is that instead of subsonic combustion, supersonic detonation is used to increase the pressure. The effect is that instead of a ‘burn’ there is more of an explosion. Because of the rapidity of the process, more of the fuel is consumed within the detonation chamber; by contrast, with a pulse jet the burn process takes longer, so that some fuel may still be burning after it has left the nozzle. Obviously this means that the energy stored in the fuel is lost as exhaust. A further

Final Report  
*Supersonic Business Jet Design Team*

limitation of the pulse jet is that it is limited to approximately 250 cycles per second (Hertz), because of the length of time needed for fuel to burn. In the PDE this process takes place at supersonic speeds, allowing up to several thousand Hertz, in theory. This would eliminate the excessive vibration found on a pulse jet, since the PDE operates in essentially a continuous manner (the V-1 flying bomb used by the Germans in World War 2 was outfitted with a pulse jet engine; it earned its nickname “the buzzbomb” from the loud operation of the engine). The volume of gas required for each detonation would also be far less than for combustion, since many more detonations are possible (Mindling).

Despite all of these perceived benefits the propulsion team could not choose to use a PDE in good faith because the technology has not been proven on a scale that is needed. Some test bed PDEs have been successfully operated, and a small PDE was installed in a modified Rutan Long-EZ (2 person home-built aircraft) but only successfully operated for about 10 seconds (Barr). Materials technologies have also not advanced to a point where a suitably efficient PDE could be made: the temperatures inside the detonation chamber are too high for current composites and the wear due to the violent nature of detonations requires that components be extremely robust (Kailasanath). Furthermore, the detonations produced would be quite loud, virtually eliminating the PDE as an option for a commercial aircraft.

Another, briefly considered, propulsion system was the Supersonic-Magnetic Advanced Generation Jet Electric Turbine (S-MAGJET) which was announced in conjunction with the HyperMach SonicStar supersonic business jet in 2011. This S-MAGJET is a variable-bypass ratio turbofan with counter-rotating compressor fan blades. Both the fan and turbine are to be held in place magnetically, without the use of a central axle. The five-stage superconducting turbine is said to produce all the electrical power needed to drive the bypass fan, which generates the majority of thrust, and power all onboard electrical systems. Decoupling the turbine, compressor, and fan efficiency “...raises overall efficiency of the engine by 70%...” (Rousset). The SonicStar is meant to fly at Mach 3.3 with specific fuel consumption under 1.05.

The information presented in the previous paragraph is virtually all that is available for the S-MAGJET. While it would have been convenient to choose this concept and move on, the team had considerable doubts. Chief among these doubts was the use of

Final Report  
*Supersonic Business Jet Design Team*

superconducting technology, which thus far has only been used in the field of medical imaging, microscopy, and some magnetometers (Eck).

Certain reports on the subject of supersonic flight came to the conclusion that if such a design were to be economically viable the efficiency would be far and above anything produced as of late. A Royal Aeronautical Society report on future supersonic transports concluded that an ideal engine could either be low bypass turbojet or turbofan, but either way would need to be variable cycle (Lowrie). The propulsion system must be able to operate efficiently at takeoff and cruise. The propulsion system necessary for a successful SBJ undoubtedly relies on technologies that have yet to be developed. With this in mind the propulsion group sought to embrace a traditional and proven engine technology and then apply a “future factor,” such as enhanced efficiencies and better materials, to produce the required engine.

The first step in this was to compile a database of all engines used in supersonic aircraft since the Concorde. One immediate issue with this was that all of aircraft that fit this criterion were military, usually of the attack or fighter variety. Military aircraft are not subject to the same efficiency, emission, or noise standards that commercial aircraft are. With regard to the noise restriction, for a time the group was operating under the assumption that this SBJ would obtain an exception from the Federal Aviation Administration and European Aviation Safety Administration to allow either unrestricted “noisy” operation (supersonic, potentially with an afterburner in use) or allow it in certain pre-determined corridors. When flying over open water sonic boom and jet noise may be unrestricted. Most of the design work to improve the engine was to be in the areas of increasing efficiency and reducing greenhouse gases, such as NO<sub>x</sub> emissions.

Another technological advancement to be incorporated into the engine is a prognostics and health monitoring (PHM) system. This will take the form of a computer dedicated to continually monitor the engines performance and making small adjustments, as necessary, to squeeze every last bit of performance out of it. Recall that the Concorde had the most fuel efficient propulsion system ever implemented on an aircraft; a successful SBJ will have to match, if not surpass, that performance.

The PHM system will also be able to identify and diagnose many issues within the engine, thereby reducing the amount of time it takes for support staff on the ground to

Final Report  
*Supersonic Business Jet Design Team*

perform maintenance. For some parts that are easily replaceable the PHM can “call ahead” to maintenance crews to alert them of service that needs to be performed once the plane has landed. This will minimize the costs associated with ground crews and also maximize the amount of time that the engine is in service. This type of technology is featured in the Pratt & Whitney F-135 engine, which is used in the F-35 Joint Strike Fighter (“Proven”).

After completing the database of supersonic-capable engine platforms a choice had to be made. The F-135 engine was seriously considered but eventually the propulsion group decided it was not an option due to its size and the lack of concrete information about it. The much-older GE F110 engine was chosen in the interim because it provided thrust appropriate to the two engine configuration of the SBJ and there was enough publicly available information. Some of the more salient points are compiled in Table 7.1.1; data for the F118 (non-afterburning variant) is included, as this was the final design choice; the decision is discussed below. The proposed, improved engine would be known as the F110 Civil Derivative Engine (CDE).

**Table 7.1.1:** Design and performance statistics of the GE F110-132 and F118-100.

	F110-132	F118-100
Type	Two-shaft augmented turbofan	Unaugmented two-shaft turbofan
Fan	Three stages. Solid titanium rotor blades. Mass flow (limited by F-16 inlet) 275.6 lb/s. Bypass ratio 0.68.	Similar to F110, reduced number of blades, exceptionally wide chord. Bleed air de-icing. Bypass ratio 0.87.
Compressor	Nine stages. Overall pressure ratio 33.3.	Nine stages, virtually identical to F110. Overall pressure ratio 35.1.
Combustor	Annular, scroll type, multiple air stream burners.	Based on F110, modified for minimum emissions.
HP Turbine	Single stage with air-cooled rotor blades carried in large flat disc.	Similar to F110, air-cooled single crystal rotor blades.
LP Turbine	Two stages with rotor blades carried in rings driving via conical disc.	Two stages, modified from F110.
Fan Duct	Integrally ribbed metal, split into upper/lower halves.	
Afterburner	High-intensity, with one ring of multiple radial spray tubes in core airflow upstream of two flameholder gutters, plus one ring of nozzles upstream of a gutter in the bypass flow.	None.
Jetpipe	None	Details classified. In B-2A jets are cooled by mixing with a

Final Report  
*Supersonic Business Jet Design Team*

		secondary airflow, and appear to emerge across areas of black carbon composite.
Nozzle	Hydraulically actuated mult flap type with inner petals forming convergent/divergent profile when fully open.	None
Length	181.9 inches	100.5 inches
Overall Diameter	46.5 inches	46.5 inches
Weight	4,050 lb	3,200 lb
Thrust, Dry (Sea Level, Static)	19,100 lb st	19,000 lb st
Thrust, Augmented	32,000 lb st	-
Specific Fuel Consumption, Dry	0.64 lb/h/lb st	0.670 lb/h/lb st
Specific Fuel Consumption, Augmented	2.09 lb/h/lb st	-

Although both of the above-mentioned engine technologies are somewhat dated they are still widely used in many US-produced aircraft. The F110 was derived from the F101, which saw service in the B-1B Lancer. A derivative engine program was started to merge the technologies of the F101 with the F404 (powered the F/A-18A/B/C/D and F-20A). When the F110 was finally available it was installed in F-16C/D/E/F/N variants, F-14B/D, and F-15E/K. GE Aviation does not hesitate to state that, just accounting for engines in the F-16, it is, "the safest single-engine power plant in its class in air force history." Indeed, by 1996 it had accumulated over two million flight hours across 1,600 F-16s. Furthermore, the non-afterburning variant, F118 is installed in the B-2A and U-2S. Clearly this is a proven-in-the-field engine with millions of flight experience across a variety of platforms (Gunston). This is a key factor influencing the decision to use it as the power plant in the SBJ.

## 7.2. Diffuser Cone

The propulsion system Lockheed SR-71 (known as A-12 during development) was also studied from a very early stage in design process. It was appealing for two main reasons: it was one of the only other aircraft produced that could maintain flight speeds at high Mach numbers and it relied on a propulsion-airframe integration that was, at the time, similar to the SBJ. If group had decided to mount the engines underneath the airframe then

Final Report  
*Supersonic Business Jet Design Team*

a system of ramps very similar to the Concorde would have been a feasible method of generating good compression ratios at supersonic speeds. However due to the size of the SBJ this would unduly increase the length and weight of the landing gear and may also have a detrimental impact on the ease of servicing the aircraft. The engines for the SBJ were to be mounted above the wings, towards the rear of the craft and they were not to be integrated to the degree the Concorde's engines were. Engine nacelles shaped as a body of revolution became necessary but this allowed the group to look at introducing Mach cones as they were used on the SR-71.

The ramp system on the Concorde is, at its core, a two-dimensional flow. When using a Mach cone, however, the flow is diverted in all directions around the body of revolution. The normal two-dimensional compressible flow equations do not apply; instead the flow must be modeled using the Taylor-Maccoll differential equation, denoted below Equation 7.2.1:

$$\frac{\gamma - 1}{2} \left[ V_{max}^2 - V_r^2 - \left( \frac{dV_r}{d\theta} \right)^2 \right] \left[ 2V_r + \frac{dV_r}{d\theta} \cot \theta + \frac{d^2V_r}{d\theta^2} \right] - \frac{dV_r}{d\theta} \left[ V_r \frac{dV_r}{d\theta} + \frac{dV_r}{d\theta} \left( \frac{d^2V_r}{d\theta^2} \right) \right] = 0 \quad (7.2.1)$$

Here,  $V_r$  is a function only of  $\theta$ . This necessitates either a time-consuming table look up from any standard compressible fluids text or the implementation of an ordinary differential equation solver. Luckily, Dr. Lassaline of Ryerson University has created several MATLAB functions that, when taken together, solve the Taylor-Maccoll. Given the desired shock angle and freestream Mach number the required cone angle and Mach number adjacent to the cone can be computed.

The Mach “spike” of the SR-71 is mounted on a hydraulically driven actuator that allows it to move forward or backwards through a range of 26° through its flight envelope. This is a necessity because of the large range of Mach numbers encountered in flight.

Final Report  
*Supersonic Business Jet Design Team*

### **7.3. Engine Development**

Once the GE F110 had been chosen the propulsion group had to determine how to improve upon its design to transform it into the CDE variant. Owing to the time constraints and the groups own inexperience in the field of aero engine design, it was decided that the most expeditious method would be to use equations from Hill & Peterson to model the thermodynamics of such an engine. Things such as component efficiencies would have to be estimated until the rudimentary model matched the known performance characteristics of the F110. With this type of analysis being relatively straightforward it was a trivial matter to use MATLAB to perform the calculations. This also enabled the propulsion group to use Ryerson's supersonic cone solver in conjunction with the engine model.

A drawback of using MATLAB is that it is too rudimentary. The group was interested in studying a variable cycle engine, like the SR-71, but this was outside the scope of the MATLAB codes that were developed. This limitation precluded the study of a variable cycle engine, as the previously-mentioned Royal Aeronautical study mandated. This setup would allow for higher efficiency and specific fuel consumption at the supersonic speeds of the mission profile. While analysis could be done on a turbofan and a ramjet separately, determining how and when the transition would occur was past the skill level of the propulsion group. Also, there was concern whether this engine would need an afterburner to overcome the transonic drag. If this was the case, an engine with a turbofan core, afterburner and ramjet could simply be too large to fit on the aircraft. This system would also be very heavy, and with the SBJ it would not be worth its weight. For these reasons, this initial design was decided against, and the team continued to research the basic F110.

Somewhat of a breakthrough occurred when Virginia Techs Assistant Professor Dr. Lowe offered a special study course in aero engine design (AOE 4984). The purpose of the course was to build upon the knowledge gained in Aerospace Propulsion Systems (AOE 4234) and also begin learning to use the Numerical Propulsion System Simulation (NPSS) software written by Wolverine Ventures. NPSS was the co-winner of the NASA Software of the Year Award for 2001 ("Software"). A learning edition of NPSS was made available; this edition does not offer the full capabilities of NPSS but allows aero engine modeling at a much higher fidelity than the rudimentary MATLAB model that the group had been using

Final Report  
*Supersonic Business Jet Design Team*

previously. Furthermore, because the development environment of NPSS is similar to MATLAB, it was not out the question to design a custom element representing the supersonic diffuser cone (Stauber).

Another beneficial aspect of the course in aero engine design is that it required individual final projects that directly related to the design of the SBJ. Since three members of the design group were enrolled, three different projects were started. One was to model the F110 and investigate improvements from improved component efficiencies and newer, thermally-resilient materials; another was to investigate the transformation of the F110 to a turboramjet design much like the SR-71; the third was to implement several bleed ports that would allow some air to flow directly from the compressor to the turbine (bypassing the primary burner) and also to power some of the electrical systems onboard.

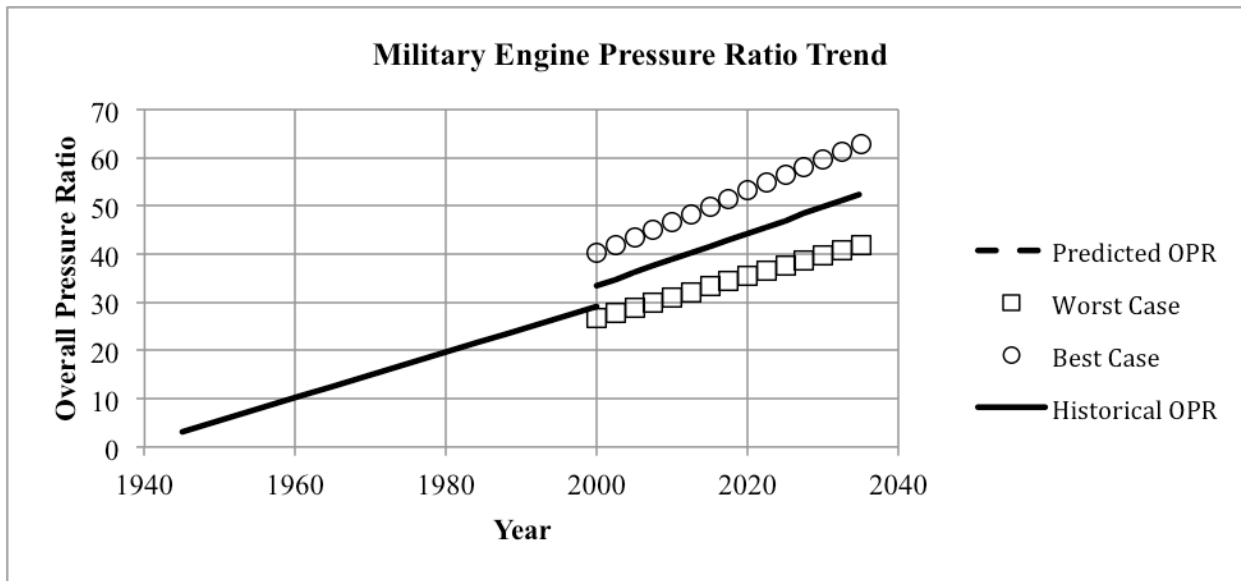


**Figure 7.3.1:** Historical data and future predictions for overall pressure ratio of military engines. "Fudge factor" of 15% applied; future data formed to include (estimated) performance of F135.

Before any of this analysis was completed figures such as thrust available, specific fuel consumption, and size and weight of the engine had to be delivered to the rest of the group so that design could continue. The compiled database of past military engines came in useful for this again. From this information historical trends in thrust to weight ratio, thrust per unit frontal area, and fuel consumption could be identified. The trends were then

Final Report  
*Supersonic Business Jet Design Team*

extended linearly 20 to 30 years in the future so that the entire group would have a solid idea of what the proposed engine would be capable of. An appropriate “fudge factor” was applied so that best and worst-case scenarios could be obtained; this way if the newly-designed engine did not perform as well as expected the rest of the design group would not be caught off guard. These data also acted a “gut check” of the new engines performance. Two of these trends, overall pressure ratio and thrust per unit frontal area for military engine, are shown in Figure 7.3.1 (above) and 7.3.2 (below), respectively. Note that the data of the trends does not include more recent engines, specifically the F135 (Gunston).

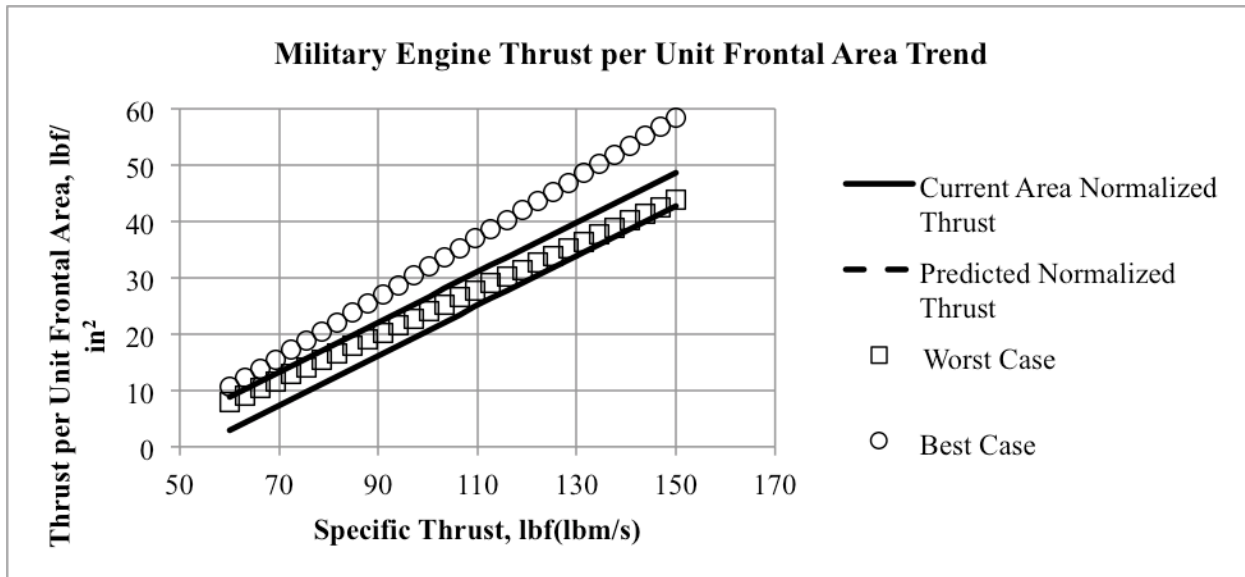


**Figure 7.3.2:** Current military thrust per unit frontal area data (as current as the year 2000) and expected future engines 20 years in the future. Fudge factor of 15% applied.

Running parallel to the engine design process was the refinement of aerodynamic models and weights estimations. Early on it was thought that the proposed F110-CDE would have to be larger and more powerful than the existing F110-132, delivering as much as 40,000 lbf with the augmenter enabled. By the Spring semester the size of the SBJ had been greatly reduced and the required thrust, per engine, was down to about 15,000 lbf. Not only did this eliminate the need for an augmenter but it also meant that a more compact and lighter engine would be acceptable. At this point in time a non-afterburning NPSS model of the F110 had been created, and so it was a trivial matter to change some of

Final Report  
*Supersonic Business Jet Design Team*

the specifications to transform it into the F118. Another convenient aspect of this change in engine is that the F118's combustor had been modified to reduce the exhaust emissions, and the elimination of the afterburner enhances the appeal of the engine with respect to jet noise near airports.

Using the powerful solver methods within NPSS the group was able to create a two-spool turbofan model that matched all the specifications (that were available) to the GE F118. The solver was then able to vary other, unknown aspects of the engine to achieve the known performance. Efficiencies for all compressors and turbines were initially kept at the default values of 85%. To transform the model into the CDE variant, component efficiencies were increased by a modest amount, mass flow of air was decreased, and maximum turbine inlet temperature was increased. These changes reflect expected technological advances in materials and computer-aided design methodologies. The resulting engine, due to the increase in efficiency, is able to generate the requisite amount of thrust while maintaining considerably lower internal temperatures. As a result, the material constraints of the turbine blades may be lower. As a factor of safety, however, the turbine blade materials are the same as the original F118 so that in an engine-out scenario the specific fuel consumption may be increased by about 40% to generate the necessary thrust to keep the aircraft aloft. Table 7.3.3 highlights some of the improvements of the F118-CDE over its military counter-part.

**Table 7.3.3:** Comparison of physical and performance characteristics of F118-100 and F118-CDE. *Estimated values are denoted with asterisk.*

	F118-100	F118-CDE
Weight	3,200 lb	3,000* lb
Length	100.5 in	130* in
Diameter	46.5 in	35* in
Thrust, Takeoff, Sea Level	19,000 lb	11,500 lb
Specific Thrust	4,090 ft/sec	3,030 ft/sec
SFC	0.67 lbm/(hr*lb)	0.50 lbm/(hr*lb)
Air Mass Flow	280 lbm/sec (found with NPSS)	227 lbm/sec
Maximum Turbine	3,210 °R	3,690 °R

Final Report  
Supersonic Business Jet Design Team

Inlet Temperature		
Overall Pressure Ratio	35.1	44.4

Estimated values are denoted with an asterisk. As much as possible, these estimates are correlated to historical trends in engine sizes. To achieve the performance level of the CDE component efficiencies were improved between 4% and 8%. Overall pressure ratio at takeoff has improved by more than 25% and this does not account for the supersonic cone diffuser that will be in effect at cruise conditions. This pressure ratio could be considerably higher if one looks at the trends in Figure 7.2. The maximum turbine inlet temperature was also increased by 15% although the inlet temperature is still less than 2000 Rankine for the performance values quoted in Table 7.3.3. Figure 7.3.4, below, shows the temperature and relative entropy across various stages of both engines.

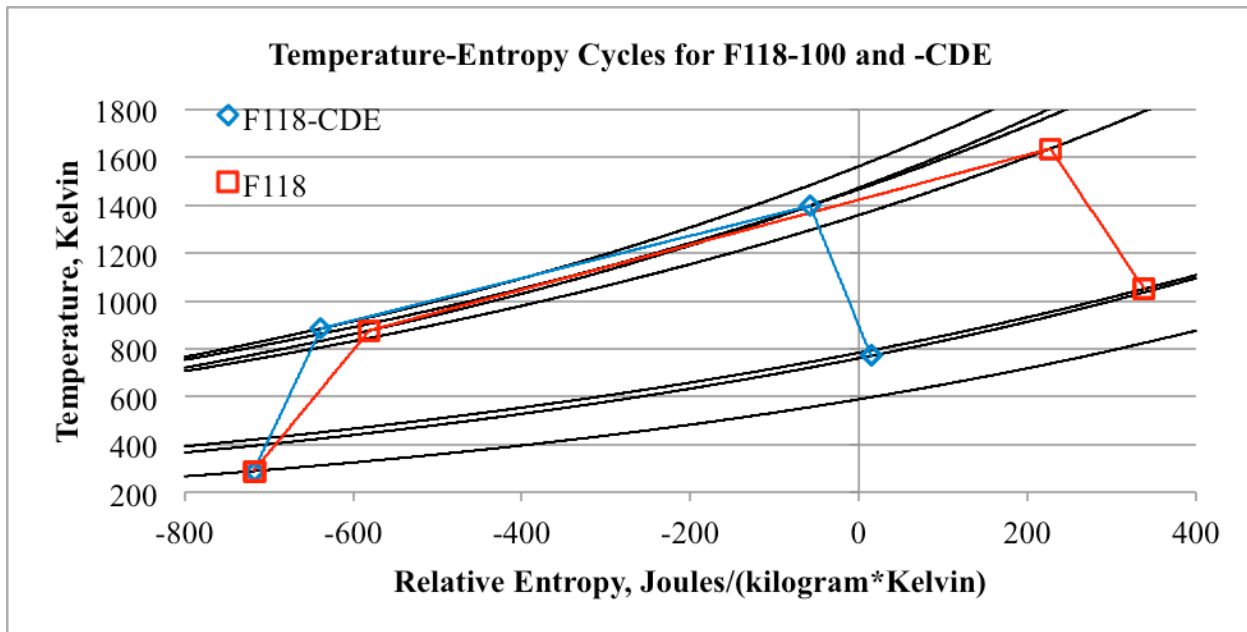


**Figure 7.3.4:** Temperature-entropy cycles for F118-100 and -CDE engines. Red square is -100, blue diamond is -CDE, curved lines are isobars.

At takeoff conditions the performance improvements of the CDE are highly visible: turbine inlet temperature is much lower, process efficiencies are better, and the overall entropy

Final Report  
*Supersonic Business Jet Design Team*

change is much less. The curved lines represent isobars at the pressure for each stage in the engine.

With the size of the powerplant determined, the supersonic diffuser cone could be designed. The SR-71 used a “spike” with a cone half-angle of approximately  $25^\circ$  (determined from photographs). The F118-CDE will be fitted with a cone of similar half-angle,  $20^\circ$ . When the SBJ is travelling at cruise condition of Mach 2.2, the air speed sensed by the engines will be Mach 1.9 due to the shock formed at the front of the aircraft. A diffuser cone with this angle allows a compression ratio of 3.6 before the flow even enters the engine, allowing for an overall compression ratio of over 120, assuming relatively constant efficiencies of fan and high pressure compressors. The Mach number after this oblique shock will be 1.49; once this turned flow interacts with and reflects off of the inlet wall it will terminate with a normal shock. The benefits of this additional compression are mitigated by the increase in flow stagnation temperature. This temperature rise is acceptable, however, due to the margin of safety at the turbine inlet.

During the acceleration from subsonic to supersonic cruise the diffuser cone will need to be adjusted by 12 inches. This will be accomplished by a hydraulic piston powered by bleed air from the engine. This air bleed will also power some engine accessories and other electronics onboard the SBJ.

An added feature of the lower operating temperature of the combustor is that the possibility of dissociation of exhaust particles is greatly lowered (Hill). The direct effect of this is a reduction in NOx emissions, which are detrimental to the atmosphere. The Federal Aviation Administration (FAA), European Aviation Safety Agency (EASA), and International Civil Aviation Organization (ICAO) have published goals on the reduction of NOx emissions. Most of these goals are very aggressive in their timetables, meaning that an aircraft coming into service 20 years from now will be subject to quite stringent regulations (European, Holsclaw).

## 8. STRUCTURAL ANALYSIS

### 8.1. Structural Configuration Design

The primary goals surrounding the structural design of the aircraft is most importantly an analysis, which identifies wing-tip deflection and maximum internal stresses. Secondly some conceptual layout of the load-bearing elements for each major component is produced. These results must be presented for several materials, which are chosen to minimize weight and cost as well as take into account environmental and servicing conditions.

The wing is the primary load-bearing component of the aircraft. Much information concerning turning performance and structural weight is gained from exclusive analysis of the wing. Thus the most emphasis is placed on this element. However other lifting surfaces are also analyzed.

Research into successful airframe designs reveals that typical structures for supersonic airfoils consist of multiple spar elements joined by ribs at several locations along the span. Figure 8.1.1 shows a cutaway view of the Concorde delta-wing structure. This serves as an extreme example of the use of multiple spars. This layout is generally required for wings with supersonic airfoils, which for aerodynamic reasons must have characteristically low thickness-to-chord ratios. The pressure load which integrates to become the lift force has a large moment arm about any single point along the chord. Thus an uneven pressure loading over the top and bottom surfaces generates force couples about a single spar which tend to distort the airfoil shape, an effect which is not desired. By placing multiple spar elements in the wing the maximum moment arms for the pressure force couples are reduced to an acceptable level, as determined by numerical analysis of the wing.

Final Report  
*Supersonic Business Jet Design Team*

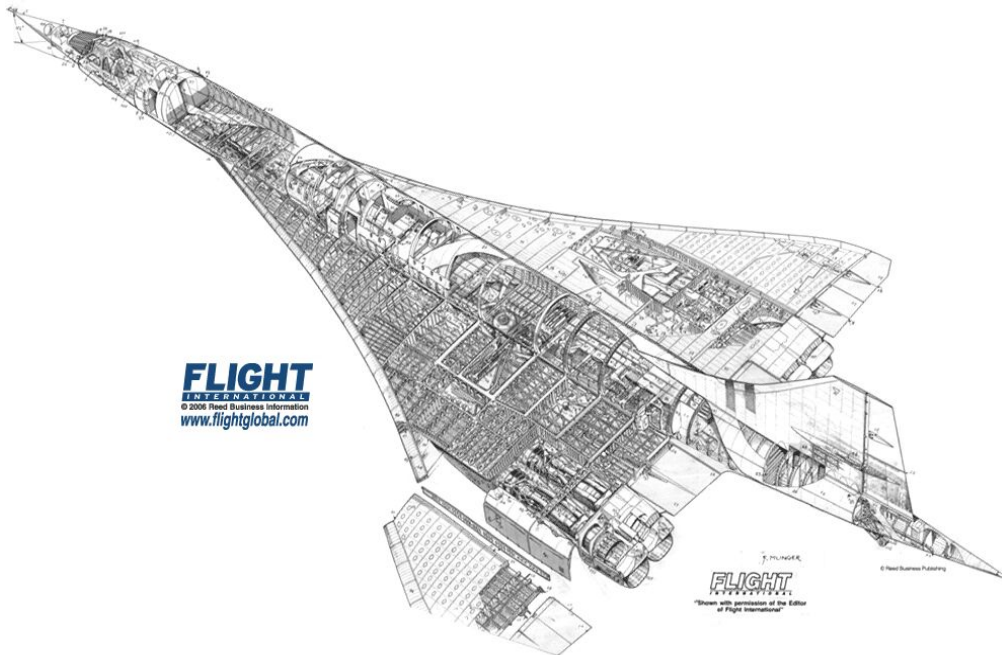


**Figure 8.1.1:** Cutaway view of the Concorde showing the structure for a wing with low thickness-to-chord ratio

## 8.2. Analysis: Intro

Given the specified structural configuration, a set of analysis procedures was selected. The primary goal of these calculations is to verify that a given structure provides the strength required by a set of aerodynamic loads. This has allowed designers to assess changes to aircraft geometry and the structural configuration.

During the first semester of the project, efforts were focused on producing first-order estimates of the internal stress and tip deflection of the wing. Once these values were calculated, work transitioned to a focus on the development of a variety of analysis procedures for the critical load-bearing elements. These procedures were codified and integrated into the multi-disciplinary optimization (MDO) framework.

Final Report  
*Supersonic Business Jet Design Team*

### 8.3. Analysis: Loading Conditions

The wing is the primary structural element which is intended to support the aircraft weight in flight. Thus it is imperative that the wing withstand the pressure loading in all flight scenarios which are expected to occur. Several key loading conditions were chosen to accurately represent the spectrum of aerodynamic loading conditions, and specifically to take into account the cases which were expected to limit sizing of important structural elements.

The V-N diagram in Figure 8.3.3 provides a visualization of the load factors in the context of performance expectations. The critical design load factors for the structure were found by applying a set of requirements and subsequently determining the structural support needed. Tables 8.3.1 and 8.3.2 show the collection of load factors considered. The most critical factors were chosen for the design and implemented into the analysis code.

**Table 8.3.1:** Load Factors assessed during structural configuration design

Method	Load Factor
Maximum bank angle	1.1547
Pull-up maneuver	0.0004
Push-down maneuver	-0.0002
Typical maneuver limit	2.5
Safe landing limit	3.1
Category System limits	3.8
	-1.52

**Table 8.3.2:** Load Factor Results

Load Factor	Final Value
Maximum positive	3.80
Minimum negative	-1.52

Final Report  
*Supersonic Business Jet Design Team*

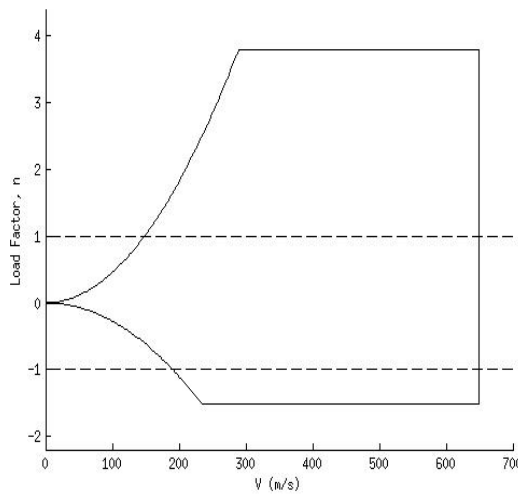


**Figure 8.3.3:** V-N diagram

The three loading conditions considered are takeoff conditions, subsonic cruise with one engine, and a maximum g-force pull-up maneuver. Maximum takeoff gross weight is used for both the takeoff and level flight conditions. The second loading condition ensures the ability of the vertical tail to support necessary lateral load. Lastly the max-g pull-up tests the structural integrity of all lifting surfaces.

The loads for all cases are modeled as elliptical. Figures 8.3.4 and 8.3.5 respectively show the distributed load concept and elliptic loading function. This first-order simplification allows for a reasonable approximation of all loading scenarios of interest in a timely manner, which has enabled efficient optimization.

Final Report  
*Supersonic Business Jet Design Team*

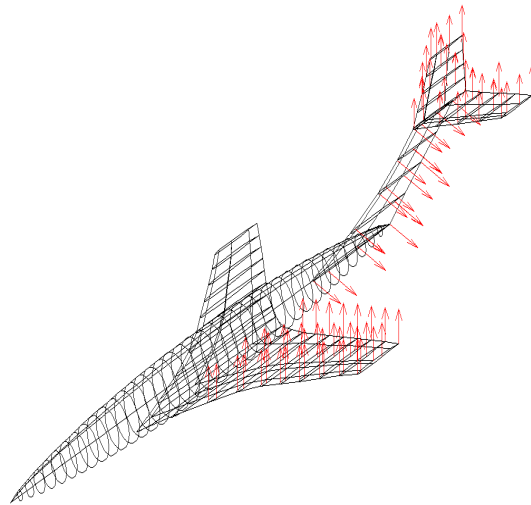


**Figure 8.3.4:** Generalized aerodynamic pressure loads applied to lifting surfaces.  
 (Screenshot at 2012-04-20 20:53:07)

$$f(y) = c \sqrt{1 - \left(\frac{y}{a}\right)^2}$$

$$a = b/2$$

$$c = \frac{4W}{\pi b}$$

**Equation 8.3.5:** Elliptic loading as a function of spanwise position. Units are Newtons per meter.

**Table 8.3.6:** Loading conditions for wing

<b>Loading Case</b>		<b>Integrated Normal Force (kN)</b>	<b>Constants</b>
1	Takeoff conditions	21.77	$a = 5.019 \text{ m}$ $c = 2.761 \text{ kN}$
2	Subsonic cruise with engine-out	21.77	$a = 5.019 \text{ m}$ $c = 2.761 \text{ kN}$
3	Max-g pullup	82.69	$a = 5.019 \text{ m}$ $c = 1.049 \text{ kN}$

**Table 8.3.7:** Loading conditions for the horizontal tail

<b>Loading Case</b>		<b>Integrated Normal Force (kN)</b>	<b>Constants</b>
1	Takeoff conditions	5.490	$a = 3.00 \text{ m}$ $c = 1.166 \text{ kN}$
2	Subsonic cruise with	5.490	$a = 3.00 \text{ m}$

Final Report  
*Supersonic Business Jet Design Team*

	engine-out		$c = 1.166 \text{ kN}$
3	Max-g pullup	20.88	$a = 3.00 \text{ m}$ $c = 4.432 \text{ kN}$

**Table 8.3.8:** Loading conditions for the vertical tail

<b>Loading Case</b>		<b>Integrated Normal Force (kN)</b>	<b>Loading Function</b>
1	Takeoff conditions	0	$a = 0 \text{ m}$ $b = 0 \text{ kN}$
2	Subsonic cruise with engine-out	11.160	$a = 4.00 \text{ m}$ $b = 1.776 \text{ kN}$
3	Max-g pullup	0	$a = 0 \text{ m}$ $b = 0 \text{ kN}$

## 8.4. Analysis: Stress Based Design

The limiting factor in stress-based design is the maximum internal (principal) stress encountered in each structural element. Allowing a structure to deform such that the stress approaches the material yield stress within a factor of safety provides a numerical fence for the weight-optimized structure. For an airworthy vehicle, this concept of weight optimization is key to success from both technical and economical points of view.

One additional consideration which ensures a realistic structure is a set of deformation limits. The wing, tail and fuselage are expected to retain their shape within some reasonable limit outlined in Table 8.4.1. These deflection limits in practice are rarely encountered by the structure, and are not strictly defined by the stress-based design procedure. However they do offer a simple numerical check that the structure performs in a qualitatively reasonable manner.

**Table 8.4.1:** Deflection limits for major structural components

<b>Component</b>	<b>Deformation Limit</b>
Wing	0.9 m at the wingtip
Horizontal Tail	0.2 m at the tip
Vertical Tail	0.1 m at the tip
Fuselage	0.2 m away from centerline, at all points

## **8.5. Analysis: Material Limits**

It is important to consider the materials that will be used for this aircraft, because it will not be produced for the next several decades. Current airplanes under construction have made wide use of composite materials, mainly due to their increased strength and time to failure when compared with regular metals. Previous airplanes have used a mixture of metals, such as aluminum, steel and titanium alloys to construct the fuselage, wings and tail. Over time, composite materials have been added to non-stress bearing parts, such as winglets and stabilizers. These composites are much lighter than their metal counterparts, making the switch an easy choice.

The drawback to composites and why they were not used on parts where critical loads are expected, is the fact that they do not show fatigue like metals do. As a result a normal inspection of cracks may not show when a composite is about to fail. After a number of years of using composites in this way, enough research had been done that companies believed composites could be utilized in more crucial roles in commercial aircraft. Taking a major leap with the new 787 Dreamliner, Boeing will be using composites as the main material for the fuselage and wings. This aircraft will be using advanced composites for 50% of the plane, with the remaining percentage made up of aluminum, titanium and steel. The steel is used mostly on the landing gear, as this is where the highest stresses will be encountered.

Using such a high percentage of composites has many advantages over conventional designs. The weight of the plane will be greatly reduced, and the maintenance cost should be lower as well. This assessment comes from the maintenance of the composite tail of the Boeing 777 as compared with the aluminum tail on the Boeing 767. While the composite tail is larger than its aluminum counterpart, it required less routine maintenance hours. The same held true for non-routine maintenance. Aluminum floor beams have long been used in Boeing aircrafts, but the 777 experimented using a composite floor beam. This also proved to be an immediate advantage, with none of these floor beams needing to be replaced in over 10 years of flights. The main source of non-routine maintenance for most

Final Report  
*Supersonic Business Jet Design Team*

aircrafts is due to the corrosion and fatigue of the metal. This will not be as big of an issue due to the high amounts of composites being used.

By the time the supersonic business jet is being produced, using composite materials may be the norm for all new aircraft. The data for the strength and weight of the specific composites used by Boeing is classified, but several studies have been performed which yield useful information about the practicality of the use of composite materials. Carbon fiber reinforced plastic (CFRP) is the main composite material that has been used for aerospace applications. The qualities of this material can vary greatly based on how it is manufactured, and can be altered for specific uses. Another possible future material is carbon nanotube reinforced plastic (CNRP). These carbon nanotubes are extremely strong and light, with some tests showing them to be 80 times stronger than high carbon steel while being six times lighter. The Lockheed Martin F-35 Lightning 2 is implementing carbon nanotube reinforced epoxy, which will be the first such use of this new material.

Due to the limited data, uncertainty and cost of these carbon nanotubes, the design vehicle will not be using them. Using CNRP does seem viable, however. Table 8.5.1 shows the material properties of aluminum, titanium, steel and carbon fiber. In order to do a rough cost estimate, approximate material prices were found. These prices would not be applicable on the scale of building an entire aircraft, but the ratio may be similar.

**Table 8.5.1:** Comparisons of Carbon Fiber with Common Metals

Material	Ultimate Tensile Strength (psi)	Yield Strength (psi)	Modulus of Elasticity (psi)	Density (lb/in <sup>3</sup> )	Price (\$/lb) *Estimate
6061 Aluminum Alloy	18000	8000	$10 \times 10^6$	0.0975	1.50
Titanium	50000	30000	$17 \times 10^6$	0.16	8
A36 Steel	58000	35000	$29 \times 10^6$	0.28	<1
Carbon Fiber	435000	200000	$29 \times 10^6$	0.065	16

As is evident from the data in Table 8.5.2, carbon fiber is the strongest material while also being the lightest. It would be easy to look at this table and simply choose carbon

**Final Report**  
*Supersonic Business Jet Design Team*

fiber as the material, but there are many other factors. The CFRP is not pure carbon fiber, but a plastic or polymer, often epoxy, which has been reinforced with this carbon fiber. CFRP is also extremely expensive, which is why current airplanes use a mixture of materials. While steel is strong enough for any applications, it is also very dense which would negatively impact the weight of the airplane. The aluminum alloy, being relatively cheap and low density, can be used places where the greatest forces will not be seen. Titanium is relatively light and strong, but it is rather expensive. This would be used to reduce cost somewhat, rather than using more CFRP. These materials were input into the MDA code to analyze what weight and cost impact they would have on the aircraft. It was expected that the material selection would be close to that of the Boeing 787 due to its futuristic yet economical design.

Several materials were considered for the aircraft structure. In the context of stress-based design the limiting factor is the maximum internal (principal) stress encountered in each element. As such the maximum internal stress is designed to match the allowable material stress and a measure of fitness is the percent error between the two.

Each material is prevalent in the aircraft industry, and each has benefits in terms of strength-to-weight ratio and cost. A tradeoff is needed in order to select the most appropriate material for each part of the structure. The factor of safety for the entire structure is taken to be 1.5.

**Table 8.5.2:** Material Properties

<i>Material</i>	<i>Yield Stress (MPa)</i>	<i>Maximum Stress in Tension (MPa)</i>	<i>Allowable Stress (MPa)</i>	<i>Modulus of Elasticity (GPa)</i>	<i>Poisson's Ratio</i>
1. Aluminum 6061-T6	276	310	218.5	68.9	0.33
2. Titanium Ti-6Al-4V	880	950	700	113.8	0.342
3. Titanium-Ti13V-11Cr-3Al	1140	1210	902.5	110	0.3
4. AISI 4130 Steel	435	670	344.4	205	0.29

Final Report  
*Supersonic Business Jet Design Team*

## 8.6. Wing

### *Stresses in Initial Configuration*

At the close of the first semester, a first-order estimation of the internal stresses and tip deflection of the wing was presented. Initially three wing sections were selected, containing 5, 4, and 3 spars in root-to-tip order. These numbers were chosen based on engineering intuition after examination of similar aircraft structures, and were intended to act as a starting point for further analysis.

The cross section contains rectangular wing spars, circular spar caps, and the aircraft skin. This model accounts for all major structural elements and is often used in shear flow and buckling analyses for other projects. Adaptation of simple beam bending for this cross section is also straightforward, and for first-order analysis requires cross section information to be represented compactly by the second moment of inertia, which is a scalar at a given spanwise location.

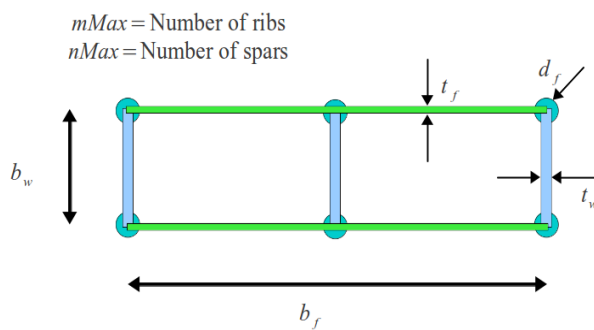


**Figure 8.6.1:** Wing box geometry specification

Exclusively one material, Aluminum 6061, was chosen for the structure. This material is the current industry standard for critical structural elements, with the exception of the steel main spar in most passenger airlines. Only one analysis procedure, which a matrix-based adaptation of technical beam theory, accounts for piecewise-varying moments of inertia.

Final Report  
*Supersonic Business Jet Design Team*

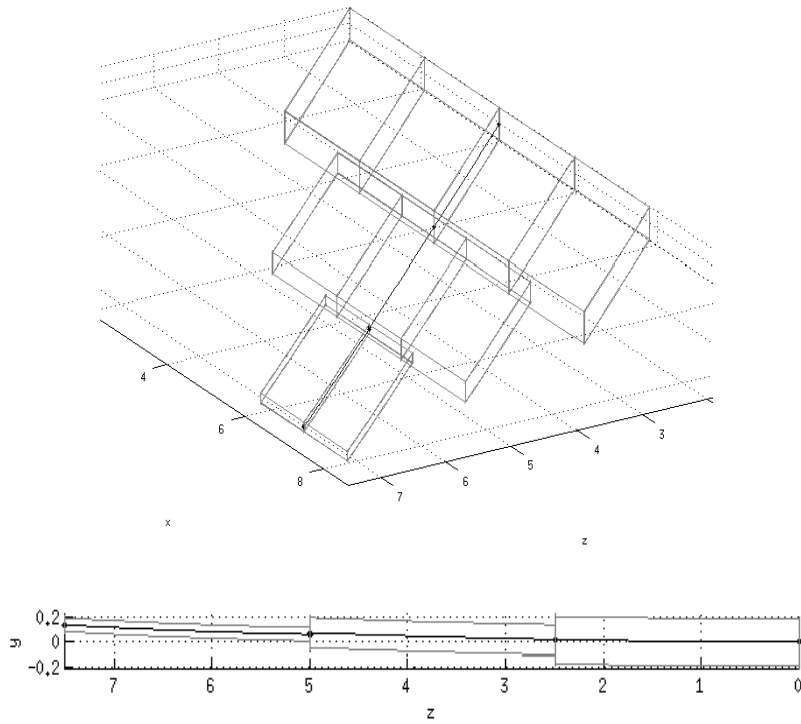


**Figure 8.6.2A/B:** Wing internal structure and wing tip deflection (includes sweep)

The maximum internal stress under an elliptic load occurs at the root. The value of this stress is tabulated for each loading condition in Table 8.6.3. These values are well within those specified by the material allowable stress in Table 8.5.2. Positive percent error indicates a within-bounds difference between the maximum design stress and maximum computed internal stress. Tip deflection is also provided, and does not exceed maximum value.

**Table 8.6.3:** Preliminary wing beam analysis results

Loading Case	Maximum Internal Stress (MPa)	% Error	Deflection (m)
1	22.01	283.9 (favorable)	0.0372
2	22.01	283.9	0.0372
3	83.6	74.7	0.1412

Final Report  
*Supersonic Business Jet Design Team*

Material strength limits are not exceeded, and deflection is within limits for all loading conditions. However the percent error indicates that this preliminary design is heavier than necessary for the design conditions.

*Stresses in Final Configuration*

The second semester design efforts have focused on two primary goals:

- . Improving the validity of calculations by introducing the thin plate analysis procedure.
- . Optimizing the structural configuration to reduce percent difference between allowable and computed stress.

## **8.7. Beam Bending Analysis**

Wings are typically designed in the industry to be supported by a “wing box,” which is a large hollow structure passing through the fuselage and extending into the wing. For purposes of simplified analysis the wing box is understood to compose the majority of the structure, and extends from wingtip to wingtip. This box should realistically take up as much cross-sectional area as possible to maximize structural efficiency. A first-order model allows for a rectangular cross section composed of spars joined by the aircraft skin (as shown in Figure 8.6.1).

One drawback to this approach is that some wasted space is permitted. Also this model is slightly unrealistic in the sense that the box is allowed to geometrically protrude through the skin of the aircraft. However the approximate location and size of all structural elements is maintained within reasonable limits which is acceptable in the context of configuration design with additional factors of safety used to account for this and other uncertainty.

Initially the beam analysis procedure was intended to be comprised of a coupled matrix structural analysis problem. However this method proved to be too tedious and

Final Report  
*Supersonic Business Jet Design Team*

resulted in an analysis, which contained more information than was necessary. A simplified beam model was developed which takes into account the piecewise-varying cross section.

Using the same approach as during the first semester, the wing box is treated as a composite beam composed of several beams with constant cross section. The governing equation for beam bending is a fourth-order, non-homogenous differential equation with one variable in one unknown. This model allows for planar deflection of a beam with a varying cross section, represented in Equation 8.7.1 by the term  $EI = EI(x)$ .

This equation may be solved by successive integration. By taking into account appropriate boundary conditions, the static deflection of the neutral axis at a continuum of points may be computed. It can be shown that the internal bending moment is proportional to the second derivative of deflection, and stress is proportional to the bending moment. Thus once deflection is determined, the maximum internal stress can be calculated. This is true of both beam bending and thin plate analyses.

$$\frac{d^2}{dz^2} \left( EI \frac{d^2 w}{dz^2} \right) = q(z)$$

**Equation 8.7.1:** Technical beam theory governing differential equation

$$\begin{aligned} \frac{d}{dz} \left( EI \frac{d^2 w}{dz^2} \right) &= \int q(z) dz + C_0 \\ EI \frac{d^2 w}{dz^2} &= \int \int q(z) dz dz + C_0 z + C_1 \\ EI \frac{dw}{dz} &= \int \int \int q(z) dz dz dz + \frac{1}{2} C_0 z^2 + C_1 z + C_2 \\ EI w(z) &= \int \int \int \int q(z) dz dz dz dz + \frac{1}{6} C_0 z^3 + \frac{1}{2} C_1 z^2 + C_2 z + C_3 \end{aligned}$$

**Equations 8.7.2:** Derivation of deflection curve equation

Final Report  
*Supersonic Business Jet Design Team*

$$Q(z) = \int \int \int q(z) dz dz dz$$

$$EI \begin{pmatrix} w_1(z) \\ w_2(z) \\ \vdots \\ w_m(z) \end{pmatrix} = Q(z) + \frac{1}{6} \begin{pmatrix} C_{0,1} \\ C_{0,2} \\ \vdots \\ C_{0,m} \end{pmatrix} z^3 + \frac{1}{2} \begin{pmatrix} C_{1,1} \\ C_{1,2} \\ \vdots \\ C_{1,m} \end{pmatrix} z^2 + \begin{pmatrix} C_{2,1} \\ C_{2,2} \\ \vdots \\ C_{2,m} \end{pmatrix} z + \begin{pmatrix} C_{3,1} \\ C_{3,2} \\ \vdots \\ C_{3,m} \end{pmatrix}$$

**Equation 8.7.3:** Deflection curve equations for m-component composite beam

Equations 8.7.2 shows how the beam deflection may be obtained from successive integration of the governing differential equation (GDE). This is performed for as many wing sections as necessary, as shown in Equation 8.7.3. Obtaining the coefficients may be transformed into a matrix equation, the solution of which gives the composite beam deflection.

$$M(z) = -EI \frac{d^2 w}{dz^2}$$

$$V(z) = -\frac{d}{dz} \left( EI \frac{d^2 w}{dz^2} \right)$$

$$\sigma_{zz}(z) = \frac{M_x y}{I_{xx}}$$

$$\sigma_{zz}(z) = \left( \frac{y}{I_{xx}} \right) EI_{xx} [w''(z)]$$

**Figure 8.7.4:** Important equations: Internal bending moment, internal shear force, & internal normal stress.

Final Report  
*Supersonic Business Jet Design Team*

## 8.8. Thin Plate Analysis

The wing being designed for the supersonic business jet is required to be thin for aerodynamic purposes. While beam bending analysis offers an estimate of the normal and shear stresses at the wing root, it uses a model that takes into account simplified physics. In reality the wing will both bend and twist, as well as warp in ways that cannot be addressed by the previous method. One readily applicable solution is known as thin plate analysis.

The governing differential equations of solid mechanics may be reduced under a set of assumptions that qualify a structure as a “thin plate.” These assumptions are:

1. Material follows Hooke's law
2. The plate is flat initially
3. The plate middle surface remains unstrained
4. Height is no greater than one tenth of the lateral plate dimensions
5. Out-of-plane deflection is small compared to lateral plate dimensions
6. Middle surface slopes are small
7. Plane sections remain plane during the deformation
8. Stress in the transverse direction is small

For a thin plate the governing differential equations reduce to one fourth-order, nonhomogeneous differential equation (referred to as a nonhomogeneous biharmonic equation). Solution in this case is more involved than for simpler techniques. Several analytical solutions exist, but only for plates whose boundary conditions involve at least three sides restrained from moving. For analysis of an aircraft wing the only available approaches which take into account the boundary correct conditions are numerical.

The finite element and finite volume methods offer the most exacting and adaptable results. However, their complexity and computation time prohibits implementation into structural analysis procedures within a realistic time frame. A better option is the finite difference method. This technique provides direct solution of an arbitrarily-shaped plate under a distributed load.

A discrete number of points are selected at which deflection will be calculated to occur. The primary setup of a matrix equation which can numerically solve the GDE

Final Report  
*Supersonic Business Jet Design Team*

involves the introduction of one equation for each unknown deflection value. The appropriate equation to use at each point is the GDE, which by definition must be solved at each point. The governing differential equation may be represented in terms of discrete values by a finite difference formulation. This can be easily derived by a truncated second-order Taylor series expansion in two variables about the point of interest. The GDE is represented by the discrete fourth derivatives set equal to the value of the distributed load at the point.

The governing differential equation represented by finite differences can be visualized with the help of an aid called the stencil. A set of points in the neighborhood of the point of interest are multiplied and set equal to the load at that point. The stencil graphically represents the finite difference expression by showing the multiplicative values in their appropriate location relative to a point under consideration.

Examples of stencils are shown in Figure 8.9.2. For points in the vicinity of a boundary additional information is needed. Equations which apply at the boundary can be used in conjunction with the GDE to mathematically eliminate points which are outside the region of interest.

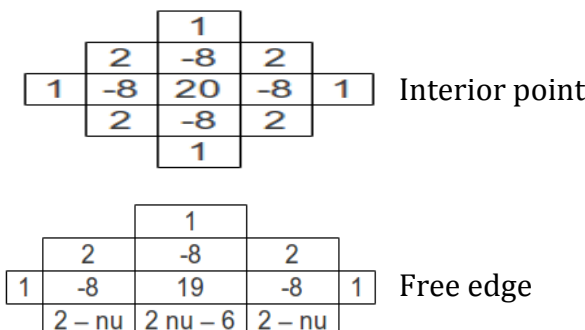


**Figure 8.9.2:** Finite difference stencils for various boundary conditions

Application of the finite difference stencils at all points in a region of interest constitute a closed algebraic system for these points. A solution of this system is possible by any inverse matrix or reduced Echelon form method. The steps taken in the finite difference implementation are therefore:

1. Create matrices which represent a rectangular plate that extends at least over the

Final Report  
*Supersonic Business Jet Design Team*

region of interest.

2. Specify the region of interest (ROI) as the interior points in a closed polygon (for example, the wing planform)
3. For each point in the ROI, add the finite difference expression values to the coefficient matrix
4. Remove points outside the ROI, resulting in a closed algebraic system containing only relevant information
5. Solve the system for the displacements at discrete points
6. Take discrete derivatives of solution as appropriate to obtain internal stress
7. Determine the largest absolute value of internal stress

A simple plate analysis procedure carried out for a rectangular flat plate is shown in Figure 8.9.3. Steps two through four are not relevant, since all points in the rectangle are considered. The boundary conditions applied to the plate are fixed around three sides and free on the negative x face.

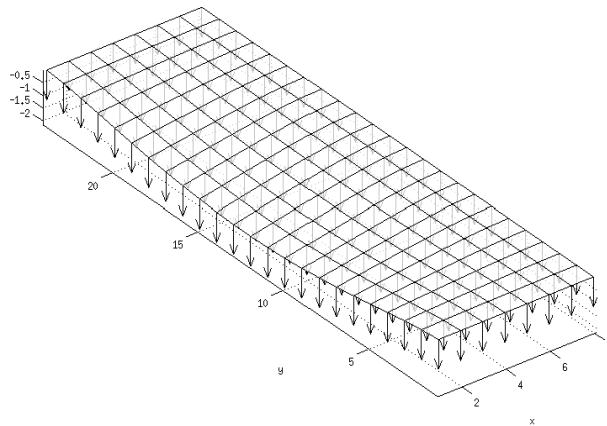


**Figure 8.9.3:** Results for a rectangular thin plate model subjected to uniform load

The method described above comprises a single-solution-step procedure for solving the deflection in an isotropic plate. Several steps are necessarily more complex for a material that is considered to be anisotropic. This is an important point for analysis of the aircraft lifting surfaces. The internal structure has been designed to be orthotropic.

Final Report  
*Supersonic Business Jet Design Team*

With the end goal of a weight-optimized structure in mind, resistance must be provided to aerodynamic loads in the direction opposite of their action. The vast majority of loading occurs normal to the plane of the lifting surface. Thus structurally the primary support is essentially a beam undergoing in-plane bending. Some resistance to out-of-plane deflections, known as warping, must be provided. In addition the aircraft skin must not encounter a load sufficient to induce excessive buckling.

Thus the need for a fundamentally orthotropic wing structure can be seen. With more resources and time it would be possible to model the wing and tail surfaces as orthotropic plates. However the procedure is sufficiently more involved than an isotropic analysis, and because only a first-order estimate of structural weight and internal stress are needed this is the method chosen.

Figure 8.9.3 shows a visualization which represents an approximation made to take into account the orthotropic nature of the plate. In isotropic plate analysis one scalar parameter contains information about the cross section's resistance to bending. This variable is termed *flexural rigidity*, and is defined for solid rectangular cross-sections in Figure N.

$$D = \frac{E h^3}{12(1-\nu^2)} \quad (\text{a}) \text{ Flexural rigidity, isotropic plate}$$

$$D^* \approx \frac{E_0 I^*}{1-\nu_a^2} \quad (\text{b}) \text{ Equivalent flexural rigidity, composite plate}$$

$$I^* \approx \int_{-h_2}^{h_1} \frac{E_k}{E_0} z^2 dz \quad (\text{c}) \text{ Equivalent area moment of inertia}$$

**Figure 8.9.4:** Flexural rigidity approximation

An approximation sometimes used for low-fidelity models in practice is to collapse information about a more complicated (anisotropic) cross section into the flexural rigidity. This has been done for composite materials and is adapted for the aircraft's partially

Final Report  
*Supersonic Business Jet Design Team*

hollow structure. The essential reasoning is that the relative widths of each cross-sectional layer can be related by scaling to their maximum value.

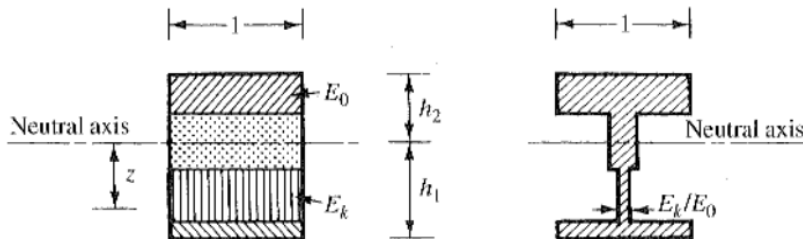


**Figure 8.9.5:** Engineering approximation used to compute equivalent isotropic plate parameter

## 8.9. Optimization

The above analysis procedures are intended to operate in conjunction to determine whether a given structure is within numerical limits. As explained in the “Stress-Based Design” section these limits are internal stress and tip deflection. These limits must not be exceeded by any analysis method for any loading condition.

In the context of a multi-disciplinary optimization process, structural analysis needs to provide an accurate weight estimation. Given a particular configuration and material, the structures code module needs to determine the minimum-volume structure that accomplishes the goals of keeping stress and deflection within limits.

With these goals in mind, a sub-optimizer was implemented into the structures portion of the MDO code. This sub-optimizer is allowed to vary three parameters – spar thickness, spar cap area, and skin thickness. Realistic limits were set on these values, and the sub-optimizer was assigned the task of determining values for these parameters which result in a minimum-weight structure.

The sub-optimizer calls an objective function. In this function, all analysis methods are executed for all loading conditions. Any failures are reported to the sub-optimizer in a way that causes automatic correction. This optimization structure is able to improve the design of the aircraft structure, which is a complicated task to perform analytically. In

Final Report  
*Supersonic Business Jet Design Team*

addition, numerical optimization is a robust technique which can handle new parameters and design limitations as they arise.

### **8.10. Configuration case study**

To test a variety of configurations a custom script was written. The set of configurations to be tested was saved as an array, and the structural sub-optimizer was run for each configuration. The number of ribs dictates the number of wing sections, and the number of spars in each section was varied around the initial values.

The goal of this study was to determine if significant improvements in strength-to-weight ratio could be obtained from a different configuration. In particular the variations in performance with changes in specific parameters without regard to material were of interest. Results are tabulated in Table 8.10.1.

**Table 8.10.1:** Configuration Case Study Results, Material 1

Number of Ribs	Number of Spars		Maximum Stress (Gpa)	% Error in Stress	Maximum Deflection (m)	Weight	Flange Area ( $m^2$ )	Web Thickness (m)	Skin Thickness (m)	0.0011
	Section 1 (Root)	Section 2								
3.0000	8.0000	6.0000	6.0000	0.5037	9.6281	0.7695	210.5600	5.4815e-05	0.0075	0.0011
3.0000	8.0000	6.0000	7.0000	0.5514	1.0598	0.8424	196.8600	5.4928e-05	0.0071	0.0010
3.0000	8.0000	7.0000	4.0000	0.5084	8.7827	0.7767	204.2100	5.4813e-05	0.0073	0.0011
3.0000	8.0000	7.0000	5.0000	0.5271	5.4245	0.8053	210.3500	5.5123e-05	0.0090	0.0010

Final Report  
*Supersonic Business Jet Design Team*

### 8.11. Materials Case Study

When making a selection of the material it was of interest to obtain data regarding the approximate strength-to-weight ratio of the structure for a variety of materials. In general the material has a direct impact on the cost of the structure, and a compromise between cost and structural efficiency must be made.

This information was obtained by assessing the wing internal stress and tip deflection for several materials, tabulated in Table 8.11.1. Both titanium alloys offer high strength-to-weight ratios. For the given configuration they are able to maintain above a 68% safety margin in terms of internal stress. This is in addition to the safety factors otherwise built into the procedure. However their cost is in many ways prohibitive in comparison to that of typical aircraft aluminum.

It is likely that the safety net provided by the use of advanced materials such as these could be understood to be the reduction of one spar in each wing section. Whether weight optimization is a priority over production cost is the deciding factor. For primarily economic reasons, and also because small numbers of additional structural elements increase operational safety, the less expensive options are selected – namely the Aluminum 6061-T6 for most of the structure, and steel for the critical parts such as the connection between wing and fuselage.

The results outlined above hold in general for the primary load-bearing structure throughout the airplane. Thus general information about the construction and affordability of the aircraft has been determined.

**Table 8.11.1:** Materials case study showing results for optimized structure.  
Configuration contains 8-7-4 spars in the root-to-tip wing sections.

Material	Maximum Stress (Gpa)	% Error in Stress	Maximum Deflection (m)	Weight (kg)	Cost (USD)
1. Aluminum 6061-T6	0.1683	3.7391	0.4395	81.2620	78.9950
2. Titanium Ti-6Al-4V	0.1736	68.8520	0.2652	133.3300	1620.1000

**Final Report**  
*Supersonic Business Jet Design Team*

3. Titanium-Ti13V -11Cr-3Al	0.1551	78.5150	0.2773	145.0700	1939.0000
4. AISI 4130 Steel	0.1508	45.2630	0.1491	0.2363	0.1723

## **8.12. Final Wing Results**

Using the combined analytical and numerical approaches described above, a final wing structure was selected. A nonzero percentage difference between allowable and actual internal stress indicates that the structural optimizer was unable to vary the parameters sufficiently to satisfy the primary requirement of a stress-based design. Of the configurations tested, most fall into this category of less-than-optimal designs – however the error margin is less than 10% and thus is acceptable for the configuration design stage.

One of the smaller numbers of spars in the root section for Material 1 that does satisfy the numerical requirements is 8. The finalized configuration of the wing was chosen such that some redundancy in structural elements exists. The purpose of this is to improve safety throughout the lifetime of the aircraft. Following this general guideline the number of spars chosen for each wing section is 8 in the root section, 6 in the middle section, and 7 in the tip section. To reduce the layout complexity 3 ribs are chosen.

The materials case study clearly shows a benefit in terms of strength-to-weight ratio for the titanium alloys. However the cost of these materials is prohibitive. Reasonable compromises are available from the aluminum alloy, and with regards to both an economical and safe design this material was chosen.

A qualitative allowance for additional sources of structural failure, which have not been taken into account, such as buckling of the aircraft skin, was made in the optimization. Optimized structural parameters were obtained for the selected configuration and material, and results from both analysis procedures are presented in Table 8.12.1. All methods show that the maximum internal stress lies safely within material limits, and deflections do not exceed reasonable values.

Final Report  
*Supersonic Business Jet Design Team*

**Table 8.12.1:** Final wing design results

<b>Method</b>	<b>Loading Case</b>	<b>Maximum Internal Stress (MPa)</b>	<b>% Error</b>	<b>Deflection (m)</b>
Beam bending	1	43.998	16.6	0.1146
	2	43.998	16.6	0.1146
	3	167.191	1003.8	0.4355
Thin plate	1	167.19	4.35	0.4367
	2	167.2	4.35	0.43668
	3	635.3	263.5	1.660

The values for the structural parameters are shown in Table 8.12.2. When compared with values for structural components on real aircraft, reasonable agreement exists.

**Table 8.12.2:** Final Wing Design Specifications

<b>Classification</b>	<b>Parameter</b>	<b>Value</b>	
Primary Material	Designation	Aluminum 6061-T6	
	Yield Stress (MPa)	276	
	Elastic Modulus (GPa)	68.9	
	Poisson's Ratio	0.33	
	Density (kg / m <sup>3</sup> )	2700	
	Cost (USD / kg)	14064.0399	
Configuration	Number of ribs	3	
	Number of spars	8	(Section 1)
		7	(Section 2)
		6	(Section 3)
	Wing box height (m)	0.138192193	(Section 1)
		0.1105537544	(Section 2)
		0.0829153158	(Section 3)
	Wing box width (m)	3.454804824	(Section 1)
		2.7638438592	(Section 2)
		2.0728828944	(Section 3)
Structural parameters	Spar cap area	5e-05	

Final Report  
*Supersonic Business Jet Design Team*

Spar web thickness	0.0010
Skin thickness	0.0010

### 8.13. Horizontal Tail

#### *Stresses in Initial Configuration*

In addition to a preliminary configuration for the wing, at the close of the first semester a configuration for the horizontal tail was described. Relying also on beam bending, the internal stress and tip deflection were computed to be within bounds. The concept of discrete spanwise sections of the wing having similarly parameterized wing box geometry was used for the horizontal tail as well. The configuration consisted of three spars at the root, followed by three in the outboard section. This number of spars was found to support the required load more than adequately.

Aluminum 6061 was chosen as the primary material for the structure, as in the case of the wing. Results of the beam analysis procedure for the horizontal tail are summarized in Table 8.13.2. The internal stress does not approach material limits. This design can be understood to be safe for all given loading conditions, but is a less than economical approach owing to the unnecessarily high weight of the structure.

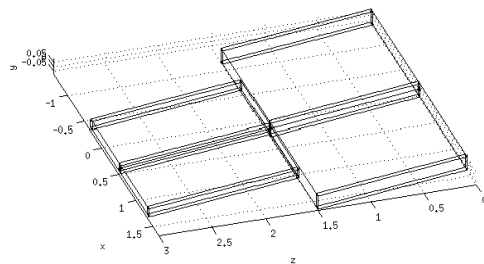


**Figure 8.13.1:** Horizontal tail internal structure (includes sweep)

Final Report  
*Supersonic Business Jet Design Team*

**Table 8.13.2:** Preliminary Horizontal Tail Results from Beam Analysis

Loading Case	Maximum Internal Stress (MPa)	% Error	Deflection (m)
1	18.89	83.1	0.0002
2	18.89	83.1	0.0002
3	72.0	21.8	6.06e-04

*Stresses in Final Configuration*

As explained for the wing, the final configuration was chosen with the help of a structural sub-optimizer. The objective function takes into account both beam bending and thin plate analysis. The cross section is parameterized in the same way as for the wing. For a given material and configuration the optimizer can determine the set of parameters (spar web thickness, spar flange area, and skin thickness) which results in a minimum structural weight for the given loading cases.

#### **8.14. Horizontal Tail Configuration case study**

Utilizing an adaptation of the script used for the wing, a set of configurations was tested for the horizontal tail structure. Results of the study, which utilized the sub-optimizer to determine optimal values of the structural parameters, are presented in Table 8.14.1.

Final Report  
Supersonic Business Jet Design Team

**Table 8.14.1:** Configuration Case Study Results, Material 1

	Skin Thickness	Web Thickness	Flange Area (m^2)	Mass (kg)	Maximum Deflection	% Error in Stress	Maximum Stress	Section 1 (Root)	Section 2	Section 3 (Tip)
3.0000	6.0000	8.0000	4.0000	0.0091	94.8120	0.0109	74.7070	2e-05	0.0010	0.0010
3.0000	6.0000	8.0000	5.0000	0.0090	94.8240	0.0109	77.6360	2e-05	0.0010	0.0010
3.0000	6.0000	8.0000	6.0000	0.0090	94.8360	0.0108	80.5650	2e-05	0.0010	0.0010
3.0000	6.0000	8.0000	7.0000	0.0090	94.8490	0.0108	83.4940	2e-05	0.0010	0.0010
3.0000	7.0000	5.0000	4.0000	0.0091	94.7810	0.0110	67.8840	2e-05	0.0010	0.0010

## 8.15. Horizontal Tail Final Results

Using the approaches described above, a final horizontal tail structure was selected. In keeping with several design features in the wing a small amount of redundancy was desired. From the configuration case study it is evident that it is possible to over-constrain the problem with too many spars. With tradeoffs similar to those made in the case of the wing, a 6-8-7 selection of number of spars per wing section was made.

**Table 8.15.1:** Final Horizontal Tail Design Results

Method	Loading Case	Maximum Internal Stress	% Error	Deflection (m)
Beam bending	1	2250006.5	362.3150349458	0.0027039738
	2	2250006.5	362.3150349458	0.0027039738
	3	8550024.6	309.9971327939	0.0102751004
Thin plate	1	8.57e+06	95.095809697	0.0103021401

Final Report  
*Supersonic Business Jet Design Team*

	2	8.57e+06	95.095809697	0.0103021401
	3	3.26e+07	81.3640768488	0.0391481324

The computed deflections and other pertinent parameters are presented in Table 8.15.2.

**Table 8.15.2:** Final Horizontal Tail Design Specifications

Classification	Parameter	Value	
Primary Material	Designation	Aluminum 6061-T6	
	Yield Stress (MPa)	276	
	Elastic Modulus (GPa)	68.9	
	Poisson's Ratio	0.33	
	Density (kg / m <sup>3</sup> )	2700	
	Cost (USD / kg)	14064.0399	
Configuration	Number of ribs	3	
	Number of spars	6	(Section 1)
		8	(Section 2)
		7	(Section 3)
Structural parameters	Spar cap area	5e-05	
	Spar web thickness	0.0010	
	Skin thickness	0.0010	

## 8.16. Vertical Tail

### *Stresses in Initial Configuration*

At the close of last semester preliminary results for the vertical tail were also presented. These are summarized by Table 8.16.1. As for the other cases, the structure is significantly over-designed. One goal is to reduce the structural volume taken up by each member.

Final Report  
*Supersonic Business Jet Design Team*

**Table 8.16.1:** Preliminary Vertical tail Results from Beam Analysis

Loading Case	Maximum Internal Stress (GPa)	% Error	Deflection (m)
1	1.961	8.382	1.102e-4
2	1.961	8.382	1.102e-4
3	7.47	2.2	4.2e-04

*Stresses in Final Configuration*

A similar analysis procedure for the vertical tail was carried out. The primary load-bearing situation which could be encountered by the structure is the yawing moment from the engine-out scenario. Planning for this case the internal structure was sized. A configuration study much like that performed for the vertical tail yields similar trends, as may be seen in Table 8.16.2.

**Table 8.16.2:** Configuration case study results, Material 1

Number of Ribs	Number of Spars	Section 1 (Root)	Section 2	Section 3 (Tip)	Maximum Stress	% Error in Stress	Maximum Deflection	Mass (kg)	Flange Area ( $m^2$ )	Web Thickness	Skin Thickness
3.0000	6.000	6.000	5.000	0.5458	0.0000	0.2074	70.4720	5e-05	0.0010	0.0010	
3.0000	6.000	6.000	6.000	0.5435	0.0000	0.2065	73.4390	5e-05	0.0010	0.0010	
3.0000	6.000	6.000	7.000	0.5411	0.0000	0.2057	76.4050	5e-05	0.0010	0.0010	

Final Report  
*Supersonic Business Jet Design Team*

### 8.17. Vertical Tail Final results

Using the approaches described above, a final vertical tail structure was selected. Similar results to those for the wing and horizontal tail are obtained, and a structure with 6, 6, then 5 spars in root-to-tip order was selected. Results from the analysis procedures are presented in Table 8.17.1 and the final design parameters are shown in Table 8.17.2.

**Table 8.17.1:** Final Horizontal Tail Design Results

Method	Loading Case	Maximum Internal Stress	% Error	Deflection (m)
Beam bending	1	0	0	0
	2	5.32e+08	2.005e+02	0.195
	3	0	0	0
Thin plate	1	0	0	0
	2	5.41e+08	2.10e+02	0.206
	3	0	0	0

**Table 8.17.2:** Final Horizontal Tail Design Specifications

Classification	Parameter	Value	
Primary Material	Designation	Aluminum 6061-T6	
	Yield Stress (MPa)	276	
	Elastic Modulus (GPa)	68.9	
	Poisson's Ratio	0.33	
	Density (kg / m <sup>3</sup> )	2700	
	Cost (USD / kg)	71.39	
Configuration	Number of ribs	3	
	Number of spars	6	(Section 1)
		6	(Section 2)
		5	(Section 3)
Structural parameters	Spar cap area	5e-05	
	Spar web thickness	0.0010	
	Skin thickness	0.0010	

## 8.18. Future Work

The above structural analysis allows for a thorough numerical treatment of the internal supporting structure. However some deficiencies do exist, as well as areas for general improvement. For more advanced stages of design more accurate procedures would likely be needed.

The beam analysis approach used does make the approximation that part of the structure which is curved (the airfoil cross section) is straight. In addition this wing box geometry is allowed to physically protrude through the skin of the aircraft, which results in a reasonably accurate estimate of cross-sectional parameters but is physically inaccurate.

Thin plate analysis offers improved accuracy in a more generalized loading scenario. This can lead to more technically accurate solutions which take into account non-planar deformation. However the code currently in use was assembled in a single semester, and several undesirable approximations had to be made. The most important of these is the treatment of the aircraft lifting surfaces as isotropic plates, which is a fundamentally incorrect assumption.

One structural limitation in practice that has not been addressed numerically is buckling. Aircraft skin can tend to warp out of plane and reduce the torsional rigidity of a wing if buckling stresses are exceeded. Neither thin plate nor composite beam analysis takes this into account. However, the code structure to integrate a buckling analysis procedure exists and has proven to work reliably in the context of both a structural sub-optimizer, and the overall MDO code.

Throughout the use of the structural sub-optimizer it was found that the initial values given to the optimizer were necessarily near the center of the desired range. Having placed realistic limits on all structural parameters, averages of these limits were taken. These acted as the seed values for the optimizer. It was found that if beginning at the upper bounds of these limits, in many cases the optimization function used was not able to successfully explore the design space. This is a noteworthy fact for future design efforts that utilize the current code base to be aware of.

One further observation made while running the structural sub-optimizer was that when exploring the design space, the optimizer tends to utilize the maximum allowable

Final Report  
*Supersonic Business Jet Design Team*

values for skin thickness and spar flange area. The parameter varied in a most weight-efficient manner was the spar web thickness. This makes sense as the skin and flange have the most direct impact on bending stiffness (for the beam bending code) and flexural rigidity (the equivalent parameter for plate analysis). This acts as a measure of confirmation that the analysis and optimization codes are working together to generate a meaningful solution.

Thin plate analysis works well for simple rectangular plates, as shown at the beginning of the semester. One suggestion for further detailed structural design is to model control surfaces as rectangular plates. Procedures to implement this exist in the current code base, and this would be a straightforward task.

*Rectangular Plate Verification Study*

A study was carried out with the finished thin plate code to determine the accuracy with which computations are being performed. Data for several plates was available to be cross-checked with, and one plate problem which was straightforward to replicate was chosen. A rectangular plate with a 10x10 grid is subjected to a uniform load. The left and right boundaries are held fixed, while the top and bottom are simply supported. Shown in Figure 8.18.1 are the resulting deflections using a late iteration of the plate analysis code (a consistent choice of integer constants was made for load intensity and flexural rigidity).

0	-1E-015	8E-015	1.6E-014	0
-7E-015	2.8502247528	4.6848067126	3.6885825592	0
-6E-015	3.8568774348	6.3950854061	5.0306263111	0
-1E-015	2.8502247528	4.6848067126	3.6885825592	0
0	0	0	0	0

**Figure 8.18.1:** Rectangular plate deflections before out-of-bounds correction for fixed and simple boundary conditions. Notice the asymmetric values.

A fundamental flaw in the results was identified. Deflections with these boundary conditions are expected to be symmetric about the plate centerlines. However this was not the case.

Final Report  
*Supersonic Business Jet Design Team*

As a result of this study changes were made to sections of the code, which addressed the issue. Symmetric results from the corrected plate analysis code are shown in Figure 8.18.2. Percent error between these results and results from a reliable source on plate deflection theory agreed to within 26%. This margin is deemed acceptable a) given the small number of points, which reduces all solution accuracy, and b) in light of other qualitative and quantitative verification with more complex boundary conditions.

0	1E-015	8E-015	8E-015	0
-6E-015	2.4668008048	3.7303822938	2.4668008048	0
0	3.3158953722	5.0503018109	3.3158953722	-7E-015
-2E-015	2.4668008048	3.7303822938	2.4668008048	0
0	0	0	0	0

**Table 8.18.2:** Results after out-of-bounds correction. Values are symmetric about both centerlines within machine error.

## 9. WEIGHTS ESTIMATION

Aircraft component weights have been estimated using semi-empirical methods, based on a compromise between civilian transport jet aircraft statistical data and high speed military fighter aircraft. The vehicle we are designing is structurally similar to a high-speed business jet, such as the Gulfstream G650 or Cessna Citation X, but operates at much higher Mach numbers. Therefore, the semi-empirical method of integrating empirical data from supersonic aircraft and civilian jets has been deemed satisfactory at this stage in the design process.

To further refine the semi-empirical weights estimation, in depth structural analysis of the wing allows us to further refine the estimate of the wing weight. Since the wing has a low thickness-to-chord ratio governed by supersonic aerodynamic considerations, the weight of the wing could be slightly higher than the semi-empirical method would suggest. To account for this, the wing has been given a ‘penalty’ for the low thickness-to-chord ratio of 5%. As suspected, the statistically estimation for wing weight was lower than the flat plate analysis yielded, and the component weight was updated accordingly.

A breakdown of weights is included in Appendix I. When compared to the Cessna Citation X (a recent vehicle with similar passenger capacity, range, wing area and empennage), the structural weight is very similar (within 12%), but the take-off gross weight of our vehicle is significantly higher. This is due to having significantly larger quantities of fuel when compared to the Citation X. At take off, up to 64.2% of the weight is fuel.

## 10. Stability and Control Surface Sizing

### 10.1. Definitions of Variables

$C_{m\alpha}$ : The change in pitch moment coefficient with respect to angle of attack ( $\frac{dC_m}{d\alpha}$ )

$C_{m0L}$ : Pitch moment coefficient at zero lift

$C_{n\beta v}$ : Change in yaw moment with respect to change in rudder angle of attack for the vertical tail

$C_{n\beta f}$ : Change in yaw moment with respect to change in rudder angle of attack for the fuselage

$S_w$ : Area of the wing

$S_h$ : Area of the horizontal tail

$S_v$ : Area of the vertical tail

$x_w$ : Distance from aerodynamic center of the wing to the c.g.

$c$ : Mean aerodynamic chord

$L_h$ : Distance from the nose of the aircraft to the leading edge of the horizontal tail

$C_{Lah}$ : The change in lift coefficient of the horizontal tail with respect to angle of attack

$C_{Law}$ : The change in lift coefficient of the wing with respect to angle of attack

### 10.2. Calculations

The first goal of the stability and control team was to determine whether or not the supersonic business jet was statically stable. The first resources used were lecture notes from AOE 3134: Stability and Control by Professor Sultan. Based on these notes, the team concluded that the stability equations and requirements would work for both subsonic and supersonic flight. However, we found difficulty applying some of these lectures to our aircraft because of the difference in perspectives used. In order to prove that our aircraft was longitudinally stable, we calculated the static margin. Static longitudinal stability requires that the following two assumptions be true:

1.  $C_{m\alpha} < 0$
2.  $C_{m0L} > 0$

These assumptions are satisfied if the static margin is positive. The equation used for static margin was:

Final Report  
*Supersonic Business Jet Design Team*

$$\frac{x_w}{c} - \frac{C_{Lah}S_hL_h}{C_{Law}S_w c} + \text{fuselage effects} = -\text{static margin} \quad (10.2.1)$$

with our calculated value of static margin being 5.51% which is indeed positive and within our initial goal of 5%-10%.

Once static longitudinal stability was proved, we moved onto lateral-directional stability calculations. In order to prove lateral-directional stability the following inequality must hold:

$$C_{n\beta v} + C_{n\beta f} > 0 \quad (10.2.2)$$

For our aircraft this sum was found to be 0.2568 which is indeed greater than zero, thus proving static lateral-directional stability.

Once the values for lateral-directional and longitudinal static stabilities were obtained, empennage sizing was optimized according to these values. The horizontal tail size was obtained from our chosen target static margin and trim conditions. The vertical tail was sized so that the inequality above was satisfied. The following tables display the results of our empennage sizing:

**Table 10.2.1:** Horizontal Tail Sizing

Mean Chord	2.76 m	9.33 ft
Span	3.0 m	9.84 ft
Area	11.0 m <sup>2</sup>	37.19 ft <sup>2</sup>

**Table 10.2.2:** Vertical Tail Sizing

Mean Chord	3.36 m	11.36 ft
Span	4.0 m	13.52 ft
Area	8.0 m <sup>2</sup>	27.05 ft <sup>2</sup>

The remaining control surface sizing to be done was found statistically from existing aircraft data through fractional relationships of the wing horizontal and vertical tail. The

Final Report  
*Supersonic Business Jet Design Team*

table below displays the fraction used for each remaining control surface and its nominal value.

**Table 10.2.3: Control Surface Sizing**

Aileron	$0.1S_w$	$4.5 \text{ m}^2$
Elevator	$0.4S_h$	$4.4 \text{ m}^2$
Rudder	$0.3S_v$	$2.4 \text{ m}^2$

With this static stability framework in place, the calculations were integrated into the MDO code. These calculations take into account the subsonic flight regime, and the supersonic flight regime – making considerations for significant aerodynamic differences at supersonic speeds. Within the optimizer, subsonic and supersonic marginal stability is required. With this condition set, the empennage sizing occurs dynamically with each iteration of the model, in which each final iteration is known to be at least marginally stable.

It was decided that the scope of this design project would be limited to assuring static stability in the subsonic and supersonic flight. The transonic flight regime was not investigated, but it is assumed to be “survivable” on the basis that other vehicles that are statically stable can successfully pass through transonic speeds.

Dynamic stability was not investigated due to its inherent complexity and large resource demands. Flight computers would assist in assuring dynamic stability if the vehicle is later determined to be dynamically unstable.

## 11. PERFORMANCE

### 11.1 Preliminary Performance Challenges and Investigations

The biggest challenge to the design's performance goals is the high level of drag at supersonic speeds. To maneuver and increase the service ceiling, drag must be reduced well below available thrust. Figure 11.1.1 shows an example plot of the total thrust required at a range of altitudes from a much earlier iteration in the design. Increasing cruising altitude to 20 kilometers from typical values between 10 – 15 kilometers reduces the required drag at Mach 2.2 by more than 50%.

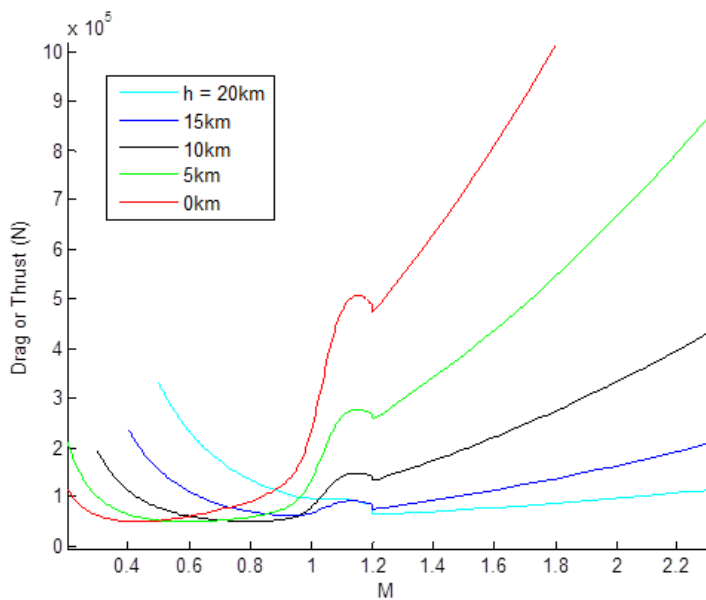


**Figure 11.1.1:** Minimum thrust required versus Mach number for the initial supersonic business jet design.

However, at higher altitudes, the available thrust decreases. For early analysis, thrust available was assumed to be directly proportional to the freestream air density. This, however, does not take into account beneficial compressibility effects due to shockwaves at supersonic speeds. A more detailed investigation on available thrust is described later.

Final Report  
*Supersonic Business Jet Design Team*

Figure 11.1.2 shows thrust required and thrust available at supersonic speeds from the initially aircraft design. From this chart, we found that the drag is too high to be overcome by the available thrust. Thus, it was impossible for the current design to fly at supersonic speeds, and significant changes needed to be made to the aircraft size and configuration. Even taking into account compressibility effects, drag would need to be reduced significantly to make supersonic flight feasible.

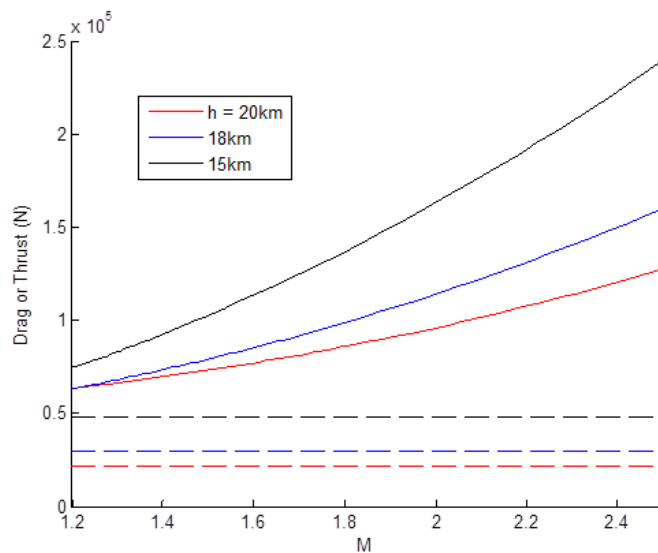


**Figure 11.1.2:** Drag and Thrust plotted versus Mach number for supersonic speeds of the initial design. Dashed lines indicate available thrust. Solid lines indicate required thrust.

Thrust required for subsonic and transonic flight is shown in Figure 11.1.3. From this curve, we found that the minimum subsonic drag is about 50 kN. In comparison, the Boeing 737-300 has a minimum drag of 36.9 kN. The ceiling for the supersonic business jet was approximately 14,000 meters, a fairly typical value for a business jet. However, that fell short of the design goal of 20,000 meters where drag and noise impact would be lower.

Final Report  
*Supersonic Business Jet Design Team*

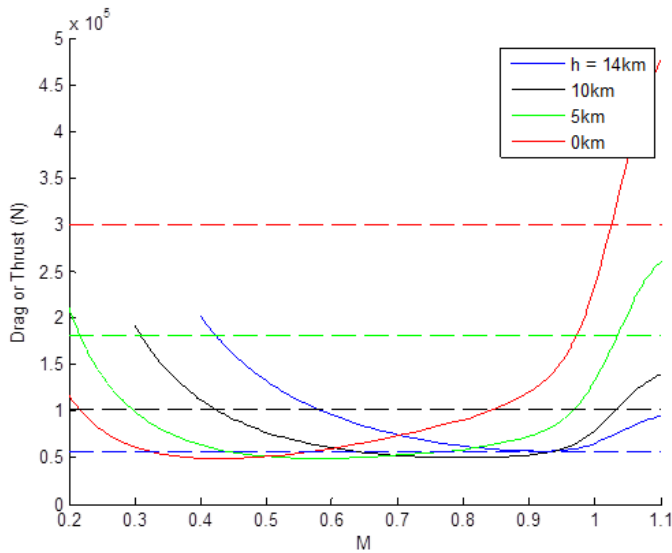


**Figure 11.1.3:** Drag and Thrust plotted versus Mach number for subsonic speeds. Dashed lines indicate available thrust. Solid lines indicate required thrust.

Performance calculations at subsonic speeds resulted in a maximum range of 7000 km without reserve fuel occurring at  $M = 0.92$  and  $h = 14$  kilometers. If the aircraft had enough thrust to continue flight into supersonic freestream velocity, the anticipated range would be approximately 6370 km, again without fuel reserves. These numbers fell short of our design goal due to higher than expected drag.

Due to the problems described above, several investigations were done to determine ways to reduce drag and increase available thrust of the aircraft. One of the measures to reduce drag is to reduce the weight of the aircraft. This reduces induced drag by directly reducing the required induced drag. Figures 11.1.4 and 11.1.5 show the impacts of weight reduction on required thrust of our preliminary design. At supersonic speeds, every weight reduction of nine to ten units leads to a 1 unit reduction in drag.

Final Report  
Supersonic Business Jet Design Team

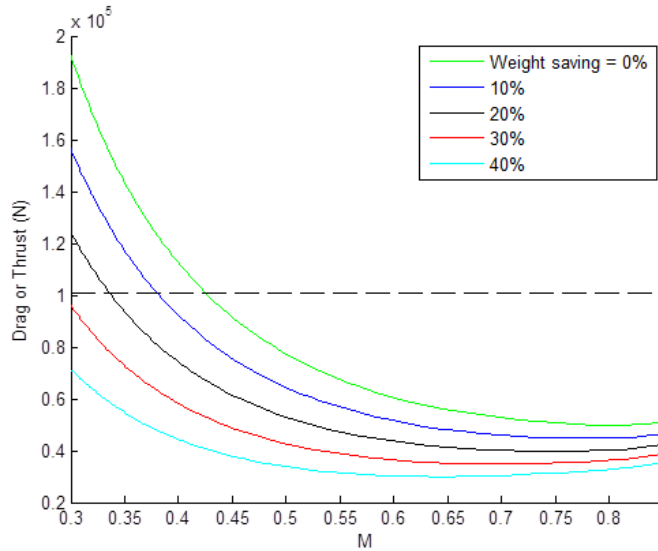


**Figure 11.1.4:** Drag vs Mach number and total weight reductions at 10 km altitude.

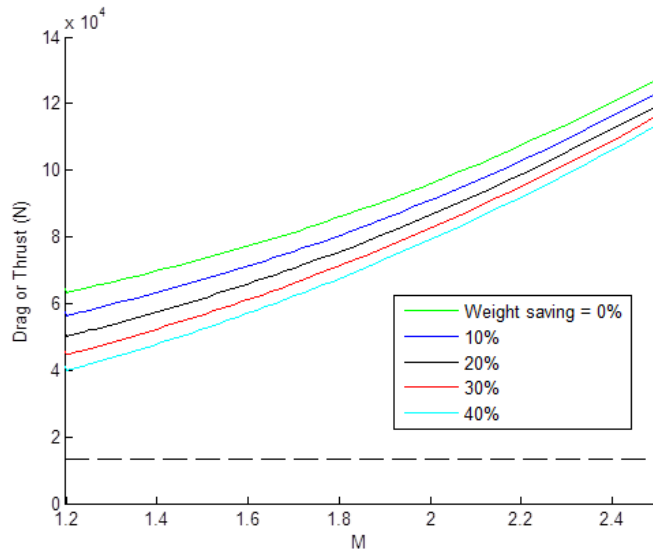


**Figure 11.1.5:** Drag vs Mach number and total weight reductions at supersonic speeds at 20 km.

After the investigation, the poor aircraft performance was attributed to several factors. Firstly, the aircraft was oversized. The weight of the aircraft needed to be drastically reduced to reduce drag, and the wing area was far too large and contributed to too much drag. Secondly, the engine performance model was insufficient and too simple to consider supersonic effects on the engine inlets and needed to be revised. Thirdly, the drag

Final Report  
*Supersonic Business Jet Design Team*

and performance calculations were initially crude and needed to be redone in far more detail.

After these changes, the aircraft was able to converge to a far more acceptable design. The changes made in some of the performance calculation methods and the results of the new performance analysis are described in the following sections.

## **11.2. Available Thrust Estimation**

One of the primary performance concerns was whether the design would have enough available thrust at very high altitudes. It was anticipated that the high design cruise Mach Number ( $M = 2.2$ ) would only be achievable at altitudes higher in the stratosphere than most commercial aircraft fly. With an estimated ceiling of about 20,000 meters, the supersonic drag and required thrust would be reduced. However, at these altitudes, the drop in air density would significantly reduce the available thrust.

One of the simpler ways of predicting thrust performance during conceptual design is to assume that the thrust varies linearly with changes in air density and does not vary with speed. However, this method suggests that static thrust will be reduced by approximately 93% at 20,000 meters and by 86% at 16,000 meters. With this drop in available thrust, early performance estimations predicted that it would be nearly impossible to reach these altitudes, even with an excessively high thrust-to-weight ratios. Ratios greater than 1.0 were still insufficient.

However, according to the specification of the Concorde, the aircraft's static thrust dropped to only about one-third of its sea level rating at the Concorde's cruising altitude of 17,000 meters at Mach 2.02. Also, Aerion's SBJ conceptual design uses two Pratt & Whitney JT8D-200 series engines. These engines provided 87kN of thrust each, similar in magnitude to our design's initial thrust estimations. The Aerion's engines are noted for their excellent performance at high altitudes and take the aircraft to a ceiling of 15,550 meters. Thus, these altitudes should be achievable by the design's propulsion system.

Clearly, the above thrust estimation method was inadequate and did not take into account important factors. Our engines are designed for optimum performance at high

Final Report  
*Supersonic Business Jet Design Team*

altitudes. Also, the thrust estimation needs to consider compressive effects at supersonic speeds. Shock waves from the aircraft body and the engine inlet compress and slow down air entering the engine. The inlet is also designed with variable geometry to provide efficient performance over a range of altitudes and Mach numbers. At supersonic speeds, the inlet design can be responsible for the majority of the installed thrust. Lastly, greater Mach numbers result in a higher pressure recovery, meaning that thrust does not stay constant with speed. Rather, it increases with Mach number up to a point.

A new model (see AE 429 - Aircraft Performance) was developed to consider these effects. Subsonic thrust is still considered to vary only with air density and thus altitude. However, once speeds become supersonic, thrust increases linearly with Mach number. This results in the following thrust estimation equations:

$$(M \leq 1) \quad T_{avail} = T_0 \frac{\rho}{\rho_{sl}} \quad (11.2.1)$$

$$(M > 1) \quad T_{avail} = (T_{avail,M=1})(1.0 + 1.18[M - 1]) \quad (11.2.2)$$

Above a certain Mach number, thrust should begin to drop as air can no longer be decelerated as it enters the engine. However, we neglect to include Mach numbers above approximately 2.5 in our analysis as the aircraft is not designed to handle the aerodynamic and thermal stresses at those speeds. Also, to account for currently emerging technologies and for our engines particularly high performance at high altitude, a factor that scales with altitude has been multiplied with the available thrust. This factor is calculated by the following equation:

$$F = \frac{0.03}{\rho/\rho_{sl}} + 0.97 \quad (11.2.3)$$

Based on this new analysis, altitudes above 15,000 meters are indeed achievable with our propulsion system. Since we attempted to increase our available thrust during a previous iteration due to the poor thrust estimation model, our thrust with the current performance model became too high. Therefore, we reduced normal operating thrust to approximately 75kN per engine at sea level, and reduced it again to approximately 51kN

Final Report  
*Supersonic Business Jet Design Team*

per engine. By reducing the size of engines, there have been reductions in weight, noise, cost and drag.

With this thrust reduction, the thrust to weight ratio dropped from 0.7 to 0.51. This is still a little bit higher than other supersonic designs which typically have values between 0.35 and 0.45. However, since our aircraft is both lighter than other designs and attempting to fly at a higher altitude and Mach number, it is likely our thrust-to-weight ratio should be somewhat higher. However, this may also be an indication that some further optimization could be done.

### 11.3. Normal Operating Envelope

Figure 11.3.1 shows the specific excess power,  $P_s = 0$ , contour for the supersonic business jet design. This figure shows the limits of the aircraft's flight as determined by propulsion. The region between the solid lines show altitude and Mach number combinations in which the aircraft has excess power to maneuver or accelerate.

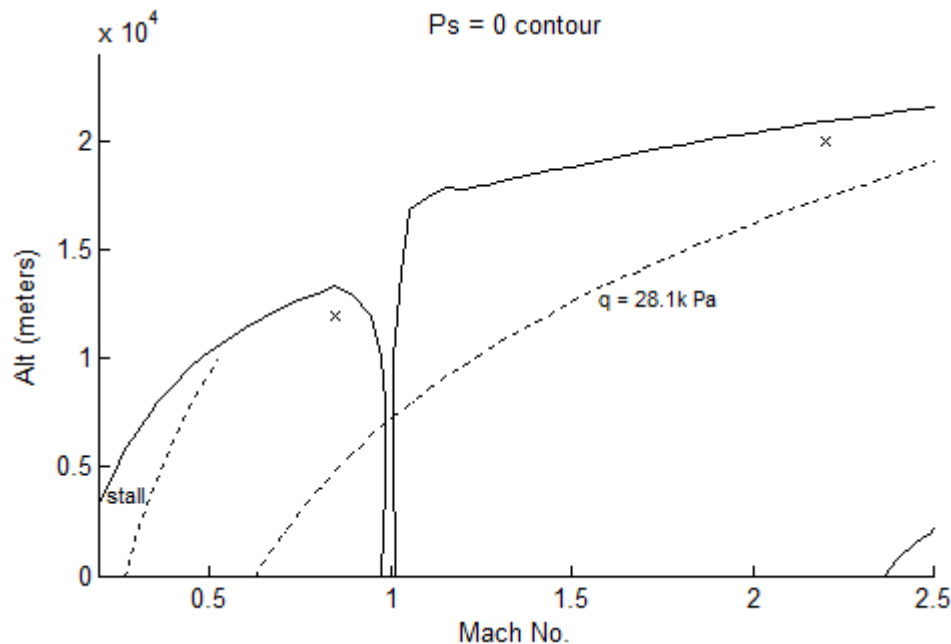


**Figure 11.3.1:**  $P_s = 0$  contour for a load factor of  $n=1$ . The two marks indicate the locations of the chosen subsonic and supersonic cruise conditions.

Final Report  
*Supersonic Business Jet Design Team*

The dotted line on the left shows the design's stall speeds at lower altitudes. The dotted line on the right side of the figure represents a notional dynamic pressure limit equal to 1.5 times the dynamic pressure that occurs at the supersonic cruise condition. While this is not the actual structural limit of the aircraft, it shows a useful trend for the potential maximum speed of the design.

The design shows that the ceiling is greater than 20,000 meter at Mach numbers greater than M=2. However, due to difference in cabin and atmospheric pressure, the aircraft would be limited to pressure altitudes no greater than 21,000 meters.

The gap in the excess power chart at Mach 1 shows that under normal conditions, there is insufficient power to accelerate through the transonic regime.

#### **11.4. Transonic Flight Considerations**

While the propulsion system normally operates at a static thrust of 51kN of thrust per engine, each engine is capable of increasing its output to 102kN for a short period of time. While this is less fuel efficient and excessive during cruising conditions, it enables the design to overcome the high drag in the transonic regime. Upon reaching subsonic cruising conditions, the aircraft would use this reserve thrust to climb and accelerate to approximately Mach 1.1. After this, the aircraft would reduce thrust back to its normal operating thrust. Figure 11.4.1 shows the increased operating envelope using this reserve power.

Final Report  
Supersonic Business Jet Design Team

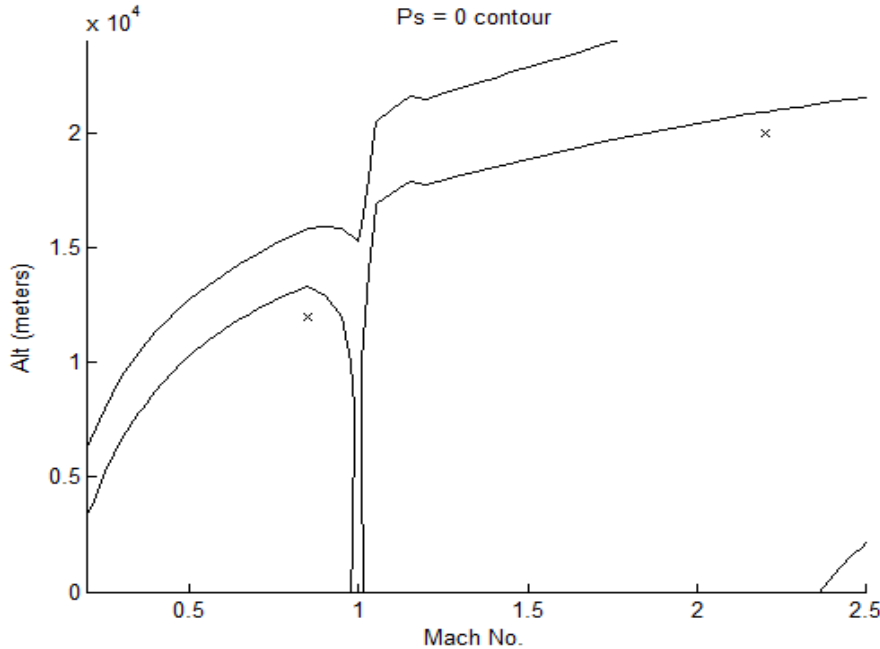


**Figure 11.4.1:**  $P_s = 0$  contours for a static thrust of 51kN and 102kN. The increased thrust allows travel through the transonic regime.

## 11.5. Range and Fuel Consumption Estimation.

Range can be quickly determined using the Breguet range equation:

$$R = \frac{V_L}{C_D} \ln \frac{W_i}{W_f} \quad (11.5.1)$$

However, this range equation assumes constant velocity, specific fuel consumption, and lift-to-drag ratio. In the case of the supersonic business jet, these assumptions are not true. Approximately half of the aircraft weight is fuel. Therefore, the lift of the aircraft at the end of cruise will be half of its value at the beginning. Similarly, since induced drag depends on the square of the lift, induced drag will be reduced by four times. Velocity may also change if the aircraft accelerates and climbs as fuel load decreases during flight.

Therefore, a more generalized form of the range equation has been used:

Final Report  
*Supersonic Business Jet Design Team*

$$\frac{dR}{dW} = \frac{V}{-CT} = \frac{V}{-CD} \quad (11.5.2)$$

By using the more generalized form of the range equation, we can account for the advantages gained by losing weight while cruising. Since this only reduces induced drag, the increase in range at most supersonic conditions is negligible since zero-lift drag is more dominant than lift-induced drag in this flight regime. However, during subsonic flight, there were range increases of approximately 20-30% at cruising altitudes and speeds.

At very high Mach numbers (approximately 2.3 and above) and at a high altitude of 20,000 meters, significant gains are made in range. Unlike at other supersonic flight conditions, induced drag is in the same order of magnitude as parasite drag. At 20,000 meters, the air density is low enough that parasite drag becomes extremely low, and induced drag, which is normally fairly insignificant at these speeds, becomes relevant again. In fact, induced drag rises slightly since the lift coefficient rises with a decrease in drag. These Mach numbers and altitudes, however, are beyond the capabilities of the current supersonic business jet design, and flying at higher altitudes may cause harm to the stratosphere.

Estimations for aircraft NBAA IFR range are as follows in Table 11.5.1.

**Table 11.6.1:** Maximum vehicle ranges

	Max Subsonic Range	Max Supersonic Range	Supersonic Cruise
<b>Range</b>	13200 km	9750 km	9200 km
<b>Mach Number</b>	0.85	1.9	2.2
<b>Altitude</b>	12 km	20 km	20 km
<b>Ground Speed</b>	903 km/h	2018 km/h	2335 km/h
<b>Fuel per distance</b>	0.94 kg/km	1.27 kg/km	1.35 kg/km
<b>Fuel per time</b>	849 kg/h	2662 kg/h	3152 kg/h

Table 11.6.1 above shows the range of the aircraft at different conditions. Since drag is much higher at supersonic cruise than subsonic cruise, the increase in speed results in significant increases in fuel consumption. This causes a reduction in range at higher

Final Report  
*Supersonic Business Jet Design Team*

supersonic Mach numbers. However, the range at M=2.2 and 20,000 feet is greater than 9200 km, enough for a non-stop trip across the Pacific Ocean.

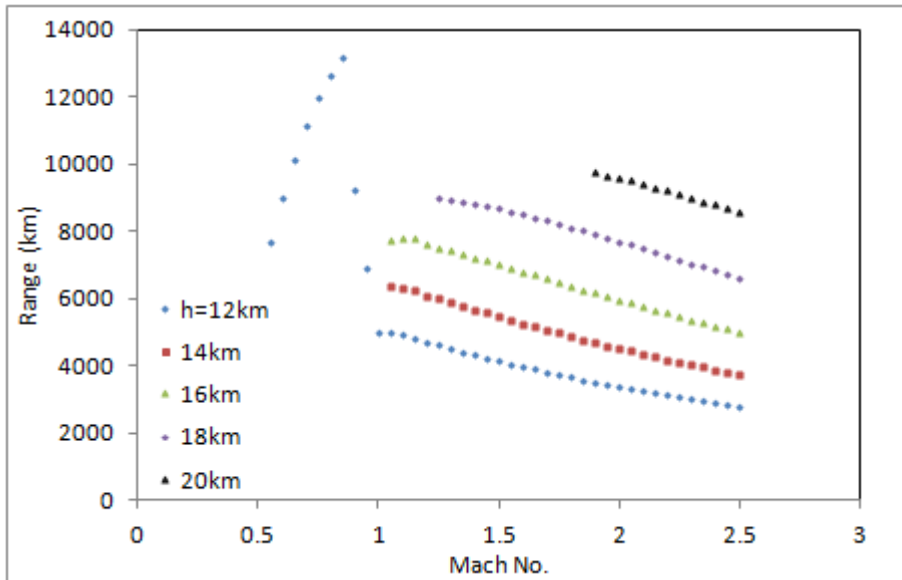


**Figure 11.5.2:** Variations in range with Mach number and altitude.

Figure 11.5.2 shows that subsonic cruise is clearly more efficient than supersonic cruise. It is slower, however, and the aircraft is unable to produce the power required to fly higher than 12-13 kilometers. For supersonic speeds, increase in altitude shows very large improvements in range, but the aircraft must fly at higher Mach numbers to maintain higher altitudes.

While not shown above and currently unachievable by the current propulsion system, at altitudes above 20 kilometers, efficiency initially increases with higher Mach numbers because induced drag becomes problematic at speeds below M=2 in the extremely thin atmosphere. However, flying at this extremely high altitude could present many structural and aerodynamic challenges. Another important issue to consider is environmental impact. Emissions from the aircraft being dumped directly this high into the stratosphere could cause significant damage to the atmosphere and ozone layer.

Final Report  
*Supersonic Business Jet Design Team*

### **11.6. Endurance Estimation**

Endurance is not a primary performance goal for this design. However, it must be considered for loitering and safety requirements. Supersonic loiter is irrelevant since it consumes more fuel than subsonic loiter. The following table shows conditions for maximum subsonic loiter:

**Table 11.6.1: Maximum Endurance**

Endurance	11.8 h
Altitude	sea level
Mach No.	0.4
Fuel consumption	1106 kg/h

### **11.7. Reserve Fuel**

Reserve fuel is stored on the aircraft in order to meet standards set by NBAA IFR recommendations. The supersonic business jet carries enough excess fuel to cruise at subsonic cruising conditions to another landing site 185 km [100 nm] away. The aircraft can then loiter at 1500 m [5000 ft] for 30 minutes. Afterwards, the aircraft can approach and land while carrying another 5 minutes of holding fuel. The reserve held by the aircraft is 632 kilograms of fuel.

### **11.8. Takeoff Calculation Method**

Takeoff distance and balanced field length were analyzed using methods described in Raymer and Marchman. The takeoff distance is the distance that includes the start of ground roll, transition to climb, and climb until the aircraft clears a 50ft [15.24m] obstacle. The distance for ground roll was determined by the following equations:

Final Report  
*Supersonic Business Jet Design Team*

$$S_{gr} = \frac{1}{2B} \ln \frac{A}{A-B V_{to}^2} \quad (11.8.1)$$

$$A = g \left( \frac{T}{W} - \mu \right) \quad (11.8.2)$$

$$B = \frac{g}{W} \frac{1}{2} \rho S (C_D - \mu C_{Lg}) \quad (11.8.3)$$

where  $\mu$  is rolling friction coefficient,  $V_{to}$  is 1.1 times the stall speed, and  $C_{Lg}$  is the lift coefficient after rotation.

Ground effect also plays a role in determining takeoff performance during ground roll. When the wing is approximately less than half a span away from the ground, induced drag can be greatly reduced. Raymer presents the following equation to account for this effect:

$$\frac{K_{effective}}{K} = \frac{33(h/b)^{1.5}}{1+33(h/b)^{1.5}} \quad (11.8.4)$$

where  $h$  is the wing height above the ground.

During transition, the aircraft follows a circular arc until it reaches its climb angle. During this phase, the average speed is approximately 1.15  $V_{stall}$  and the load factor is approximately  $n=1.2$ . The horizontal distance traveled during transition is determined by the following:

$$S_{tr} = \frac{(1.15V_{stall})^2}{0.2g} \sin \gamma_{climb} \quad (11.8.5)$$

If the obstacle height has not been cleared by the end of transition, then the distance traveled during climb can be determined from the following:

$$S_c = \frac{1}{\tan \gamma_{climb}} [h_{obs} - \frac{(1.15V_{stall})^2}{0.2g} (1 - \cos \gamma_{climb})] \quad (11.8.6)$$

The balanced field length is the total takeoff distance when additional distance is needed to brake to a halt or continue taking off if an engine fails at the decision speed. Raymer gives the following equations to estimate balanced field length:

Final Report  
*Supersonic Business Jet Design Team*

$$BFL = \frac{0.863}{1+2.3(\gamma_{climb}-0.024)} \left( \frac{W/S}{\rho g C_L_{Climb}} + h_{obs} \right) \left( \frac{1}{T_{av}/W - U} + 2.7 \right) + \left( \frac{665}{\sqrt{\rho/\rho_{sl}}} \right) \quad (11.8.7)$$

$$T_{av\ jet} = 0.75 T_0 \left[ \frac{5+BPR}{4+BPR} \right] \quad (11.8.8)$$

where BPR = the bypass ratio and U =  $0.01C_{L\max} + 0.02$ .

### 11.9. Takeoff Results

The takeoff distance and balanced field length were determined for the conditions shown in Table 11.9.1. While the takeoff distances at sea level meet the takeoff distance goal of 1800 meters, these distances do not include any safety buffers in case of an engine problem. The balanced field length, however, does account for this. While the balanced field lengths at sea level do not meet the 1800 meter goal, it does meet the 2400 meter requirement.

**Table 11.9.1:** Takeoff distance and balanced field length.

	Sea Level - Dry	Sea Level - Wet	Hot and High (Denver, 32°C)
Takeoff Distance	1521 m [4990 ft]	1572 m [5158 ft]	2204 m [7231 ft]
BFL	2240 m [7350 ft]	2240 m [7350 ft]	3222 m [10570 ft]

At high altitudes and temperatures, the balanced field length fails to meet to requirement set for the design. This will have to be compensated by finding longer runways at high altitudes. However, an addition of a lifting canard to the design would improve takeoff performance, both at sea level and altitude, and would be worth investigating in detail.

## 12. SYSTEMS

### 12.1. Landing Gear

Our primary concern while choosing a landing gear configuration was its placement and size constraints. Tip back and side turnover prevention, load distribution, take-off clearance and wing tip clearance were key considerations while determining the main and nose gear placements. We chose retractable landing gears with oleo-pneumatic shock absorbers. The tire selection was made so that it meets all the performance requirements. The main gears were placed a little aft of the center of gravity. The height of the main gear was determined by an iterative method to account for the take-off clearance. To provide sufficient tail clearance this angle must be greater than the take-off pitch angle. The minimum fuselage clearance was taken to be 20 cm. The clearance requirement was checked by using the following equation:

$$\alpha_c = \tan^{-1} \frac{Hg}{AB} \quad (12.1.1)$$

Where  $H_g$  is the height of the main gear and  $AB$  is the distance from the main gear to the tail of the aircraft.

The wheel base and the placement of nose and main gears were determined to satisfy the static and dynamic load distribution. The loads on the main gear and nose gears were calculated using the following equations.

$$Fm = \frac{l_n}{l_m + l_n} W \quad (12.1.2)$$

$$Fn = \frac{l_m}{l_m + l_n} W \quad (12.1.3)$$

Where  $l_m$  and  $l_n$  are the distance measured from the aircraft cg to the main and nose gear respectively. The load on the nose gear was taken to be 10% of the total aircraft weight. The placement of the main gear was determined by the following equation.

Final Report  
*Supersonic Business Jet Design Team*

$$X_{mg} = \frac{X_{cg}W - X_{ac}L + Z_T T - Z_D D - M_{ac} - 0.4W}{Fm} \quad (12.1.4)$$

Where  $X_{cg}$  is the distance from the nose of the aircraft to the center of gravity,  $X_{mg}$  is the distance from the nose of the aircraft to the main gear,  $Z_T$  is the thrust moment arm from c.g,  $Z_D$  is the Drag moment arm from c.g,  $L_{wf}$  is the wing fuselage lift at takeoff,  $L_t$  is the tail lift,  $D$  is the drag force,  $T$  is the thrust and  $M_{ac}$  is the moment at the aerodynamic center.

The distance  $l_m$  was calculated by using the equation:

$$l_m = X_{cg} - X_{mg}. \quad (12.1.5)$$

The distance  $l_n$  was calculated by using equation 12.1.3. The wheel track was determined by accounting for a maximum turn radius to prevent overturn. The following equation was used to calculate the wheel track.

$$T = \frac{2 F_c H_{cg}}{W} \quad (12.1.6)$$

Where  $H_{cg}$  is the distance of the aircraft center of gravity from the ground and  $F_c = mV^2/R$ . Where  $R$  is the turn radius and  $V$  is the ground speed.

Aircraft classification number (ACN) is the classification of the aircraft's impact on the ground as well as the load carrying capabilities of typical airfield surfaces and has a value between 40 and 80. A two wheel configuration was chosen for each gear considering the loads on the gears and accounting for the lowest ACN possible. The tire diameter was determined by using the equation:

$$d = \sqrt{\frac{TGOW}{32 n r}} \quad (12.1.7)$$

Where  $r$  is the ratio between tire width and diameter,  $n$  is the number of wheels,  $TGOW$  is the take-off gross weight.

**Final Report**  
*Supersonic Business Jet Design Team*

The weight and volume of the tire will decrease with an increase in inflation pressure. A decrease in the tire contact area will induce a higher bearing stress on the pavement and braking will also become less effective due to a reduction in the frictional force between the tire and the ground. Therefore, a high inflation pressure was chosen for the landing gear tires.

Since a very thin wing airfoil is used on the aircraft to allow for supersonic flight, it is not possible to retract the landing gears into the aircraft wing. In order to account for the wheel track and still have a retractable landing gear, the gears are placed on the aircraft wings and the wheels are retracted into the fuselage laterally.

The cross section of the gear strut is primarily a function of the aircraft mass, load per wheel and strut material. The material chosen to use for the landing gear strut is a Titanium 6-4 (Ti-6Al-4V) alloy.

**Table 12.1.1:** Landing Gear Sizing

	<b>Main gear</b>	<b>Nose gear</b>
Load on gear	19594 kg	2177 kg
Gear Height	1.2 m	1.2 m
Distance from C.G	1.7 m	14.3 m
Wheel Track	4.46 m	
Wheel Diameter	0.83m	0.31 m
Wheel Width	0.3m	0.11 m
Strut Radius	0.039 m	0.0102 m

The main gear retraction system (see Figure 12.1.2) that was selected consists of a retraction shaft and a drag strut. The retraction shaft extends from the aircraft fuselage to the gear and the drag strut is attached to the wing. The gear strut also consists of an oleo-pneumatic shock absorption system.

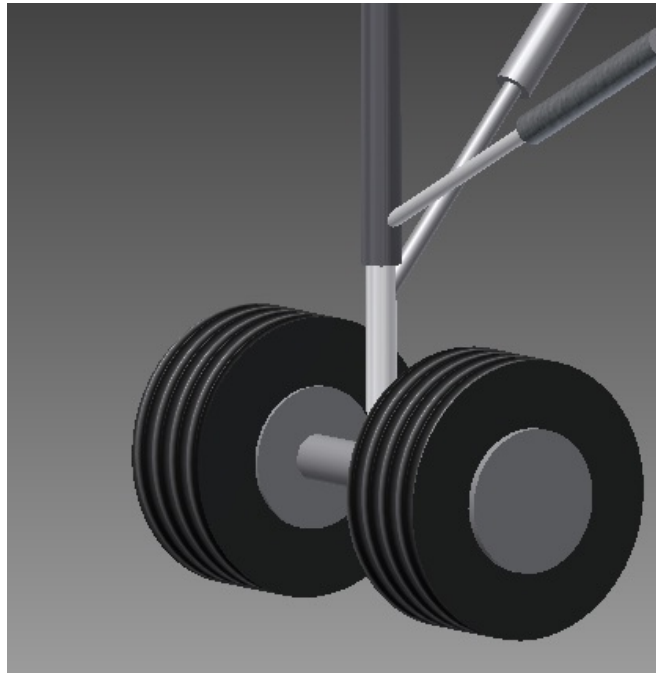


**Figure 12.1.2:** Main gear configuration.

## 12.2 Fuel Systems

The primary fuel storage location is the fuselage since the wings have a low thickness to chord ratio, necessitated by supersonic aerodynamics. The nose has small trim tanks nestled around the landing gear and extendable nose boom, used primarily as ballasts to control center of gravity while the other fuel tanks are drained. Running the length of the fuselage, below the cockpit and cabin floor, are the larger, primary tanks. Traditionally this area would be used for cargo space and avionics, but these items are instead stored at the aft end of the cabin.

Seventy percent of the wing volume is occupied by fuel, a feat proved to be possible by the MiG-29. Additionally, sixty percent of the vertical tail volume is estimated to be used for fuel storage purposes. The vertical tail will be used as a trim tank in conjunction with the nose tank. A summary of the fuel volumes stored in each tank is summarized in Table 12.2.1:

Final Report  
*Supersonic Business Jet Design Team*

**Table 12.2.1:** Fuel Volumes

Wing	5.228 m <sup>3</sup>	184.601 ft <sup>3</sup>
Vertical Tail	1.163 m <sup>3</sup>	41.066 ft <sup>3</sup>
Fuselage	9.9745 m <sup>3</sup>	352.200 ft <sup>3</sup>
Total	16.3061 m <sup>3</sup>	575.768 ft <sup>3</sup>

Electric fuel pumps will be used to deliver fuel and limit center of gravity changes during flight as fuel is transferred between partitioned tanks. This system is monitored and control semi-autonomously from the cockpit.

Since fuel is stored in the belly of the vehicle, a gear up landing would prove catastrophic. As such, methods to dump fuel from the belly tanks would be integrated, allowing for the vehicle to deplete the belly tanks while on final approach in the event of an engine out, gear up landing.

Additionally, the Kevlar lined fuel tanks would be implemented in response to the BAC Concorde crash. The use of Kevlar lining would significantly reduce the rate at which a fire would spread (Concorde SST).

### **12.3: Internal Configuration**

The internal configuration of the aircraft is complicated due to the long, slender nature of a business jet, with significant changes in fuselage cross section to account for area rule considerations. Additionally, a large portion of the fuselage needs to be devoted to fuel storage since the wings are thin due to supersonic aerodynamic necessities.

The nose of the vehicle houses the extendable nose boom, forward landing gear and forward fuel tanks. These components are all located ahead of the forward pressure wall. The forward pressure tanks are small, but act as variable ballasts to increase control on center of gravity location during flight.

Aft of the forward pressure wall is the cockpit area, avionics panels and partial avionics. The remaining avionics and electronic flight controls are located aft of the lavatory (before the aft pressure wall). This positioning will allow for temperature and

Final Report  
*Supersonic Business Jet Design Team*

pressure control for the avionics, and for ease of maintenance. Aft of the cockpit is the cockpit-cabin dividing wall for security reasons.

The cabin layout was sized to allow for a maximum of 12 passengers. Figure 12.3.1 shows a sample configuration for an 8 passenger luxury layout. The cabin will be explained in more detail in section 12.6.

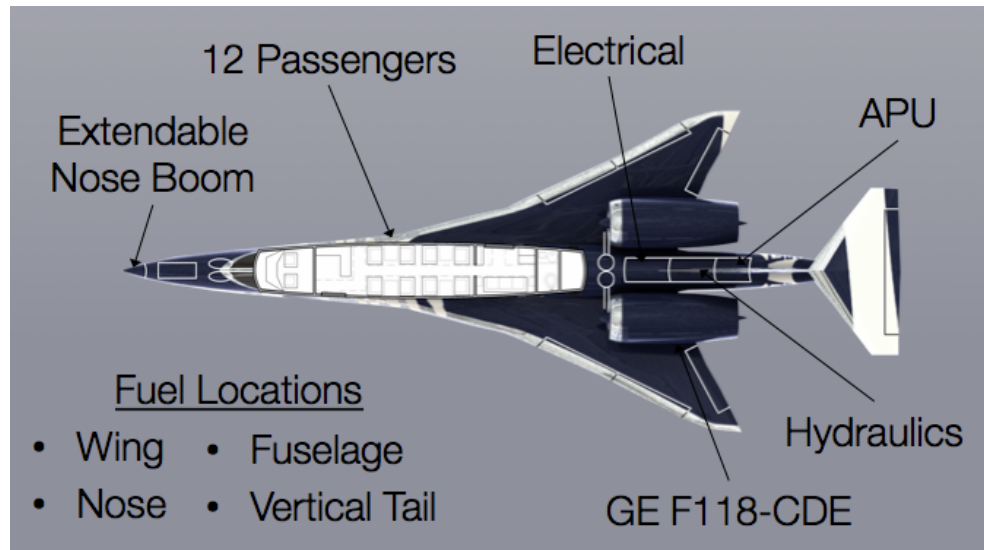


**Figure 12.3.1:** Planform Configuration

## 12.4: Hydraulic and Electrical Systems

Aft of the rear pressure wall is the electrical and environmental systems, auxiliary power unit and hydraulic systems. These occupy the rear third of the fuselage, aft of the main landing gear. These systems are expected to occupy 70% of the aft fuselage, with the remaining volume to be devoted to rear fuel tanks.

The control surfaces and high lift devices are powered hydraulically. For redundancy, three hydraulic systems are used. The electrical system will power the avionics, nose boom extension, fuel transport systems and cabin environment systems.

To minimize structural weight, and allow for higher pressure gradients, the vehicle will use a combination of traditional and synthetic windows. From the outside, the vehicle

Final Report  
*Supersonic Business Jet Design Team*

will appear to have conventional windows. From the inside, every second window is synthetic – replaced with an OLED display and camera system. These OLED displays double as presentation/display surfaces during flight, or act as a traditional window.

## 12.5 Cockpit

The cockpit will have room for a pilot and a co-pilot, and will feature state of the art glass avionics as primary instruments. Secondary backup instrumentation will be included as well, as per FAR for IFR flight. Pilot visibility will be limited due to the long slender nature of the vehicle, so synthetic vision systems were chosen instead of a “drooping nose” as seen on the Tupolev Tu-144. The areas requiring synthetic vision has been estimated in Figure 12.5.1:

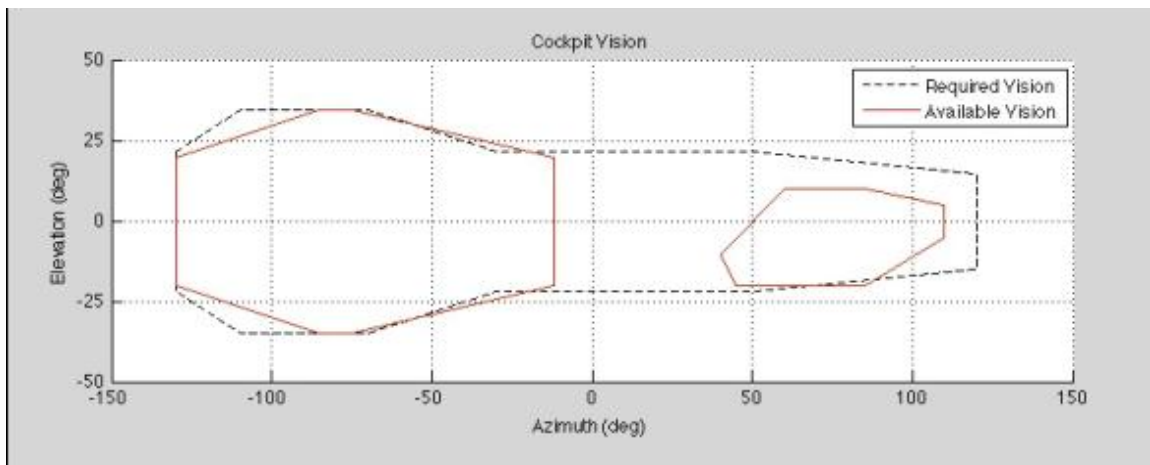


**Figure 12.5.1: Synthetic Vision Requirements**

The weights and volumetric requirements for avionics were taken into account during the cockpit sizing process. Weights were estimated statistically (Raymer, Nelson). Volumetric requirements were taken from aircraft with similar complexity, but discounted to account for the increase in glass components and therefore the trend in decreasing volumetric needs. The length of the cockpit was determined to be 1.62 meters to allow for integration of the nose boom and landing gear systems.

Final Report  
*Supersonic Business Jet Design Team*

This very preliminary sizing and cockpit systems accounting was decided to be sufficient for this project. If desired, future teams could easily perform further detailed avionic and ergonomic design to elaborate.

## 12.6 Cabin

The cabin was sized according to the following measurements listed in Table 12.6.1.

**Table 12.6.1:** Cabin Sizing Parameters

Width	2.00 m
Length	11.1 m
Outer Contour Cabin Lining	0.09 m
Aisle Space	0.30 m
Seat Cushion Width	0.532 m
Armrest Width	0.114 m
Seat Height	1.33 m
Seat Depth	0.6034 m

These standards are based on typical first class parameters, many obtained from Airbus designs. The SonicSwift's cabin capacity is currently 12 passengers, with a typical layout being tailored to around 8 passengers. The interior will ultimately be user-configured, as is standard to the aviation world.

The scope of the SonicSwift's use is V.I.P.'s such as senators, world leaders, cabin members, etc. Because of this, the cabin design will emphasize luxury over other qualities. A sample layout is given in Figure 12.6.1 below.

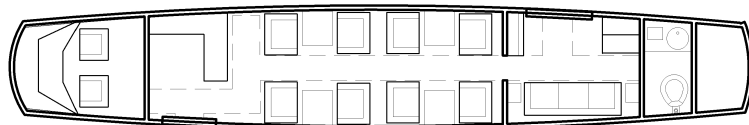


**Figure 12.6.1** Sample Cabin Configuration

Final Report  
*Supersonic Business Jet Design Team*

This particular example features tables for use by the individual passengers along with first class-rated seats, and a multi-purpose couch aft of the cabin. The storage for luggage is included in the rear, along with a coat rack while also including a bar in the front of the cabin for refreshments and drinks. Again, the interior can and will be tailored to any specific user's preferences.

## **12.7 Emergency**

The alert system will provide audio and visual warnings for the flight crew and passengers. This will consist of a beeper and flashing light within the flight compartment and in both vestibules within the cabin. When the arming and control switch in the flight deck is turned to the ON position, the system will automatically actuate at all three stations. The cabin control switch may sound the alert system if the flight deck's control switch is set in the ARM position. If the cabin's switch is set to ON, but the flight deck's switch is in the off position, only the flight deck's flashing light visual will be actuated. The audio alert warnings at each station may be individually turned ON or OFF at the flight crew's discretion.

The flight deck compartment's emergency and safety equipment will include a flashlight and smoke goggles for each crew member at his/her station. There will be one portable oxygen mask and pack in the equipment rack, along with a CO<sub>2</sub> fire extinguisher, one axe, one pair of asbestos gloves, a first aid kit and two life jackets.

The passenger cabin will have three fire extinguishers. Two CO<sub>2</sub> extinguishers will be placed by the forward left-hand door and rear right-hand door. The water extinguisher will be placed at the rear right-hand door. One ditching line will be placed at the entrance's vestibule along with an escape rope, escape slide, and life raft. The front vestibule will also store one emergency pack, a radio beacon, and a megaphone. One life jacket will be placed under each passenger seat. Two adult and one infant life jacket will be placed in the rear vestibule as extras along with a first aid kit and one portable oxygen set.

There will be two emergency oxygen systems: one for the flight crew and one for the passenger. They will be independent of one another, and will employ oxygen from their

Final Report  
*Supersonic Business Jet Design Team*

own storage cylinders. However, an interconnection will allow one system to draw oxygen from the other system in case of failure. The crew's control panel will be located in the flight deck and the passenger's control panel will be located near the front vestibule.

## **13. SONIC BOOM MITIGATION AND ESTIMATION**

The commercial success of this vehicle relies heavily on the ability to minimize the sonic boom impact on the ground. FAR and ICAO regulations currently prohibit supersonic flight over land, which severely limits the feasibility of this vehicle design. NASA, Gulfstream and other companies recognize the fact that if the perceived loudness (PldB) of a vehicle can be sufficiently low, there stands a high chance to change current international regulations to allow for supersonic flight over land. NASA has set a goal of 70.0 PldB on the ground as an acceptable level – in comparison the BAE Concorde routinely topped 104 PldB (“N+2”).

The shape and strength of a the sonic impact on the ground is determined by vehicle geometry, weight, flight altitude and speed, and atmospheric perturbations. At a distance a few body lengths from the vehicle (“near field”), the sonic boom pattern is very defined, with sawtooth overpressure jumps. As this near field boom radiates from the vehicle towards earth, passing through the atmosphere, the sawtooth overpressures coalesce into what is known as an “N-wave” for its apparent shape, as seen in Figure 13.1:

Final Report  
*Supersonic Business Jet Design Team*

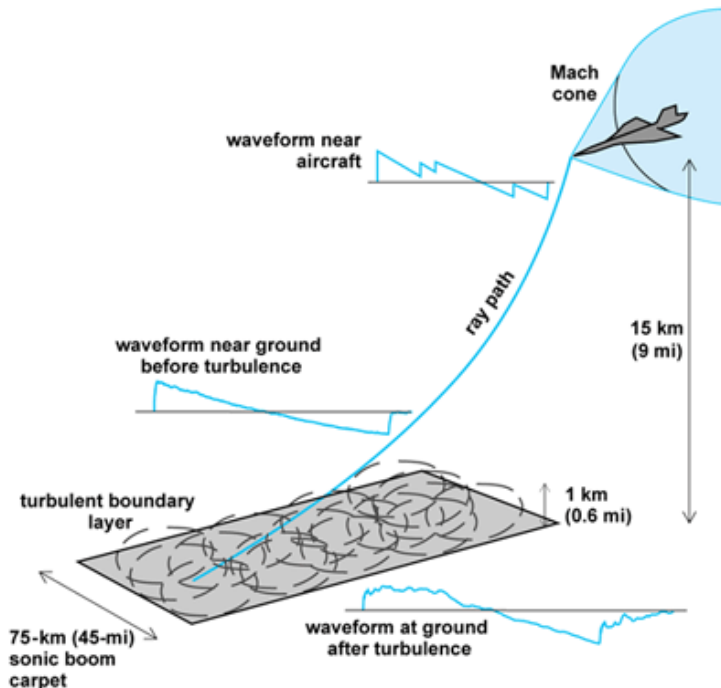


**Figure 13.1:** Sonic Boom Evolution through Atmosphere  
([www.assessscience.com /content/Sonic-boom/636800](http://www.assessscience.com/content/Sonic-boom/636800))

Outside of aircraft sonic boom shaping technologies, a smaller aircraft flying at higher altitudes will have a smaller sonic boom impact on the ground than the Concorde. This is due to the fact that there is less volume breaking the sound barrier, producing a boom that weakens faster. The higher the flight altitude, the more opportunity for the boom to diminish as it passes through the atmosphere.

The most damaging part of the N-wave is the initial overpressure rise, and the time in which the pressure rise occurs. A single overpressure that occurs very rapidly produces more damage than a N-wave in which the pressure rise is gradual and spread across several smaller booms (Figure 13.2).

Final Report  
*Supersonic Business Jet Design Team*

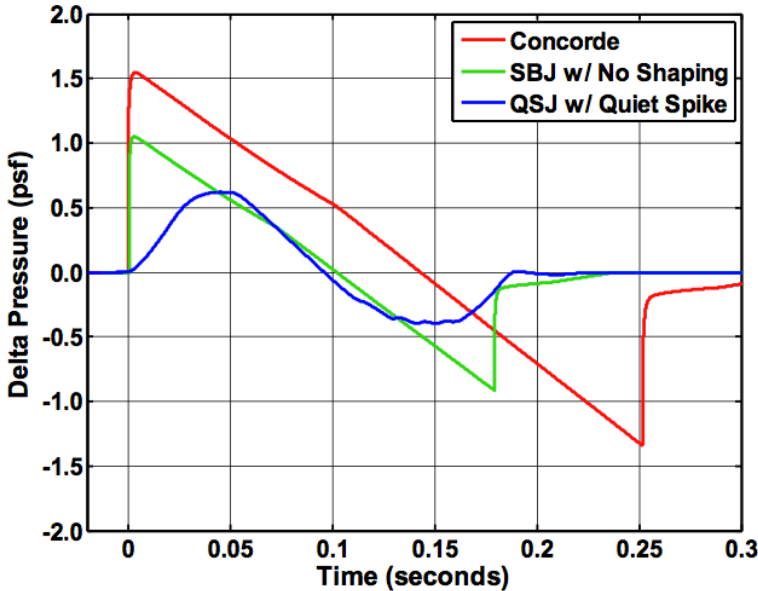


**Figure 13.2:** N-Wave Profile for Concorde, Supersonic Business Jet with and without “Quiet Spike” Technology

Gulfstream, in partnership with NASA has developed a “Quiet Spike” meant to break up the initial single overpressure into three separate shock waves, which coalesce as they travel through the atmosphere to form a pressure wave without the sharp spike seen with a single shock wave.

This “Quiet Spike” technology essentially extends the nose of the vehicle at supersonic speeds. On the ground, the spike is retracted into the body of the vehicle to allow for better ground handling characteristics. This technology is incorporated in our vehicle, and is expected to decrease the sonic boom created significantly. The figures below show spike retraction/extension positions and corresponding near field shock patterns.

Final Report  
Supersonic Business Jet Design Team

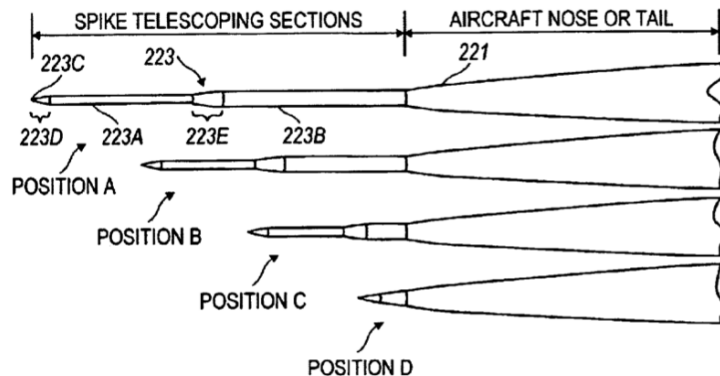


**Figure 13.3:** "Quiet Spike" retraction/extension positions  
(US Patent No. 6,698,684B1, Figure 14)

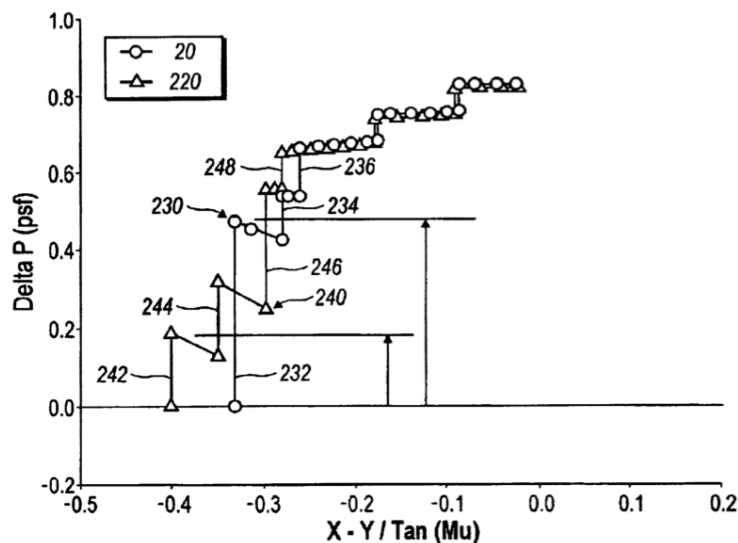


**Figure 13.4:** Near field shock wave overpressures.  
(US Patent No. 6,698,684B1, Figure 15)

Additionally, shaping the nose of the vehicle and greatly reduce the sonic boom experienced on the ground. NASA's "shaped boom" research has shown that having a non-symmetric nose section can lower the maximum initial overpressure, as seen in Figure 13.5 below:

Final Report  
*Supersonic Business Jet Design Team*

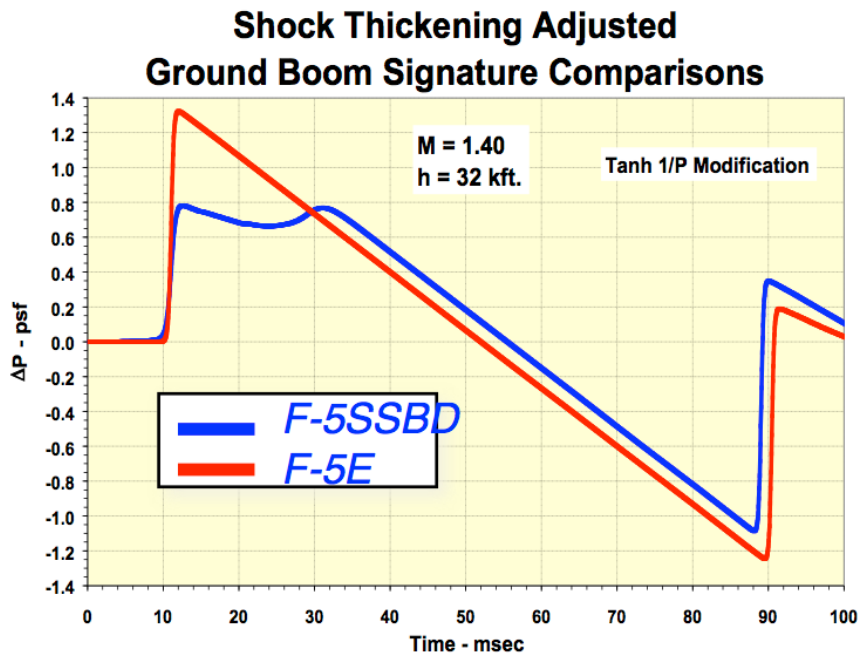
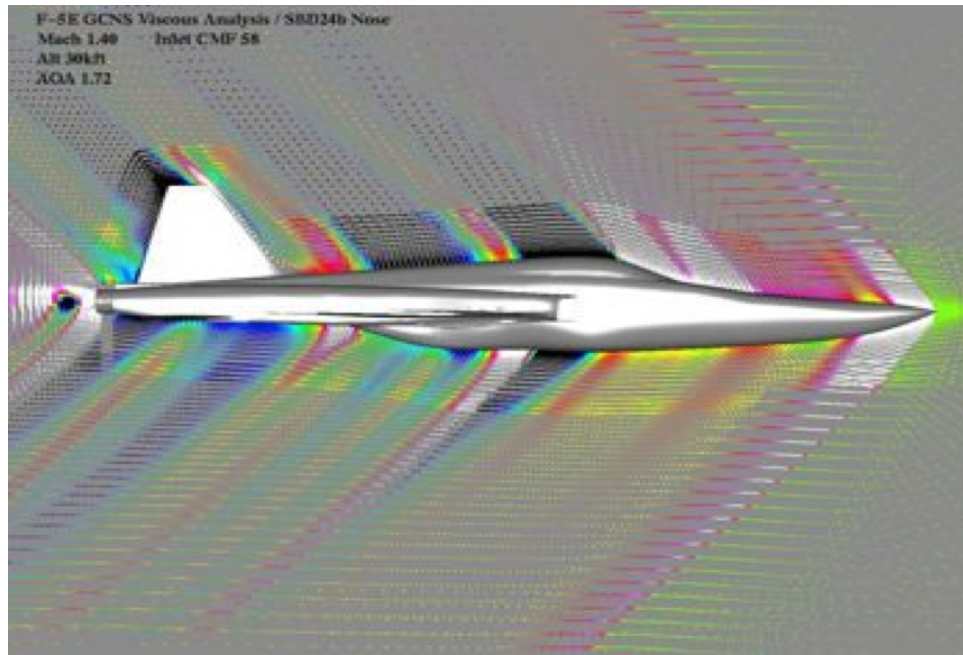


**Figure 13.5:** “Shaped Boom” ground signature (NASA).

The corresponding optimum nose shaping was implemented on a Navy F5-E, and is seen below in Figures 13.6 and 13.7:



Final Report  
*Supersonic Business Jet Design Team*

**Figure 13.6:** CFD Analysis of F5-E with Shaped Nose. “Shaped Sonic Boom Demonstrator” (NASA).



**Figure 13.7:** Actual “Shaped Sonic Boom Demonstrator” F5-E vehicle (NASA).

As a way to measure the overall impact of the sonic boom, we developed two methods of calculating the strength and impact of an idealized sonic boom that has the above sonic boom mitigation configurations. One of the methods is called the Figure of Merit (Seebass, and George). Figure of Merit is a function of the aircraft's weight, length and Mach number and is calculated by using the equation below.

$$FOM = \left( \frac{\beta W}{P_g l^{3/2} \sqrt{h}} \right) e^{h/(2H)} 10^3$$

Where,  $P_g$  is the ambient pressure,  $l$  is the length of the aircraft,  $W$  is the weight of the aircraft,  $h$  is the cruise altitude and  $\beta = \sqrt{M^2 - 1}$ .

The lower this value, lesser boom the aircraft generates. Figures of Merit values of 1.0 or lower are considered acceptable. For our aircraft with a single spike the Figure of Merit value was calculated as 1.028.

The other method involves measuring the strength of the sonic boom in terms of Perceived loudness levels. The perceived loudness of the shock depends on the shock over

Final Report  
*Supersonic Business Jet Design Team*

pressure and the rise time. For an N wave generated by a sonic boom this can be calculated by using the following equation.

$$PLdB = 55 + 20\log_{10} \frac{\Delta p}{\tau}$$

Where  $\Delta p$  is the overpressure and  $\tau$  is the shock rise time. The acceptable values of perceived loudness are 70.0 dB or lower. According to these calculations our aircraft would generate a sonic boom of perceived loudness 82.2 dB.

A perceived loudness of 82.2 dB is still louder than desired, but it is significantly quieter than the Concorde, and is the best approximation we have reached through our low-fidelity modeling. This level of modeling is sufficient for our design project, proving that it is possible to design a supersonic business jet that can operate several orders of magnitude quieter than previous vehicles, most notably, the BAC Concorde.

## 14. COSTS ESTIMATION

To estimate the project costs and fly-away costs, statistical data equations were used heavily to create an initial estimate of the costs. Traditional statistical data equations (Raymer) generally approximate costs from complex aircraft with a combination of several crucial variables: Mach number, number of engines, weight, thrust and maximum turbine inlet temperature.

The statistical data equations used (Raymer) yielded results in 1999 USD, so these values had to be adjusted for inflation to 2011 USD, which is equivalent to a 36% rise in price, as indicated by the Consumer Price Index (a primary measure of the yearly inflation in an economy). Using CPI as an indication of aircraft price trends is recognized to be quite poor, so several other factors were used to better estimate fly-away costs. For example, increases in manufacturing technology were assumed to decrease quality control hours by 15%.

Due to the inherent complexity of a supersonic aircraft and to account for engineering focus on sonic boom mitigation, a 5% overall 'fudge-factor' was included for the design hours. A 20% increase for materials was justified to account for significant

Final Report  
*Supersonic Business Jet Design Team*

increases in materials cost, and due to the increased tooling hours required for higher grade materials.

Finally, a simple trade study of high-technology business jet costs was performed. In this informal study, business jets capable of similar passengers and range were seen to cost in the range of \$19-35 million.

A critical portion of determining the project cost and fly-away cost is an estimate of the number of aircraft that will be produced. A Russian corporate study (Tupolev, 1998) found that there was a market for 200 supersonic business jets. As such, the project was assumed to produce a minimum of 200 aircraft. With this, the fly-away cost is estimated to be \$42.68 million, with the total project cost being \$8.54 billion. A tabulated summary of the various costs can be found in Appendix II.

## **15. FAA REQUIREMENTS**

The single largest design constraints are those imposed in the Federal Aviation Regulations (FAR), which define in great detail the performance and design of any civilian aircraft. Since we will be operating as a civilian aircraft, it is crucial to strictly adhere to the FAR requirements in order to operate in United States airspace. The most pertinent FAR requirements are included in Appendix III.

## **16. SIZING EVOLUTIONS**

The initial design vehicle sizing was based off the competitor research performed in the Fall of 2011. It became quickly apparent that this initial design was grossly oversized, but the sizing parameters were not altered until the beginning of 2012, when all of the component calculation codes were compiled into a single code structure. The reason for this was to minimize the confusion between analysis teams regarding what the “current

Final Report  
*Supersonic Business Jet Design Team*

“vehicle” was, before we had a single unified location to store vehicle information. For a more detailed discussion of this, see Section 4.3.

The most drastic resizing occurred in January 2012, when the vehicle was scaled down significantly. At the conclusion of the Fall semester (2011), it became obvious that the cabin was grossly oversized, on the order of 3x too large. This had ramifications for the entire vehicle being too large. Figure 16.1 shows the vehicle at the end of 2011, and Table 16.2 has the characteristic parameters.

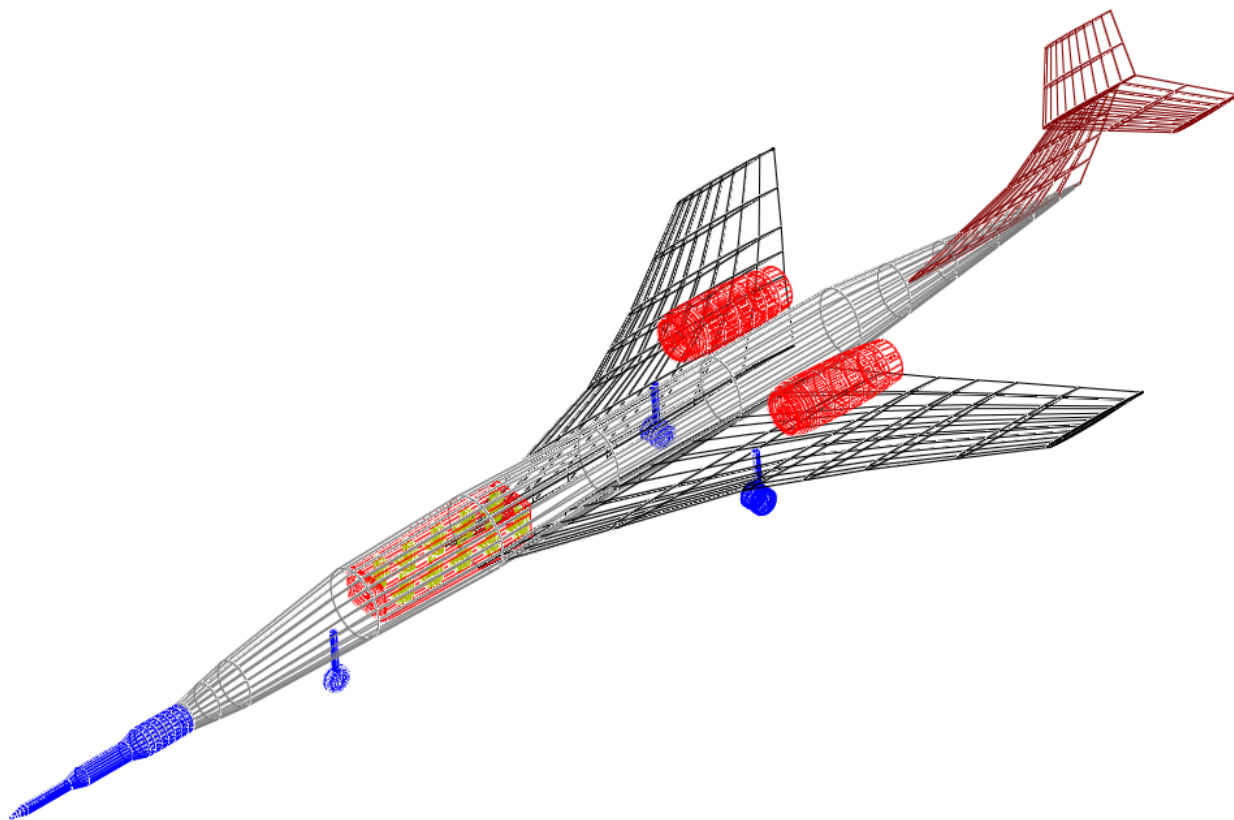


**Figure 16.1:** Initial Vehicle Design (Red box is cabin)

**Table 16.2:** Initial Vehicle Design Characteristic Parameters

Length	40 m	131.2 ft
Wing Area	150 m <sup>2</sup>	1615 ft <sup>2</sup>
Vertical Tail Area	15 m <sup>2</sup>	161.5 ft <sup>2</sup>
Horizontal Tail Area	15 m <sup>2</sup>	161.5 ft <sup>2</sup>
TOGW	35,626 kg	78,544 lbs
Wing Loading	2240.3 N/m <sup>2</sup>	46.79 lb/ft <sup>2</sup>

Final Report  
*Supersonic Business Jet Design Team*

Top Mach #	0.92
Cost	\$78.42 million

Knowing that the initial design was oversized, the fuselage length was decreased significantly, and in turn the wing and control surfaces were scaled down as well. This smaller vehicle had a lower weight, lower drag, and therefore, lower propulsion requirements. The second vehicle design is shown in Figure 16.3 and Table 16.4 below.

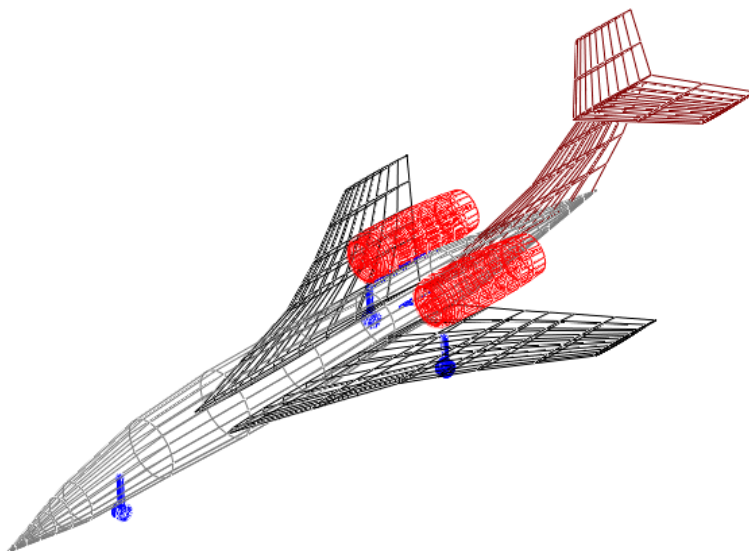


**Figure 16.3:** Second Vehicle Design

**Table 16.4:** Second Vehicle Design Characteristic Parameters

Length	25 m	82.02 ft
Wing Area	45 m <sup>2</sup>	484.4 ft <sup>2</sup>
Vertical Tail Area	8 m <sup>2</sup>	86.11 ft <sup>2</sup>
Horizontal Tail Area	11 m <sup>2</sup>	118.4 ft <sup>2</sup>
TOGW	21,771 kg	47,997 lbs
Wing Loading	4746.4 N/m <sup>2</sup>	99.13 lb/ft <sup>2</sup>
Top Mach #		2.5
Cost		\$42.68 million

At the time of the second vehicle design, the code structure was developed enough to allow for multi-disciplinary analysis, but not multi-disciplinary optimization. Following

Final Report  
*Supersonic Business Jet Design Team*

the second vehicle design, the vehicle was “close enough” to the expected final design to allow for select aspects to be analyzed and optimized with the code structure. This process is further outlined in Section 3. Heavy use of the MDO code structure, and refinements in component analysis techniques allowed us to converge to a final design vehicle, outlined in Section 17.

Iterative advancements in the vehicle design were carried out through the MDO code, with only minor changes from the second vehicle design, until there was a significant break-through with the propulsion modeling. This is outlined further in Section 7.3, but allowed for a lower weight engine, that had a lower fuel consumption. This gave us an increase in range, allowing for trans-Pacific flight. Prior to this breakthrough, the fuselage was going to be lengthened to allow for an increase in fuel volume.

## 17. FINAL DESIGN

### 17.1. Final Vehicle Design

With heavy use of the MDO code structure, and the component analysis code, developed and/or integrated in-house, our team was able to converge on a final vehicle. This vehicle takes into sonic boom mitigation techniques outlined in Section 13, low-drag aerodynamics outlined in Section 5, cutting-edge structures analysis techniques and optimization outlined in Section 8 and all major, necessary systems components outlined in Section 12. Table 17.1.1 below shows the characteristic parameters for the final design vehicle, and Section 17.2 contains a range of artist renditions of the vehicle.

**Table 17.1.1:** Final Vehicle Design Characteristic Parameters

Length	25 m	82.02 ft
Wing Area	41.86 m <sup>2</sup>	450.58 ft <sup>2</sup>
Vertical Tail Area	7.55 m <sup>2</sup>	81.27 ft <sup>2</sup>
Horizontal Tail Area	13.06 m <sup>2</sup>	140.58 ft <sup>2</sup>
TOGW	19,656 kg	43,335 lb
Wing Loading	4425.1 Pa	92.42 lb/ft <sup>2</sup>

Final Report  
*Supersonic Business Jet Design Team*

Loudness	82.2 PldB	
Subsonic Max Range	13,200 km	
Subsonic Optimal Cruise	Mach 0.92	
Supersonic Max Range	9,200 km	
Supersonic Optimal Cruise	Mach 2.20	
Top Mach #	Mach 2.50	
Cost	\$40.32 million	
# Passengers	Max: 12; Luxury: 8	

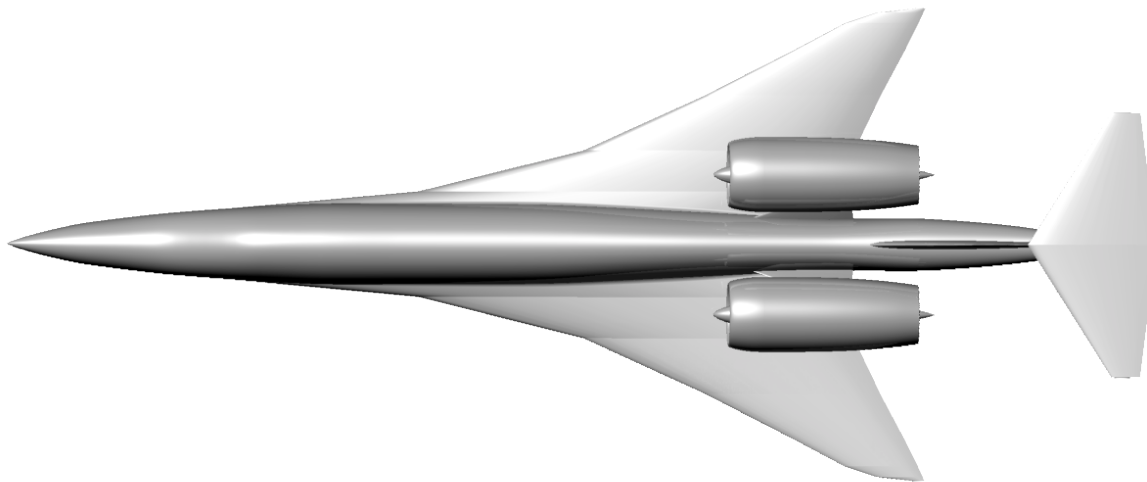


**Figure 17.1.2:** Final Vehicle Design, Top View



**Figure 17.1.3:** Final Vehicle Design, Side View

Final Report  
*Supersonic Business Jet Design Team*



**Figure 17.1.4:** Final Vehicle Design, Front View

Final Report  
*Supersonic Business Jet Design Team*

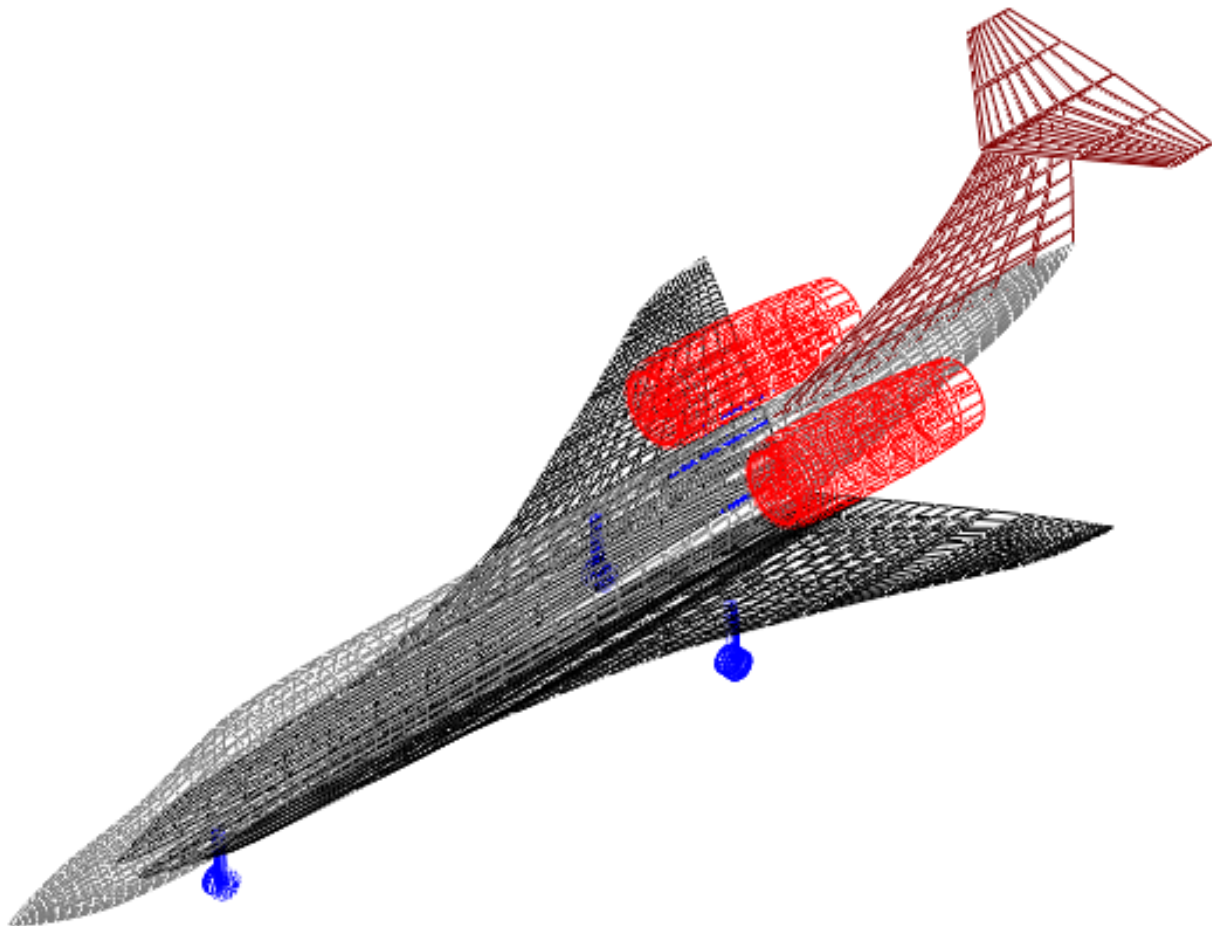


**Figure 17.1.5:** Final Vehicle Design, Isometric

Final Report  
*Supersonic Business Jet Design Team*

## 17.2. Vehicle Mockup and Branding



**Figure 17.2.1:** *SonicSwift* with paint scheme and windows.

With the assistance of an interior designer and industrial designer, the final vehicle designed has been branded as the *SonicSwift*, a name that reflects its speed and ability to fly supersonically.



**Figure 17.2.2:** *SonicSwift* Logo

Final Report  
*Supersonic Business Jet Design Team*



**Figure 17.2.3:** *SonicSwift* side view

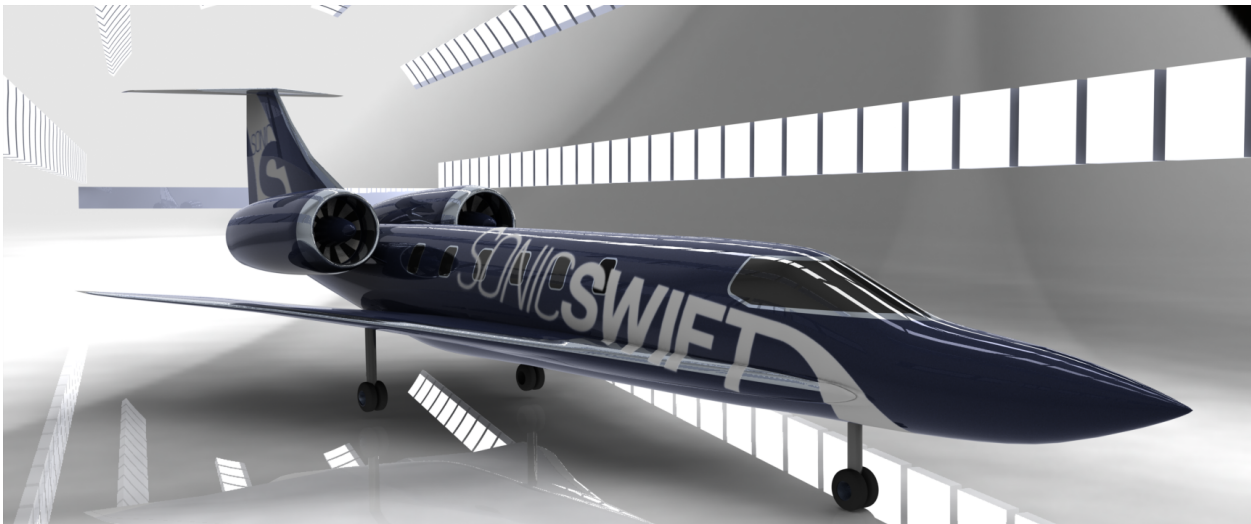


**Figure 17.2.4:** *SonicSwift* in a Hangar.

### 17.3. Comparison to the Cessna Citation X

The *SonicSwift* is remarkably, but unintentionally, similar to the recent Cessna Citation X. The Citation X is also a mid-sized business jet, with a top speed of Mach 0.92. It is widely considered as the fastest, most advanced mid-sized jet on the market today. The convergence of the *SonicSwift* to the Citation X provides a level of confidence in our analysis

Final Report  
*Supersonic Business Jet Design Team*

calculations, as our vehicle's primary differences are larger engines and careful considerations for supersonic aerodynamics. Table 17.3.1 below outlines the similarities between the two vehicles.

**Table 17.3.1:** Comparison between *SonicSwift* and Citation X

	SonicSwift	Citation X
# Passengers	12	12
Length	25 m	22.05 m
Wing Area	45 m <sup>2</sup>	48.96 m <sup>2</sup>
Vertical Tail Area	8 m <sup>2</sup>	10.31 m <sup>2</sup>
Horizontal Tail Area	11 m <sup>2</sup>	11.15 m <sup>2</sup>
TOGW	47,989 lbs	36,400 lbs
Wing Loading	99 lb/ft <sup>2</sup>	68.5 lb/ft <sup>2</sup>
Cruise Mach	2.20	0.92
Cost	\$42.4 mil	\$22 mil

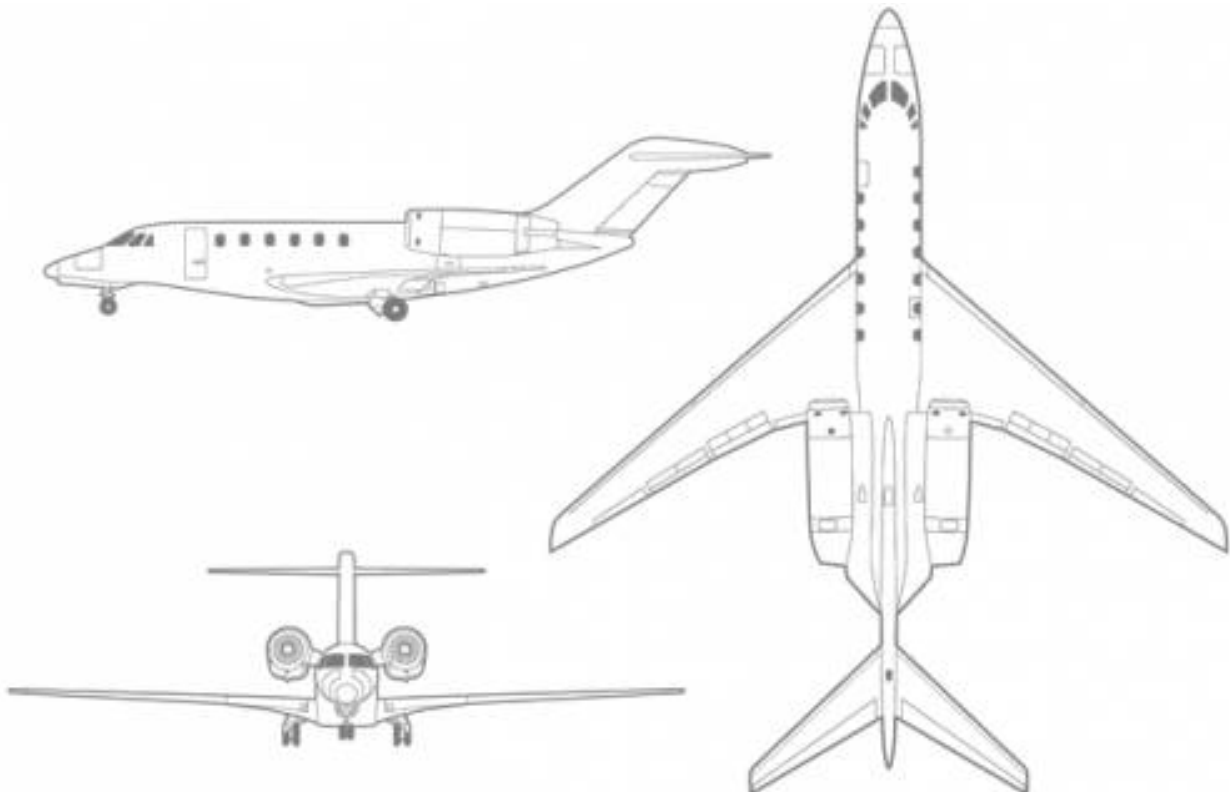


**Figure 17.3.2:** Cessna Citation X.

([http://www.the-blueprints.com/blueprints/modernplanes/cessna/40970/view/cessna\\_citation\\_x/](http://www.the-blueprints.com/blueprints/modernplanes/cessna/40970/view/cessna_citation_x/))

Final Report  
*Supersonic Business Jet Design Team*

## **18. CONCLUSION**

In conclusion, this report shows that it is economically and technology feasible for a supersonic, mid-sized business jet to enter the market and achieve low enough sonic boom impact to change current FAA/ICAO regulations to allow for supersonic flight over land. The final design vehicle, the *SonicSwift*, is unique in its merging of high performance propulsion systems, advanced aerodynamics and sonic boom mitigation techniques, and the incorporation of a luxurious interior. The vehicle is marketed to heads of state, military leaders and corporate executives, a potential market large enough to sustain this project despite the technical and manufacturing challenges involved in bringing it to market and obtaining airworthiness certificates.

Final Report  
*Supersonic Business Jet Design Team*

## REFERENCES

- "AE 429 - Aircraft Performance and Flight Mechanics." Wallace H. Coulter School of Engineering. <http://people.clarkson.edu/~pmarzocc/AE429/AE-429-6.pdf>
- "Airfoil Investigation Database". World of Krauss. <<http://www.worldofkrauss.com/foils/1602>>. Web. 25 February 2012.
- Anderson, John D. "10: Conical Flow." *Modern Compressible Flow with Historical Perspective*. 2nd ed. New York: McGraw-Hill, 1982. 295-306. Print.
- Concorde SST. "Concorde: Return to Flight".  
<<http://www.concordesst.com/returntoflight/mods.html>>. 04/23/2012.
- Colville, Jesse R., and Mark J. Lewis. *An Aerodynamic Redesign of the SR-71 Inlet with Applications to Turbine Based Combined Cycle Engines*. Tech. no. AIAA 2004-3481. Fort Lauderdale: American Institute of Aeronautics and Astronautics, 2004. Print. AIAA/ASME/SAE/ASEE Joint Propulsion Conference and Exhibit.
- "EPA Proposed NOx Emission Standards for Aircraft Gas Turbine Engines." *Environmental Protection Agency*. EPA, Jul 2011. Web.  
<<http://www.epa.gov/otaq/regulations/nonroad/aviation/420f11019.htm>>.
- Gunston, Bill. *Jane's Aero-Engines*. Coulsdon, Surrey, UK: Jane's Information Group, 2000. Print.
- Hill, Philip G., and Carl R. Peterson. *Mechanics and Thermodynamics of Propulsion*. 2nd ed. Reading, MA: Addison-Wesley, 1992. Print.
- Krammer, Paul, Klaus Rued, and Jens Truebenbach. *Technology Preparation for Green Aero Engines*. Tech. no. AIAA 2003-2790. Dayton: American Institute of Aeronautics and Astronautics, 2003. Print. AIAA/ICAS International Air and Space Symposium and Exposition.
- Lassaline, J. V. *Supersonic Right Circular Cone at Zero Angle of Attack*. Ryerson University, 13 Mar. 2009. Web. 12 Oct. 2011.
- "Load Factors: Airplane Operating Limits". Free Online Private Pilot Ground School. <[http://www.free-online-private-pilot-ground-school.com/Load\\_factors.html](http://www.free-online-private-pilot-ground-school.com/Load_factors.html)>. Web.
- Lowrie, B W, R M. Denning, and P C. Gupta. *The Next Generation Supersonic Transport Engine: Critical Issues*. London: Royal Aeronautical Society, 1990. Print.
- Mack, Robert J. NASA Langley Research Center, Hampton, Virginia. "A Supersonic Business Jet Concept Designed for Low Sonic Boom". October 2003.

Final Report  
*Supersonic Business Jet Design Team*

Marchman, James F. III. *Introduction to Aerodynamics & Aircraft Performance*. Virginia Tech. 2004. Print.

Mascitti, Vincent R. NASA Technical Memorandum 74055. "A Preliminary Study on the Performance and Characteristics of a Supersonic Executive Jet". September 1977.

Mehta, Jayesh M., Dale Shouse, Gary Holloway, Brian Cox, and David Marshall. *Optimization of Integrally Woven SiC-SiC Ceramic Combustor Liner Thermal Parameters*. Tech. no. AIAA 2004-4081. Fort Lauderdale: American Institute of Aeronautics and Astronautics, 2004. Print. AIAA/ASME/SAE/ASEE Joint Propulsion Conference and Exhibit.

Raymer, D.P. *Aircraft Design: A Conceptual Approach*. 2<sup>nd</sup> ed. Washington DC. AIAA. 1992. Print.

Seebass, Richard, and Albert George. "Figure of Merit Research." Sonic Boom Measuring. MIT, 2010. Web. 27 Oct 2011. <<http://www.mit.edu/figureofmerit>>.

Shames, Irving H., and Clive L. Dym. *Energy and Finite Element Methods in Structural Mechanics*. London: Taylor & Francis Books, Inc., 2003. 257-314. Print.

Stanford Aircraft Aerodynamics and Design Group. <<http://adg.stanford.edu/>>. Web.

Stevens, S.S. "Perceived Level of Noise by Mark VII and Decibels (E)."

Szilard, Rudolph. *Theories and Applications of Plate Analysis*. Hoboken, New Jersey: John Wiley & Sons, 2004. 247-276. Print.

Ugural, A.C. *Stresses in Plates and Shells*. New York: McGraw-Hill Book Company, 1981. 106-121. Print.

**Final Report**  
*Supersonic Business Jet Design Team*

## APPENDIX I: VEHICLE WEIGHTS BREAKDOWN

	Weight (lb)	Loc. (ft)	Moment (ft-lb)
STRUCTURES	4141.8		203490.5
Wing	1933.9	49.2	95179.3
Horizontal Tail	102.5	80.4	8242.0
Vertical Tail	483.4	80.0	38662.5
Fuselage	3099.8	41.	42519.3
Main Landing Gear	783.6	53.3	41779.4
Nose Landing Gear	413.2	4.1	1694.6
Engine Mounts	115.2	68.1	7842.7
Nacelle	144.0	67.7	9744.4
Firewall	45.9	4.9	225.7
Nose Boom	120.0	2.0	240.0
PROPELLSION	6573.0		429187.1
Engines-installed	6000.0	67.7	393720.0
Engine controls	53.6	65.6	3519.7
Starter	129.7	68.9	8934.7
Fuel Systems & Tanks	389.7	59.1	23012.7
EQUIPMENT	2456.1		71769.8
Flight Controls	382.9	12.3	4711.4
Instruments	179.8	9.8	1769.7
Electrical System	1015.2	49.2	49963.7
Avionics	625.0	9.8	6151.7
Furnishings	198.4	32.8	6508.6
Air Cond. & Anti-Ice	28.3	55.8	1578.4
Handling	26.5	41.0	1086.3
USEFUL LOAD	31574.0		1527913.6
Crew	360.0	32.8	11811.6
Fuel	28764.0	49.2	1415621.4
Passengers	1800.0	41.0	73822.5
Cargo	350.0	41.0	14354.4
Seats	300.0	41.0	12303.8
TAKE OFF GROSS WEIGHT (lb)	44744.8		
DRY WEIGHT (TOGW - FUEL, lb)	15980.8		
WING LOADING (lb/ft <sup>2</sup> )	92.41		
CENTER OF GRAVITY	0.60824		

Final Report  
*Supersonic Business Jet Design Team*

## APPENDIX II: VEHICLE COSTS BREAKDOWN

### ENGINE DESIGN

Hours:	7289650
Rate:	\$ 116.96
Total:	\$ 852.60 million

### TOOLING

Hours:	9289075
Rate:	\$ 119.68
Total:	\$ 1111.72 million

### MANUFACTURING

Hours:	25171147
Rate:	\$ 99.28
Total:	\$ 2498.99 million

### QUALITY CONTROL

Hours:	2363126
Rate:	\$ 110.16
Total:	\$ 260.32 million

### DEVELOPMENT SUPPORT

Total:	\$ 533.08 million
--------	-------------------

### FLIGHT CONTROL TESTING

Total:	\$ 42.48 million
--------	------------------

### MATERIALS COST

Total:	\$ 1577.78 million
--------	--------------------

### ENGINE

Total:	\$ 7.00 million
--------	-----------------

Total for 200 Aircraft: \$ 8063.55 million

Cost per Aircraft: \$ 40.32 million

Final Report  
*Supersonic Business Jet Design Team*

## APPENDIX III: RELEVANT FAR REGULATIONS

### Appendix III.1: Performance

**--§ 25.113 Takeoff distance and takeoff run.**

(a) Takeoff distance on a dry runway is the greater of—

- (1) The horizontal distance along the takeoff path from the start of the takeoff to the point at which the airplane is 35 feet above the takeoff surface, determined under §25.111 for a dry runway; or
- (2) 115 percent of the horizontal distance along the takeoff path, with all engines operating, from the start of the takeoff to the point at which the airplane is 35 feet above the takeoff surface.

**--§ 25.125 Landing.**

(a) The horizontal distance necessary to land and to come to a complete stop (or to a speed of approximately 3 knots for water landings) from a point 50 feet above the landing surface must be determined (for standard temperatures, at each weight, altitude, and wind within the operational limits established by the applicant for the airplane)

### Appendix III.2: Performance/Controllability and Maneuverability

**--§ 25.143 General.**

(a) The airplane must be safely controllable and maneuverable during—

- (1) Takeoff;
- (2) Climb;
- (3) Level flight;
- (4) Descent; and
- (5) Landing.

(b) It must be possible to make a smooth transition from one flight condition to any other flight condition without exceptional piloting skill, alertness, or strength, and without danger of exceeding the airplane limit-load factor under any probable operating conditions, including—

- (1) The sudden failure of the critical engine;

### Appendix III.3: Structures

**--§ 25.301 Loads.**

(a) Strength requirements are specified in terms of limit loads (the maximum loads to be expected in service) and ultimate loads (limit loads multiplied by prescribed factors of safety). Unless otherwise provided, prescribed loads are limit loads.

(b) Unless otherwise provided, the specified air, ground, and water loads must be placed in equilibrium with inertia forces, considering each item of mass in the airplane. These loads must be distributed to conservatively approximate or closely represent actual conditions. Methods used to determine load intensities and distribution must be validated by flight load measurement unless the methods used for determining those loading conditions are shown to be reliable.

(c) If deflections under load would significantly change the distribution of external or internal loads, this redistribution must be taken into account.

### Appendix III.4: Flight Loads

**--§ 25.321 General.**

(a) Flight load factors represent the ratio of the aerodynamic force component (acting normal to the assumed longitudinal axis of the airplane) to the weight of the airplane. A positive load factor is one in which the aerodynamic force acts upward with respect to the airplane.

(c) Enough points on and within the boundaries of the design envelope must be investigated to ensure that the maximum load for each part of the airplane structure is obtained.

Final Report  
*Supersonic Business Jet Design Team*

**--§ 25.365 Pressurized compartment loads.**

For airplanes with one or more pressurized compartments the following apply:

(d) The airplane structure must be designed to be able to withstand the pressure differential loads corresponding to the maximum relief valve setting multiplied by a factor of 1.33 for airplanes to be approved for operation to 45,000 feet or by a factor of 1.67 for airplanes to be approved for operation above 45,000 feet, omitting other loads.

## Appendix III.5: Cabin, Systems and Other Configurations

**Emergency Landing Conditions --§ 25.561 General.**

(c) For equipment, cargo in the passenger compartments and any other large masses, the following apply:

- (1) these items must be positioned so that if they break loose they will be unlikely to:
  - (i) Cause direct injury to occupants;
  - (ii) Penetrate fuel tanks or lines or cause fire or explosion hazard by damage to adjacent systems
  - (iii) Nullify any of the escape facilities provided for use after an emergency landing.

**--§ 25.807 Emergency exits**

(a) *Type*. For the purpose of this part, the types of exits are defined as follows:

- (1) *Type I*. This type is a floor-level exit with a rectangular opening of not less than 24 inches wide by 48 inches high, with corner radii not greater than eight inches.
- (2) *Type II*. This type is a rectangular opening of not less than 20 inches wide by 44 inches high, with corner radii not greater than seven inches. Type II exits must be floor-level exits unless located over the wing, in which case they must not have a step-up inside the airplane of more than 10 inches nor a step-down outside the airplane of more than 17 inches.
- (3) *Type III*. This type is a rectangular opening of not less than 20 inches wide by 36 inches high with corner radii not greater than seven inches, and with a step-up inside the airplane of not more than 20 inches. If the exit is located over the wing, the step-down outside the airplane may not exceed 27 inches.
- (4) *Type IV*. This type is a rectangular opening of not less than 19 inches wide by 26 inches high, with corner radii not greater than 6.3 inches, located over the wing, with a step-up inside the airplane of not more than 29 inches and a step-down outside the airplane of not more than 36 inches.
- (7) *Type A*. This type is a floor-level exit with a rectangular opening of not less than 42 inches wide by 72 inches high, with corner radii not greater than seven inches.
- (8) *Type B*. This type is a floor-level exit with a rectangular opening of not less than 32 inches wide by 72 inches high, with corner radii not greater than six inches.
- (9) *Type C*. This type is a floor-level exit with a rectangular opening of not less than 30 inches wide by 48 inches high, with corner radii not greater than 10 inches.

(b) *Step down distance*. Step down distance, as used in this section, means the actual distance between the bottom of the required opening and a usable foot hold, extending out from the fuselage, that is large enough to be effective without searching by sight or feel.

(c) *Over-sized exits*. Openings larger than those specified in this section, whether or not of rectangular shape, may be used if the specified rectangular opening can be inscribed within the opening and the base of the inscribed rectangular opening meets the specified step-up and step-down heights.

(d) *Asymmetry*. Exits of an exit pair need not be diametrically opposite each other nor of the same size; however, the number of passenger seats permitted under paragraph (g) of this section is based on the smaller of the two exits.

(e) *Uniformity*. Exits must be distributed as uniformly as practical, taking into account passenger seat distribution.

(f) *Location*.

- (1) Each required passenger emergency exit must be accessible to the passengers and located where it will afford the most effective means of passenger evacuation.

**Final Report**  
**Supersonic Business Jet Design Team**

(2) If only one floor-level exit per side is prescribed, and the airplane does not have a tailcone or ventral emergency exit, the floor-level exits must be in the rearward part of the passenger compartment unless another location affords a more effective means of passenger evacuation.

**(g) Type and number required**

(2) For a passenger seating configuration of more than 9 seats, each exit must be a Type III or larger exit.

(8) If a Type A, Type B, or Type C exit is installed, there must be at least two Type C or larger exits in each side of the fuselage.

**--§ 25.809 Emergency exit arrangement.**

(a) Each emergency exit must have means to permit viewing of the conditions outside the exit when the exit is closed. The viewing means may be on or adjacent to the exit provided no obstructions exist between the exit and the viewing means.

**--§ 25.815 Width of aisle**

The passenger aisle width at any point between seats must equal or exceed the values in the following table:

<b>Passenger seating capacity</b>	<b>Minimum passenger aisle width (inches)</b>	
	<b>Less than 25 in. from floor</b>	<b>25 in. and more from floor</b>
10 or less	12	15
11 through 19	12	20
20 or more	15	20

**--§ 25.857 Cargo compartment classification.**

(a) *Class A*; A Class A cargo or baggage compartment is one in which—

- (1) The presence of a fire would be easily discovered by a crewmember while at his station; and
- (2) Each part of the compartment is easily accessible in flight.

(b) *Class B*. A Class B cargo or baggage compartment is one in which—

- (1) There is sufficient access in flight to enable a crewmember to effectively reach any part of the compartment with the contents of a hand fire extinguisher;
- (2) When the access provisions are being used, no hazardous quantity of smoke, flames, or extinguishing agent, will enter any compartment occupied by the crew or passengers;
- (3) There is a separate approved smoke detector or fire detector system to give warning at the pilot or flight engineer station.

(c) *Class C*. A Class C cargo or baggage compartment is one not meeting the requirements for either a Class A or B compartment but in which—

- (1) There is a separate approved smoke detector or fire detector system to give warning at the pilot or flight engineer station;
- (2) There is an approved built-in fire extinguishing or suppression system controllable from the cockpit.
- (3) There are means to exclude hazardous quantities of smoke, flames, or extinguishing agent, from any compartment occupied by the crew or passengers;
- (4) There are means to control ventilation and drafts within the compartment so that the extinguishing agent used can control any fire that may start within the compartment.

(e) *Class E*. A Class E cargo compartment is one on airplanes used only for the carriage of cargo and in which—

- (2) There is a separate approved smoke or fire detector system to give warning at the pilot or flight engineer station;

**Fuel System--§ 25.951 General.**

**Final Report**  
*Supersonic Business Jet Design Team*

- (a) Each fuel system must be constructed and arranged to ensure a flow of fuel at a rate and pressure established for proper engine and auxiliary power unit functioning under each likely operating condition, including any maneuver for which certification is requested and during which the engine or auxiliary power unit is permitted to be in operation.
- (b) Each fuel system must be arranged so that any air which is introduced into the system will not result in—
  - (1) Power interruption for more than 20 seconds for reciprocating engines; or
  - (2) Flameout for turbine engines.